

Fire Risk Management and Emergency Response in Mining Operations

Serhii Minieiev | Roman Dychkovskyi
Dariusz Prostański | Vladyslav Ryskykh



Gliwice, 2025

Monografia opublikowana na licencji [Creative Commons Uznanie autorstwa –
Użycie niekomercyjne 4.0 Międzynarodowe](https://creativecommons.org/licenses/by-nc/4.0/) (CC BY-NC 4.0)

<https://doi.org/10.32056/KOMAG/Monograph2025.8>

Serhii Minieiev
Roman Dychkovskyi
Dariusz Prostański
Vladyslav Ryskykh

**Fire Risk Management
and Emergency Response
in Mining Operations**



*Monografia opublikowana na licencji [Creative Commons Uznanie autorstwa -
- Użycie niekomercyjne 4.0 Międzynarodowe](https://creativecommons.org/licenses/by-nc/4.0/) (CC BY-NC 4.0)*

Authors:

Serhii Minieiev, professor
Institute of Geotechnical Mechanics named by N. Poljakov, Dnipro, Ukraine

Roman Dychkovskyi, professor
Dnipro University of Technology, Ukraine
AGH University of Krakow, Poland

Dariusz Prostański, PhD, Eng., Professor at ITG KOMAG
Instytut Techniki Górniczej KOMAG (KOMAG Institute of Mining
Technology), Poland

Vladyslav Ryskykh, associated professor
Dnipro University of Technology, Ukraine

Reviewed Scientific Monograph:

Vasyl Holinko, professor
Dnipro University of Technology, Ukraine

Magdalena Tutak, PhD, Eng., prof. PŚ
Politechnika Śląska (The Silesian Technical University in Gliwice), Poland

Cover design:

Aleksandra Strzałkowska

Copyright by *Instytut Techniki Górniczej KOMAG, Gliwice 2025*
(*KOMAG Institute of Mining Technology, Gliwice 2025*)

Editor:

Instytut Techniki Górniczej KOMAG, ul. Pszczyńska 37, 44-101 Gliwice, Polska
(*KOMAG Institute of Mining Technology*)

ISBN 978-83-65593-50-4

Contents

Foreword	2
1. Introduction	3
2. Features of gas flow distribution in isolated mine workings	6
3. Dependence of air density on temperature, humidity, and methane content	10
4. Air temperature dynamics at the fire source	14
5. Thermal depression of a fire in isolated extraction areas	25
6. Forecast of maximum temperature dynamics at the fire source	30
7. The methodology for forecasting temperature in the fire source	33
8. Methods for detecting the development of underground fires	39
9. Methodology for monitoring ignition and fire development	49
9.1. Control of coal ignition	49
9.2. Fundamental concepts on the mechanism and causes of coal self-heating and spontaneous combust	50
9.3. The rate of coal oxidation	52
9.4. Kinetics of ethylene and acetylene emission during coal heating	53
9.5. Background values of indicator gases characterizing the development of coal spontaneous combustion	54
9.6. Emission of indicator gases during combustion of disintegrated coal mass	56
9.7. Method and means for determining coal temperature based on the ratio of unsaturated hydrocarbons	61
9.8. Methodology for determining the incubation period of coal self-ignition	66
10. Passport of endogenous fire hazard of coal seams	70
11. The issue of determining the lower explosion limits of coal dust, the release of volatile substances from the coal seam, and the norms of slagging	73
11.1. The issue of preventing dust formation and dust protection in mines	73
11.2. Determination of volatile matter output from coal seam	75
11.3. Determination of slaking norms and lower explosion limits of coal dust	81
12. Selected results of the volatile matter content of the coal seam, coal dust lower explosive limits, and inert dust addition standards	84
13. The Issue of reclassifying a fire as extinguished and the specifics of conducting work in this area	87
13.1. Reclassification of fires as extinguished and opening of sections with extinguished fires	87
13.2. Mining operations in areas affected by fire hazards	89
13.3. Methodology for Reclassifying a Fire as Extinguished and Conducting Work in the Affected Area	89
Conclusions	91
References	92

Foreword

Fire remains one of the most dangerous and unpredictable hazards in the mining industry. Whether in surface or underground environments, the combination of combustible materials, confined spaces, complex ventilation patterns, and critical infrastructure creates conditions in which even a minor ignition can escalate rapidly into a large-scale emergency. As mining operations evolve toward greater mechanization, deeper extraction levels, and more intricate networks of technological systems, the need for advanced fire-risk mitigation strategies becomes increasingly urgent. This monograph addresses that need with a comprehensive and evidence-based approach.

The authors present an integrated view of fire risk management, linking theoretical safety principles with practical engineering solutions. The monograph emphasizes the preventive dimension: identifying ignition sources, assessing combustible load, evaluating ventilation characteristics, and analyzing system vulnerability. Special attention is given to modern methods for predicting fire behavior and modeling heat and smoke spread tools that have become essential for designing safer mines and supporting effective decision-making under uncertainty.

Equally important is the focus on emergency preparedness and response. Mining emergencies demand rapid, coordinated action supported by reliable communication, robust evacuation planning, and adequate rescue capabilities. This work examines best practices for organizing emergency response systems and highlights the importance of training, scenario-based exercises, and continuous safety culture development. By combining engineering, organizational, and human-factor perspectives, the monograph provides a holistic framework for managing emergency situations.

In addition, the authors explore innovative technologies that are reshaping fire safety in mining: real-time monitoring systems, smart sensors, predictive analytics, and automated control solutions. These technologies, integrated with risk-assessment models, enable earlier detection of hazardous conditions and support dynamic risk management throughout the life cycle of a mining project. Their inclusion in this monograph reflects the industry's transition toward digitalized safety management systems.

The strength of this work lies not only in its scientific rigor but also in its practical relevance. The case studies, quantitative analyses, and methodological recommendations offered in the monograph make it a valuable reference for engineers, researchers, safety managers, and policymakers. It bridges gaps between theory and practice, offering solutions that can be implemented across different mining contexts and regulatory environments.

Ultimately, this monograph contributes to a safer and more resilient mining industry. By providing an in-depth examination of fire hazards and the strategies required to control them, it supports the development of mines where risks are systematically identified, mitigation measures are deliberately designed, and emergencies are met with competence and preparedness. It is my hope that this work will serve as both a scholarly reference and a practical guide for all professionals committed to safeguarding human life and mining assets.

Serhii Minieiev, Roman Dychkovskyi, Dariusz Prostański, Vladyslav Ruskykh

1. Introduction

The acceleration of fire suppression and the reduction of the time required to resume coal extraction from reserves prepared for mining in isolated mining sections (IMS) are among the most critical tasks in mitigating the consequences of accidents and minimizing material losses. Addressing this issue imposes specific requirements on the ventilation regime of isolated workings, as ventilation plays a key role in maintaining the optimal thermal conditions of the emergency zone. The thermal regime should maximize heat removal from the fire source and enhance the cooling of heated rocks while ensuring an oxygen concentration in the IMS atmosphere that prevents fire recurrence [1–10].

Research conducted by the Research Institute of Mining Safety (RIMS) and experience in accident mitigation indicate that fires in mining sections of underground mines are accompanied by several thermal factors: thermal depression, thermal resistance, and local recirculation of fire gases near the fire source. These factors disrupt the ventilation regime of the emergency area and the mine's overall ventilation network. Among them, thermal depression poses the greatest danger from a ventilation standpoint, as it results from an extremely uneven redistribution of air mass in the workings due to a powerful heat source. Thermal depression can be comparable in magnitude to the critical depression of the workings and significantly impacts the ventilation regime after isolation. In such cases, the ventilation of the affected section is primarily driven by thermal depression, with minor air leakage through stoppings.

Since the most complex and hazardous fires in mines require isolation, any ventilation measures must be scientifically justified and their consequences thoroughly forecasted. The reliability of such forecasts depends primarily on the accuracy of assessing the dynamics of thermal depression in isolated workings.

Methodological guidelines for calculating the ventilation of workings during fires are outlined in regulatory documents [6, 10], but they were developed without considering the specific ventilation and thermal regimes of isolated mining sections and are therefore unsuitable for long-term modeling and forecasting. Until recently, there was no reliable methodological framework for determining the magnitude of thermal depression under fire conditions when the section is isolated from the mine's ventilation network.

Existing methods for evaluating the feasibility of various ventilation interventions in fire suppression—such as inducing fire gas recirculation within IMS [6, 10] – are largely based on the classical hydrostatics problem of two interconnected vessels. These methods merely illustrate the hypothesis that combustion products can be repeatedly returned to the fire source, without accounting for the spatial or temporal dynamics of the phenomenon. Thus, they should not be used for isolated fires for several fundamental reasons:

The ventilation scheme of IMS is not equivalent to a simple parallel connection of several workings with through-ventilation. Such simplifications disregard key factors:

- The distribution of air leakage and inflows along the workings, whose impact on IMS thermal conditions remains unexplored;
- The existence of isolated zones where heat transfer conditions and heat release/absorption power change significantly as the airflow progresses;
- The formation of countercurrent airflows (local recirculation of fire gases) in horizontal and inclined workings from both the incoming and outgoing ventilation streams near the fire source.

It is possible that the latter factor contributes to fire suppression under conventional isolation conditions. However, the advantages of organizing global fire gas recirculation (in a closed IMS loop) over local (natural) recirculation require scientific validation.

A reliable assessment of thermal depression magnitude in IMS can only be achieved using a ventilation scheme that accurately reflects all the above-mentioned flow distribution characteristics. Therefore, the simplified approach to determining the average air temperature in the isolated workings based on measured thermal depression, as presented in [12] and the latest edition of the Statute [6], is unacceptable. Firstly, the analytical dependence of fire-induced thermal depression on average temperature does not imply a reverse relationship from a mathematical or statistical standpoint. Secondly, the temperature field of a fire source evolves over time

and space under the influence of multiple factors: fire intensity, thermophysical properties of the surrounding environment, and the distribution of air mass within the complex system of workings and goaf areas. Thus, the concept of average temperature in such conditions lacks practical significance.

Accordingly, methods for determining thermal depression during a fire should only be applied within their valid scope – namely, for assessing the stability of airflow in an individual inclined working. Additional research is required to develop a methodology for determining thermal depression after section isolation.

Another crucial factor in ensuring the reliability of thermal calculations during fires in mining sections is the mandatory consideration of air humidity and methane content. Even under normal ventilation conditions, air humidity in mine roadways exceeds 90% [12, 13], and methane emissions in gassy mines tend to intensify after isolation.

Due to the significant difference in the thermophysical properties of water vapor and methane compared to dry air, it is essential to study the impact of humidity and gas emissions on thermal depression throughout the entire isolation period. Despite the widespread use of computational modeling for mine ventilation networks, emergency ventilation conditions are still primarily assessed using approximate engineering formulas. These formulas form the basis for various operational thermal calculation methodologies, many of which have inherent shortcomings detailed in [14].

Meanwhile, when studying the long-term processes of heat transfer in gaseous and solid media within underground mining workings (UMW), which are characterized by powerful sources of thermal gas emissions and complex ventilation connection schemes, the goal of deriving universal analytical formulas is objectively impractical. Therefore, reliable modeling of the thermal depression dynamics of a fire during the isolation of a mining section is only feasible through the development of an appropriate mathematical model and an algorithm for conducting thermal calculations.

To develop an algorithm for determining the dynamics of thermal depression during fire isolation under different ventilation measures, it is necessary to:

- Analyze the distribution characteristics of airflows in UMW workings (define the ventilation scheme of the isolated section, compile a scheme of ventilation connections, and examine the air mass balance within the emergency workings);
- Establish patterns linking air density with methane impurities, water vapor content, and temperature under isolated fire conditions;
- Determine the dependence of the air temperature at the fire source on ventilation modes, thermophysical and geometric parameters of the workings, and the surrounding rock mass at different stages of emergency mitigation;
- Establish relationships linking the dynamics of thermal fire factors (thermal depression, thermal resistance, and the critical airflow velocity that induces local recirculation) with the aerodynamic parameters of isolated workings and their ventilation mode;
- Develop a methodology for determining the dynamics of thermal depression in an isolated section using the identified patterns under the influence of ventilation on its thermal regime.

The study of thermal depression dynamics in UMW involves a comprehensive research method that includes:

- Analysis and generalization of scientific and technical achievements in ventilation and thermal calculations for fires in underground structures;
- Mathematical modeling based on the fundamental laws of thermodynamics, heat and mass transfer, and mine aerology;

- Simulation modeling of gas-air mass and heat distribution processes in mine ventilation sections isolated from the general mine ventilation network after a fire;
- Experimental studies of factors that determine the ventilation and thermal regime of emergency areas.

The research methodology follows a specific sequence. The study of heat and mass transfer processes in the gaseous medium of UMW workings and surrounding rock mass is carried out as follows: the ventilation scheme of the section is determined, the gas-air mass balance equations in the isolated workings are compiled, and a mathematical model of heat and mass transfer in UMW is developed for the entire emergency mitigation period under the influence of ventilation, with the aim of accelerating fire suppression and intensifying the cooling of heated rock formations.

2. Features of gas flow distribution in isolated mine workings

The distribution of flows will refer to the direction of air mass movement along the mine working [2, 10]. As known from [5, 6, 10], the balance of air mass within a mine working is represented by its ventilation scheme. This scheme accounts for three main factors:

- The number of airflows involved in heat and mass exchange;
- The presence of air transfers from the external environment or other co-directional or counter-directional flows;
- Variations in heat and mass exchange conditions in different sections of the scheme.

In subsequent studies, the ventilation scheme is understood as a conceptual (schematic) representation of airflow movement within the gas environment of a mine working (as opposed to classification schemes of mining district ventilation). Air transfers refer to the inflows and outflows of air into the main air stream [6].

According to the classification of ventilation schemes presented in [14], the airflow distribution in an isolated working follows a through-flow ventilation scheme (Fig. 1) [10]. This includes: the main airflow G_0 , kg/s; additional airflow intake from adjacent workings at the connection point through the initial section of the working $G_{\text{дон}}$, kg/s; uniformly distributed inflows along the working G_{np} , kg/s and air outflows G_{yt} , kg/s.

The study considers a scenario most favorable for recirculation formation (Fig. 2), where a fire occurs in an inclined longwall, and a connecting roadway (a decline) links the incoming and outgoing ventilation streams of the mining district. In this case, the ventilation scheme, in terms of heat exchange, consists of four characteristic sections: haulage roadway (AB); longwall face (BC); ventilation roadway (CD); roadway DA, which closes the potential recirculation loop ABCD.

These section names are conventional, as any other isolation scheme can be represented by a combination of these typical sections, which does not affect the fundamental conclusions of the study.

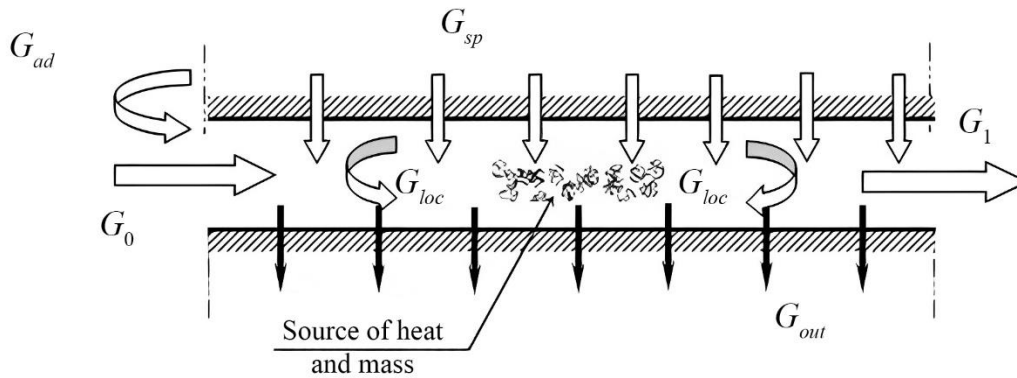


Fig. 1. Through-Flow ventilation scheme of a mine working with air transfers [10]

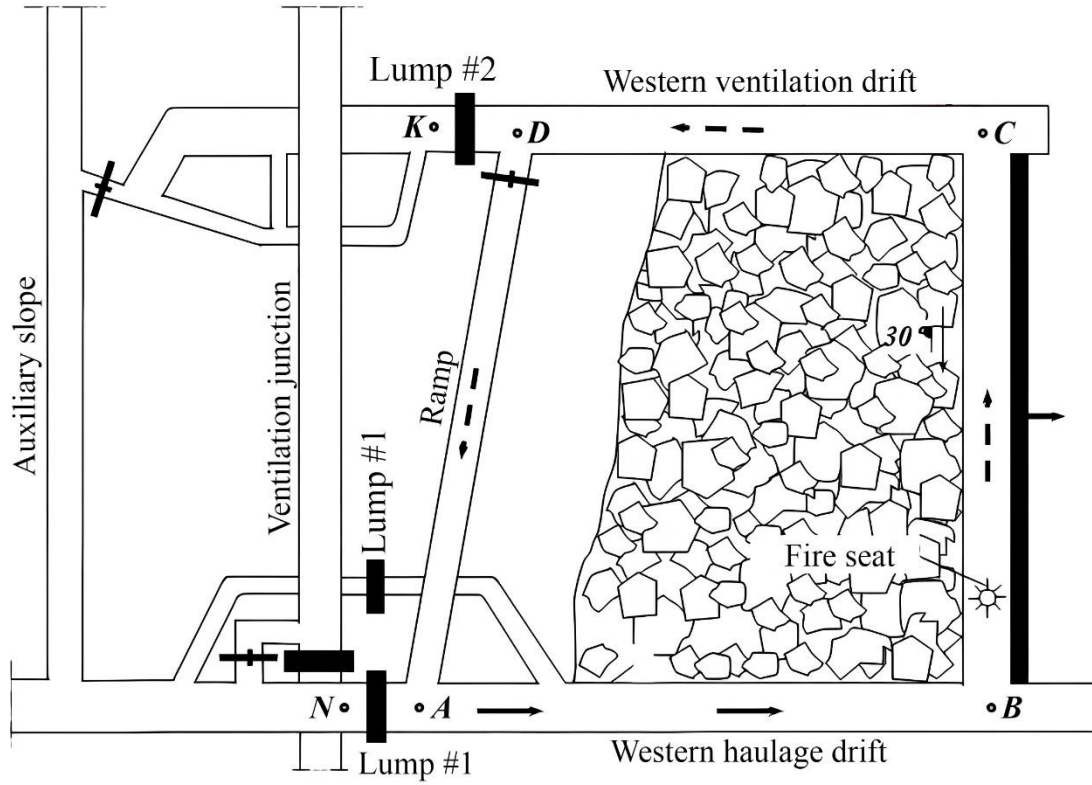


Fig. 2. Scheme of isolation of the extraction area [4]

The distribution of airflow in the examined section is presented as follows. The main airflow (commonly referred to as the "exhaust flow") G_0 enters the section through bulkhead No. 1. In the event of fire gas recirculation, it mixes with an additional airflow G_{add} coming from the inclined passage. Along the haulage drift AB , air leakage into the goaf is consistently observed.

In study [15], an empirical relationship is presented for these air leakages Q_{leak} , m^3/s (for a fully caved mining system, a U -type ventilation scheme, and complete roof collapse) as a function of the airflows Q_{sit} , m^3/s and Q_{lw} , m^3/s , which enter the section and the longwall, respectively, as well as the average rock strength f according to the Protodyakonov scale:

$$\left(\frac{Q_{lw}}{Q_{leak}}\right)^2 = \frac{a}{f^4(Q - Q_{lw})} + \frac{b}{f^5} \quad (1)$$

where $a = 4533 \text{ m}^3/s$; $b = 802$.

Based on this relationship, an analytical expression for the leakage coefficient has been obtained:

$$k_{yt} = \frac{Q_{leak}}{Q_{sit}} = \frac{\bar{a} + 1}{\bar{b} - 1} \left[\sqrt{\frac{\bar{b} - 1}{(\bar{a} + 1)^2} + 1} - 1 \right], \quad (2)$$

where $\bar{a} = 4533/(2 \cdot Q_{sit} f^4)$; $\bar{b} = 802/f^5$.

Moreover, equations (1) and (2) are defined only for $f < 3$ (the graphs in [2] also present curves for $f > 3$).

Figure 3 presents the calculated results of the air leakage coefficient according to (2) within the actual range of air consumption in the isolated working area (IWA). Thus, it is determined that as the air moves along the drifts, its mass can vary by up to 30%. For the pillar mining system, according to [6]:

$$k_{yt} = 0,04 + 0,33 \cdot f \quad (3)$$

Expressions (2) and (3) are assumed to be used for modeling the distribution of airflow within the haulage and ventilation drifts.

In the haulage drift, in addition to the main airflow and leakages, an additional counterflow directed against the main stream emerges under the roof. This so-called convective flow or free convection flow $G_{\text{лок}}$, m^3/s , is caused by the local thermal depression of the fire [5, 13, 16-18]. By convective flow or free convection flow, we refer to local recirculation flows: warm (under the roof) or cold (near the mine floor). As the distance from the fire source increases, this flow cools down and mixes with the main airflow near the floor of the working. Consequently, the ventilation scheme in section AB becomes a three-flow system.

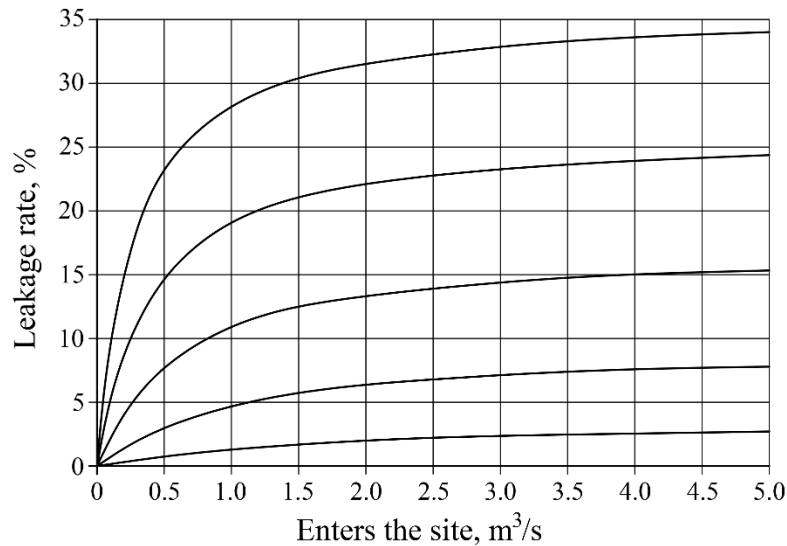


Fig. 3. Dependence of the air leakage coefficient into the mined-out space on the total airflow rate in the extraction area [5]

All the listed flows and crossflows contain moisture in the form of water vapor and other gaseous impurities, the most significant of which is methane. Heat and mass exchange occurs between these flows. In the section with the fire source, crossflows can be neglected. However, this section is considered separately, as it is here that the temperature field of the gas environment in the isolated volume is formed.

The sources of thermal draft that may arise during a fire are conventionally denoted as h_t with additional indices “l” and “g” to emphasize their division into local h_{tl} , Pa, acting inside the volume of the working, and global h_{tg} , Pa, applied to the entire air column in the working, representing the thermal depression. The symbol h_{pr} indicates a conditional source of draft caused by the overall mine ventilation, while branch 1 models the entire mine ventilation network adjacent to the ventilation network of the extraction section.

The presented scheme is developed solely for analyzing the air mass balance in the section, with the further application of the results in heat transfer modeling. It does not claim compliance with any standards or norms. In our view, it includes the minimal number of branches necessary for an accurate mathematical representation of the research object. The scheme cannot be reduced to a simple parallel-series connection of branches for the following reasons. If any marked branch is omitted, this would completely ignore certain thermal factors or prevent assessing their impact on the thermal regime of the section. Standard network transformation methods are also unsuitable under these conditions, as each branch is influenced by gravitational forces and thermal resistance forces that dynamically depend on other branches. The contribution of each section of the scheme to the overall formation of the ventilation or thermal regime can only be assessed after specialized studies.

As a result, no measurements at the stoppings should be considered a sufficient basis for predicting not only the temperature but also the thermal depression itself, as the concept of thermal depression in the extraction section extends far beyond the weight of the air column in an individual inclined working. In this research, the thermal depression of the extraction section is represented as a pressure field at all scheme nodes (Figure 3, 4), except for the pressure distribution in the absence of heat sources.

The use of the leakage coefficient values (3, 4) allows the air balance in the roadways to be represented by the following equation:

$$G_l = G_0 + \omega l \quad (5)$$

where $\omega = (k_{\text{leak}} - 1)G_0/l$ – the specific value of air leakage in the roadways, kg/(s·m);
 l – length of the roadway section, m.

Due to the variation in mass airflow over space and time, as well as its close dependence on temperature, density, and pressure, determining the airflow distribution in the ventilation network of the IVU solely based on this equation is impossible, even with known boundary conditions. To achieve this, solving additional research problems is required.

The results of the presented analysis of IVU airflow distribution were used in developing a mathematical model of the thermal regime of the section during the accident elimination period.

3. Dependence of air density on temperature, humidity, and methane content

From a thermodynamic perspective, the state of air in an isolated section is characterized by absolute temperature T (K), absolute pressure P (Pa), and mass per unit volume, i.e., density ρ (kg/m³). Under normal (standard) conditions, the temperature, pressure, and density have the following values:

$$T_H = 273,15 \text{ K}; P_H = 101,325 \text{ kPa} = 760 \text{ mm Hg} \quad (6)$$

The relationship between the state parameters is determined by the Clapeyron equation [10, 21]:

$$\rho = \frac{P}{B_g T}, \quad (7)$$

where $B_g = B/\mu$ – the specific gas constant, J/(kg·K); B – the universal gas constant, $B = 8314 \text{ J}/(\text{kmol} \cdot \text{K})$; μ – the molecular weight of the gas, kg/kmol.

The value of B can be determined based on equation (7) using the state parameters of the gas under normal conditions (6):

$$B = \frac{P_n}{\rho_n T_n}, \quad (8)$$

Accordingly, considering equations (7) and (8):

$$\rho = \frac{T_n}{T} \frac{P}{P_n} \rho_n, \quad (9)$$

Considering the dynamics of pressure, temperature, and the presence of heat and gas emission sources, the air density does not significantly change as it moves through the isolated section.

The pressure P consists of static pressure P_{st} , Pa, and dynamic pressure p , Pa. The dynamic pressure is determined by the movement of air at a velocity u , m/s:

$$p = \frac{\rho u^2}{2}, \quad (10)$$

Since the velocity of the ventilation stream in the extraction areas does not exceed 5 m/s, $p < 16 \text{ Pa}$. Therefore, considering that the magnitude of P_{st} is on the order of 10^4 , with an error of no more than 0.002%, in formula (9), we can assume $P \approx P_{st}$.

The static pressure is determined by gravitational forces and is equal to the pressure of the air column at a depth z , m, according to the standard formula [2, 10, 19, 20]:

$$P_{st} = P_n + \rho_n g z, \quad (11)$$

where $g = 9,81 \text{ m/s}^2$ – the modulus of the gravitational acceleration vector.

Under the influence of this pressure, air volumes are compressed, and its temperature can increase by 9.8°C for every 1000 meters of depth (in the absence of heat exchange with the surrounding environment) [21].

As a result, based on (9) and (11), the density of dry air as a function of pressure and temperature is represented as follows:

$$\rho = \left(1 + \frac{\gamma_n}{P_n} z\right) \frac{T_n}{T} \rho_n, \quad (12)$$

where $\gamma_n = \rho_n \cdot g$ – specific weight of air under normal conditions, N/m³.

The state of air at the surface is conventionally assumed to be normal, and its parameters are used only as a reference level when assessing the degree of change in air conditions within the mine. The presence of gas emission sources leads to the appearance of various impurities in the air, which have different state parameters compared to pure air. In the IMS, the most significant impurities are moisture (in the form of water vapor) and methane. Therefore, the air density should be considered as the density of a gas mixture, according to the following equation:

$$\rho = C_v \rho_v + C_m \rho_m = \rho_v \left[1 - C_m \left(1 - \frac{\rho_m}{\rho_v}\right)\right], \quad (13)$$

where C_v and C_m – the volumetric content of humid air and methane in the mixture; ρ_v and ρ_m – the density of humid air and methane, kg/m³.

The water vapor content in the air is measured using psychrometers [2] or determined according to specialized tables [6], based on its partial pressure P_p , Pa, which can be calculated using an empirical formula [5, 6]:

$$P_p = 611,21 \cdot \exp\left(\frac{17,5043 \cdot t}{241,2 + t}\right), \quad (14)$$

where t – air temperature, °C.

The pressure of humid air (a mixture of air and water vapor) P_v , Pa, is lower than that of dry air and is given by:

$$P_v = \left[P - \left(1 - \frac{\mu_w}{\mu_a}\right) P_p\right], \quad (15)$$

where $\mu_w = 18.016$ kg/kmol – molecular mass of water vapor; $\mu_a = 28.980$ kg/kmol – molecular mass of air;

Therefore, based on (15), expression (12) for the air density in the presence of water vapor is transformed into the following form:

$$\rho_a = \left(1 + \frac{\gamma_n}{P_n} z - \frac{P_n}{P_n} \kappa_n\right) \frac{T_n}{T} \rho_n, \quad (16)$$

where $\kappa_n = (1 - \mu_n/\mu_e) \approx 0,3783$ – coefficient accounting for the differences between the density of air and water vapor.

Based on (13) and (16), the influence of pressure, temperature, humidity, and methane admixture on air density is characterized by the "difference" function:

$$f_\rho(z, t, C_m) = \frac{\rho}{\rho_n} = (1 - C_m \kappa_m) \left(1 + \frac{\gamma_n}{P_n} z - \frac{P_n}{P_n} \kappa_n\right) \frac{T_n}{T}, \quad (17)$$

where $\kappa_m = (1 - \rho_m/\rho_a) \approx 0,4464$ – coefficient accounting for the differences in density between methane and air.

Since pressure, temperature, moisture content, and methane concentration in the air, in turn, depend on the distribution of its mass along the excavation, air density is a transcendental function of these parameters. A single expression (17) is insufficient for an unambiguous determination of the air state in an isolated section [5, 6, 10]. However, by applying (17), it is possible to assess the degree of influence of each of these factors on density.

When deriving function (17), the values of pressure, temperature, and density under normal conditions P_n , T_n , and ρ_n were used. Obviously, the relationship between the air state parameters will remain unchanged if, instead of normal conditions, the known parameters are taken as their values at the inlet of the ventilation stream into the isolated section. These values can be directly measured or reliably determined by calculation. Additionally, the coordinates x and z can be referenced from the entry cross-section of a series of isolated workings (point N in the diagram in Fig. 2). In this case, the equation takes the following form:

$$f_\rho(z, t, C_m) = \frac{\rho}{\rho_0} = (1 - C_m \kappa_m) \left(1 + \frac{\gamma_0}{P_0} z - \frac{P_n}{P_0} \kappa_n \right) \frac{T_0}{T}, \quad (18)$$

where $\rho_0 = (1 - C_{m0} \kappa)(1 - (P_{n0}/P_0) \kappa_n)$ – air density at the initial cross-section; the index "0" indicates the parameter value at the initial cross-section.

Figure 4 presents curves of air density variations depending on temperature, water vapor content, and methane concentration within the actual range of these parameters in the isolated ventilation unit (IVU). The density values are expressed as a percentage relative to the density of dry air, without impurities, at a temperature of 20°C and a barometric pressure of 110.8 kPa, which approximately corresponds to an elevation of $z = -750$ m.

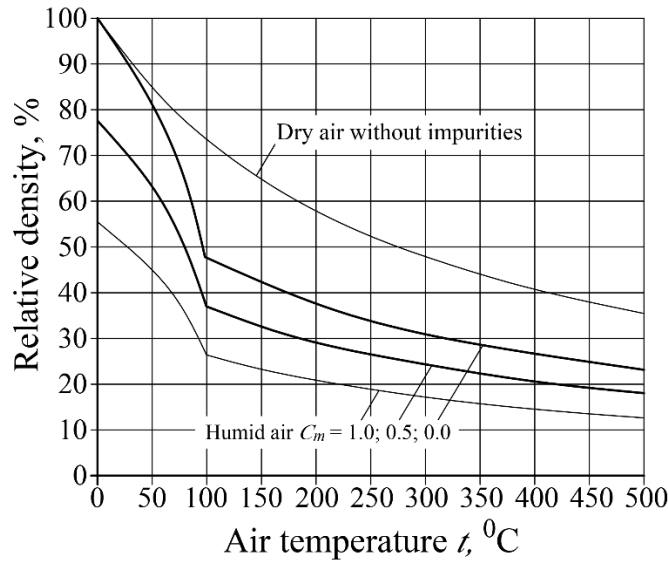


Fig. 4. Dependence of air density on humidity and methane content at different temperatures [5]

In the calculation using formula (18), 100% relative humidity of the air was assumed (under normal ventilation conditions, as the air moves through the working face and further along the ventilation drift, the relative humidity exceeds 95% [5]).

Since within the extraction area, the variation in excavation depth occasionally reaches 250 m, the term γ_z/P_0 in formula (18) can be neglected compared to 1, with an error not exceeding 3%, even if the barometric pressure at the section entrance is close to normal. Furthermore, at depths up to 1000 m, the value of $P_p \kappa_p/P_0$, assuming 100% air humidity, varies within a narrow range of 0.234–0.250 Pa. Therefore, for further calculations, it is assumed that $P_p \kappa_p/P \approx 0.242$ Pa.

The results of the analysis of air density dependence on temperature, humidity, and methane content indicate that its value can be determined with sufficient accuracy using the following formula [2]:

$$f_\rho = \frac{\rho}{\rho_0} = 0,768 \cdot (1 - 0,446 \cdot C_m) \frac{T_0}{T}, \quad (19)$$

Thus, according to (19), air density decreases by nearly 25% solely due to humidity; in the case of complete replacement of air with methane, the mass of the gas medium in the workings of the emergency area is expected to decrease by approximately half; and an increase in air temperature to 1000°C leads to an almost threefold expansion in its volume.

These factors must be taken into account when determining thermal depression, as its magnitude is directly proportional to air density.

4. Air temperature dynamics at the fire source

The thermal regime in isolated workings of the excavation area is determined by the temperature dynamics at the fire source. The dynamics of T_{fs} in this study are determined based on the heat balance equation in the fire source with a volume of V_{fs} [6]:

$$c_{pfs}\rho_{fs}V_{fs}\frac{\Delta T_{fs}}{\Delta\tau} = \theta_{cm} + \theta_{ct} + \theta_{he}, \quad (20)$$

where c_{pfs} is the specific heat capacity of air within the fire source, J/(kg·K); ρ_{fs} is the density of air with impurities within the fire source, kg/m³; ΔT_{fs} is the temperature change of air, K, over the time interval $\Delta\tau$, s, within the volume V_{fs} ; θ_{cm} is the heat release power during the combustion of materials forming the fire load of the working, W; θ_{ct} is the power of convective heat transfer by the air flow, W; θ_{he} is the power of convective heat exchange between the air volume in the fire source and the surrounding rock mass, W.

The left-hand side of equation (20) represents the change in thermal power in the fire source over $\Delta\tau$, while the right-hand side is the algebraic sum of the heat sources (sinks) acting within V_{fs} during the same time interval. For further research, the meaning of the quantities included in this equation is explained.

When solving the given problems, it is necessary to consider the air humidity and the presence of methane impurities. The specific heat capacity of dry air is $c_{ps} = 1005$ J/(kg·K). The heat capacity of humid air is determined by the formula [5]:

$$c_{pw} = c_{pa} + c_{ps} \cdot d, \quad (21)$$

where $c_{ps} = 1930$ J/(kg·K) – heat capacity of water vapor; d – moisture capacity of air, kg/kg, its maximum value is reached at 100% relative humidity (as assumed in this study) and equals:

$$d = \frac{\mu_a}{\mu_a} \frac{p_s}{p - p_s} = \frac{18,016}{28,980} \frac{p_s}{p - p_s} = 0,622 \cdot \frac{p_s}{p - p_s}, \quad (22)$$

where μ_a and μ_s – are the molecular masses of air and water vapor, respectively, in kg/mol; under standard conditions $\mu_a = 28,980$ kg/mol; $\mu_s = 18,016$ kg/mol; p and p_s – are the pressures of dry air and water vapor in moist air, respectively, in Pa.

The heat capacity of methane is more than twice that of air: $c_{pm} = 0.593$ kcal/(kg·°C) ≈ 2483 J/(kg·K). As a result, taking into account the components of air, the value of c_{pai}^r in (20) is determined as follows:

$$c_{pai}^r = \left[\left(1 + \frac{k_s p_s}{p - p_s} \bar{c}_{ps} \right) (1 - C_m) + \bar{c}_{pm} \cdot C_m \right] \cdot c_{pa}, \quad (23)$$

where $k_n = \mu_s/\mu_a \approx 0,622$ – the ratio between the molecular mass of steam and air;

$\bar{c}_{pm} = c_{pm}/c_{pa} = 1,920$ – the ratio of the heat capacity of steam to air;

$\bar{c}_{pm} = c_{pm}/c_{pa} = 2,471$ – the ratio of the heat capacity of methane to air.

It should be noted that the presented expression for the moisture capacity of air (22) is used in technical calculations of thermal power installations (steam engines, boilers, dryers). Theoretically, the steam pressure in such systems can not only reach but also significantly exceed atmospheric pressure, and the value of d is not limited when $p_s \approx p$. Therefore, unlike (22), in the present study, when determining the heat capacity of humid air, it is assumed that the moisture capacity is equal to the ratio of the absolute humidity of the air, numerically equal to the density of water vapor ρ_s , kg/m³ [2], under state parameters p_s , T , adjusted to the characteristic air density ρ_0 :

$$\tilde{d} \approx \frac{\rho_n}{\rho_0} = \frac{\rho_{s0}}{\rho_0} \cdot \frac{T_0}{T} \cdot \frac{p_n}{p_{s0}}, \quad (24)$$

In particular, at $T_0 = T_n$, the quantities in (24) have the following values: $\rho_{s0} \approx 4,84 \cdot 10^{-3} \text{ kg/m}^3$; $p_{s0} \approx 611,12 \text{ Pa}$ – density and pressure of water vapor in the air under normal conditions; $\rho_0 = 1,293 \text{ kg/m}^3$ – density of air under normal conditions.

If instead of (22), equation (24) is used to determine humidity, then equation (23) takes the following form:

$$f_c = \frac{c_{pfd}}{c_{pa}} = \left(1 + \frac{\rho_{s0}}{\rho_0} \cdot \frac{p_n}{p_{s0}} \cdot \frac{T_0}{T} \bar{c}_{ps}\right) \cdot (1 - C_m) + \bar{c}_{ps} \cdot C_m, \quad (25)$$

where f_c – the function representing the difference between the heat capacity of dry air and the heat capacity of humid air with a methane admixture.

During calculations using formulas (19) and (25), it is assumed that the air moisture capacity increases as the temperature rises from the normal value, $T_n = 0^\circ\text{C}$, to 100°C , and remains constant above this value. This assumption is based on the fact that the formation of superheated water vapor with a pressure significantly exceeding atmospheric pressure within a large isolated volume of mine workings, which have aerodynamic connections to the surface, is unlikely. The validity of this assumption requires experimental verification.

Figure 5 graphically represents the function of the dependence of air heat capacity on humidity and methane content f_c , determined under the specified assumptions.

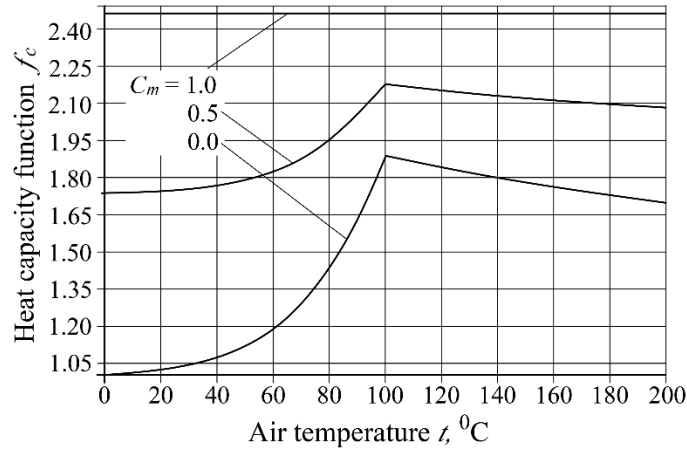


Fig. 5. The heat capacity dependences of humid air on temperature at different methane concentrations [6]

Hence, it should be noted that the dependence of air heat capacity on methane content is more significant than on humidity. The maximum heat capacity value can exceed the standard value $c_{pai} = 1005 \text{ J/(kg} \cdot \text{K)}$ by more than 2.4 times.

In the further analysis of the quantities included in equation (20), the volume of the fire source is conventionally assumed to be equal to the volume of a cylinder with a base area S , m^2 , equivalent to the cross-section of the excavation, and a generating length l ; thus, $V_{f0} = S \cdot l$. Let us assume that the heat source power is uniformly distributed within this volume. In this case, the heat source is the heat release during the combustion of materials that constitute the fire load of the excavation. Its power is determined by the combustion rate of these materials per unit surface area m_g , $\text{kg}/(\text{m}^2 \cdot \text{s})$, and the air flow rate entering the fire source G_0 , kg/s .

Based on the analysis of research results [5], this power can be determined as follows:

$$\theta_{gm} = \eta_m \cdot \left[1 - \left(1 - \frac{m_g F_g}{G_0} f_p\right) \frac{\mu_{a0}}{\mu_{al}} \cdot \frac{C_{O_2 l}}{C_{O_2 0}}\right] \cdot C_{O_2 0} \frac{\mu_{O_2}}{\mu_{a0}} G_0, \quad (26)$$

where η_m – the heat of combustion per unit mass of materials (or methane) in the fire source per unit mass of oxygen that has participated in the combustion reaction. Approximate values of η_m for materials that contribute to the fire load in mine workings are as follows: wooden support structures – 17.5 MJ/kg; conveyor belt – 33.0 MJ/kg; scattered coal dust – 31.0 MJ/kg; signal and power cables – 29.0 MJ/kg; methane – 55.5 MJ/kg; F_g – the surface area of burning materials, m^2 ; μ_{a0} , μ_{al} and μ_{o2} – the molecular mass of oxygen and air entering and exiting the source, respectively; according to [5], it is assumed $\mu_{a0} = \mu_{al} = \mu_a = 28,980$ kg/mol; $\mu_{o2} = 31,999$ kg/mol; $C_{O_{20}}$, $C_{O_{2l}}$ – the volumetric content of oxygen in the air entering and leaving the fire source; under normal conditions $C_{O_{20}} = 0,2095$ [5, 6]; f_ρ – The function of the differences in the mass flow rates of air entering the fire source G_0 and leaving it G_l due to changes in density is determined according to (19) based on the air temperature in the source.

The expression $m = m_g \cdot F_g$ represents the rate of mass combustion in the fire source, measured in kg/s. In the conditions of mine workings, the burning surface may include the front side of wooden support structures (lagging, frames), the area of a burning conveyor belt (either one or both branches), the surface of coal dust scattered on the floor of the working, the sheath of signal and power cables, and other materials. Throughout all phases of a fire – initial stage, development stage, steady combustion, and extinction – the rate of material combustion continuously changes depending on numerous factors. These include the thermophysical and chemical properties of the burning materials, the distribution of their mass within the fire source, the dynamics of air consumption and its gas components, temperature, humidity, and more. It is impossible to derive an analytical expression for this dependence. Therefore, in further studies, the value of m_g is determined using well-known empirical data [5, 7, 9] on the spread rate of the fire front v_{op} (m/s) for various fire load scenarios in the workings (burning support structures, lagging, conveyor belts, etc.), and it is assumed that:

$$m_m = m_{fl} \cdot v_{op}, \quad (27)$$

where m_{fl} – The fire load of the mine working [5], measured in kg/m, can be determined for different materials as follows: timber supports (the fire load is approximately $m_{fl} \approx 22$ kg/m); rubber-fabric conveyor belt (the fire load is given by $m_{fl} \approx 22.5 \cdot b - 0.5$ kg/m, b is the belt width in meters); sheath of signal and power cables (the fire load is given by $m_{fl} \approx 0.017 \cdot D + 1.07$ kg/m, D is the cable diameter in meters).

As a result, the heat release power during the combustion of materials in the fire source can be determined using the following formula:

$$\theta_{cm} = [1 - (1 - k_g f_\rho) \cdot \bar{C}_{O_2}] \cdot \bar{\mu}_{O_2} \cdot \eta_m \cdot C_{O_{20}} \cdot G_0, \quad (28)$$

where $k_g = m_{fl} v_n / G_0$ – the combustion rate coefficient of materials in the source; $\bar{C}_{O_2} = (\mu_{a0} / \mu_{al}) \cdot (C_{O_{2l}} / C_{O_{20}}) \approx C_{O_{2l}} / C_{O_{20}}$ – relative change in oxygen content at the source; $\bar{\mu}_{O_2} = \mu_{O_2} / \mu_{a0} \approx 1,104$ – the ratio of the molecular weight of oxygen to the molecular weight of air.

In expression (28) for the thermal power of a fire, additional unknowns are included: the combustion rate of materials and the oxygen content in the air entering and leaving the fire source. It is assumed that these parameters will be determined based on statistical data, known experimental research results, or empirical methods.

The power of convective heat transfer θ_{kp} , W , which is represented by the second term on the right-hand side of (20), is proportional to the mass flow rate of air and its temperature. Taking into account that $G_l \approx G_0 + m_z \cdot F_z$, this component of thermal power can be expressed as:

$$\theta_{ct} \approx [T_0 - (1 + k_g) T_{fs}] \cdot f_\rho f_c c_{pa} G_0, \quad (29)$$

Since the temperature of the air entering the source is lower than that of the air exiting it, the thermal power (29) characterizes the intensity of heat removal from the source.

Convective heat exchange between the volume of air in the fire source and the surrounding rock mass (the last term of the thermal power on the right-hand side of (20)) is represented by the heat outflow power into the

surrounding space, which is determined as follows:

$$\theta_{he} = \alpha \Omega l (T_{lw} - T_{fs}), \quad (30)$$

where T_{lw} – temperature of the workings' walls, K; α – convective heat transfer coefficient, W/(m²·K) or kcal/(m²·h·°C); Ω – perimeter of the working, m.

The value of the convective heat transfer coefficient between the airflow and the workings' walls under normal ventilation conditions $\alpha = \alpha_0$, according to [13, 21], depends on the airflow velocity, the cross-section of the working:

$$\alpha_0 = 2,9 \cdot \varepsilon \cdot u^{0,8} \cdot D^{-0,2}, \text{ kcal}/(\text{m}^2 \cdot \text{h} \cdot ^\circ\text{C}). \quad (31)$$

where u – airflow velocity, m/s; ε – roughness coefficient of the workings' walls, varying within the range of 1...3, depending on the type of support; $D = 4 \cdot S / \Omega$ – equivalent diameter of the working's cross-section, m.

During fires, according to experimental studies [5], in the velocity range of 0.5...5.0 m/s, the following empirical formula was obtained:

$$\alpha = \alpha_m = 4,42 + 3,54 \cdot u, \text{ kcal}/(\text{m}^2 \cdot \text{h} \cdot ^\circ\text{C}). \quad (32)$$

Based on the analysis of the values included in (20), this equation transforms into the following:

$$\begin{aligned} c_{pa} \rho_0 V_{fs} f_c f_\rho \frac{dT_{fs}}{d\tau} = & [1 - (1 - k_g f_\rho) \bar{C}_{O_2}] \bar{\mu}_{O_2} C_{O_2 0} \eta_m G_0 + \\ & + [T_0 - (1 + k_g) T_{fs}] f_\rho f_c c_{pa} G_0 + \alpha_m \Omega l (T_{lw} - T_{fs}) \end{aligned} \quad (33)$$

Unlike in (20), in (33), the final increments of temperature and time are represented by their differentials, and the problem of determining the temperature dynamics in the fire source is reduced to solving a first-order differential equation. To transform this equation into its canonical form, it is necessary to determine the characteristic values of the dependent and independent variables involved.

The independent variable is time τ . Its characteristic value is chosen as the air flow passage time through the fire source τ_0 , s, which is given by:

$$\tau_0 = \frac{\rho_0 V_{fs}}{G_0} \sim \frac{l}{u_0}, \quad (34)$$

According to (32), the maximum temperature increase at the fire source, ΔT , K, may reach:

$$\Delta T^* = \frac{f_g \eta_m G_0 \tau_0}{f_\rho f_c c_{pa} \rho_0 V_{fs}} \sim \frac{f_g \eta_m}{f_\rho f_c c_{pa}}, \quad (35)$$

where $f_g = [1 - (1 - k_g \cdot f_\rho) \cdot \bar{C}_{O_2}] \cdot \bar{\mu}_{O_2} \cdot C_{O_2 0}$ – the dimensionless function of the combustion rate of materials at the source.

The functions f_ρ , f_c , and f_g , characterize the dependence of the thermophysical properties of air on temperature, humidity, methane and oxygen content, and the combustion rate of materials at the source. In the absence of a fire, for dry, impurity-free air, the values of f_ρ , f_c , and k_g in equation (33) take the values $f_\rho = f_c = 1$; $k_g = 0$. When moisture and methane impurities are present in the air f_ρ decreases, while f_c – exceeds one.

The results of the study on k_g , under actual fire load conditions in the workings, based on data from [7], indicate that it is of the order of 10^{-1} . Figure 6 presents a graph of changes in the function f_g within the typical oxygen content range C_{O_2} for mine fires in air exiting the source (0.08–0.21) and for variations in $(k_g f_\rho)$ from 0 to 0.01. It follows that the value of $k_g f_\rho$ has virtually no impact on f_g , and therefore, it can be neglected in comparison to 1.

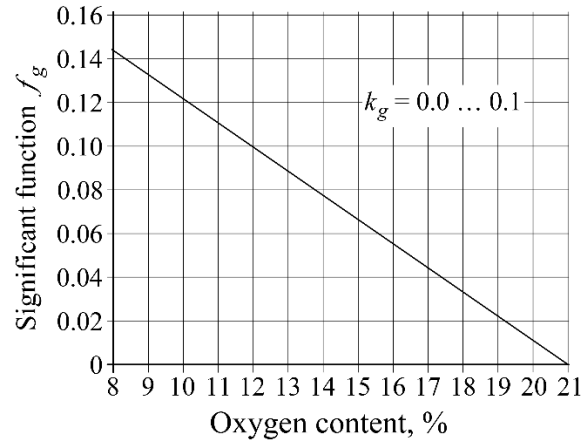


Fig. 6. Dependence of the function f_g on the oxygen content in the air originating from the fire source [5, 7]

The dependence of the product of the functions $f_p f_c$ is presented graphically in Figure 7. Over a wide temperature range (up to 500°C), this product deviates from the average value of 0.8 by 0.5, varying from 1.3 to 0.3.

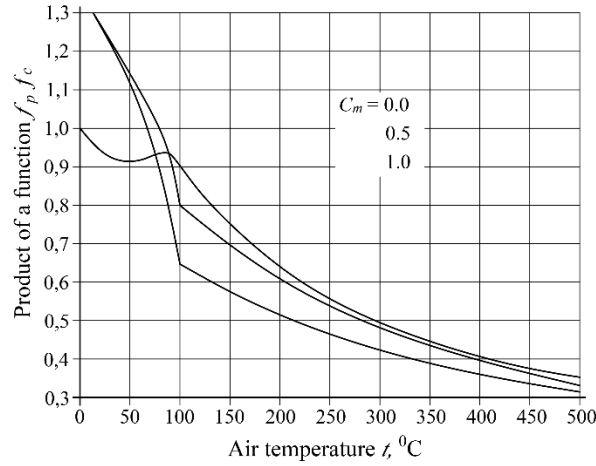


Fig. 7. Dependence of the product of density and heat capacity functions $f_p f_c$ on air temperature [7]

Taking into account the analysis of the dimensionless values of the functions f_g , f_p , and f_c , the value ΔT_{op}^* is considered to be equal to ΔT^* under the conditions: $C_{O_2 0} \approx 21\%$; $C_{O_2 l} \approx 8\%$; $\bar{\mu}_{O_2} \approx 1,1$; $1 - k_g f_p \approx 1$; $f_g = f_{g0} \approx (C_{O_2 l} : 100\%) \cdot \bar{\mu}_{O_2} \approx 0,088$; and $f_p f_c \approx 0,3$ is regarded as the limiting value for temperature increment (according to statistical data, the oxygen content in the air exiting the source, with some exceptions, is not lower than 8%). Henceforth, $T^* \approx \Delta T_{op} = \text{const}$ and ΔT_{op} is used as the characteristic temperature value at the source. After introducing two new dimensionless variables:

$$\bar{\tau} = \frac{\tau}{\tau_0}; \quad t = \frac{T_{fs} - T_0}{\Delta T_{op}}, \quad (36)$$

The heat balance in the fire source is modeled by the equation:

$$\frac{dt}{d\bar{\tau}} = 1 + \phi \cdot \text{St} \cdot t_{\Omega} - (1 + \phi \cdot \text{St}) \cdot t, \quad (37)$$

where $\phi = \phi(t, \bar{\tau}, C_m) = 1/f_p f_c$ – the function of the differences in density and heat capacity of humid air with methane impurities from the standard values of these parameters for dry, impurity-free air; $t_{\Omega} = (T_{lw} - T_0)/\Delta T_{op}$ – The relative temperature value T_{st} ; $\text{St} = \alpha_m \Omega l / c_{pa} G_0$ – the dimensionless complex (analogous to the Stanton number for thermal similarity), characterized by the ratio between heat exchange

intensity and the physical heat capacity of air.

Equation (37) has the standard form of a first-order differential equation:

$$\frac{dt}{d\bar{\tau}} + f_1 \cdot t = f_0, \quad (38)$$

Where $f_1 = f_1(\bar{\tau}, t, t_\Omega, C_m) = 1 + \phi \cdot St$; $f_0 = f_0(\bar{\tau}, t, t_\Omega, C_m) = 1 + \phi \cdot St \cdot t_\Omega$ – functions of the independent variable $\bar{\tau}$ and the dependent variables t, t_Ω .

Obtaining such a solution in an analytical form is possible only in certain cases of dependencies f_1 and f_0 on $\bar{\tau}$, or when:

$$t_\Omega = t_{\Omega 0} = \text{const}; \quad \phi = \phi_0 = \text{const}, \quad (39)$$

Solution (38) for constant values f_1 and f_0

$$t = \frac{f_0}{f_1} (1 - e^{-f_1 \cdot \bar{\tau}}) = \frac{1 + \phi \cdot St \cdot t_\Omega}{1 + \phi \cdot St} \{1 - \exp[-(1 + \phi \cdot St) \cdot \bar{\tau}]\}, \quad (40)$$

This particular solution models the temperature dynamics at the source under standard air density and heat capacity conditions, assuming constant wall temperature. Hereafter, this solution for the temperature at the fire source will be referred to as the standard solution.

In other cases, equation (38) can only be solved using numerical methods. Figure 8 presents temperature curves obtained from one of the modeling scenarios of temperature dynamics at the fire source, where $S_t=0.067$, $t_\Omega = 0.0$, and $\Delta T_{op} = 1000$ °C, corresponding to an air flow velocity of $u_0 = 0.5$ m/s with a cross-sectional area of the excavation $S = 10.0$ m² and a combustion zone length of $l = 2.0$ m. Temperature values were determined based on equation (38) using the numerical integration method for differential equations by Runge-Kutta [7, 10].

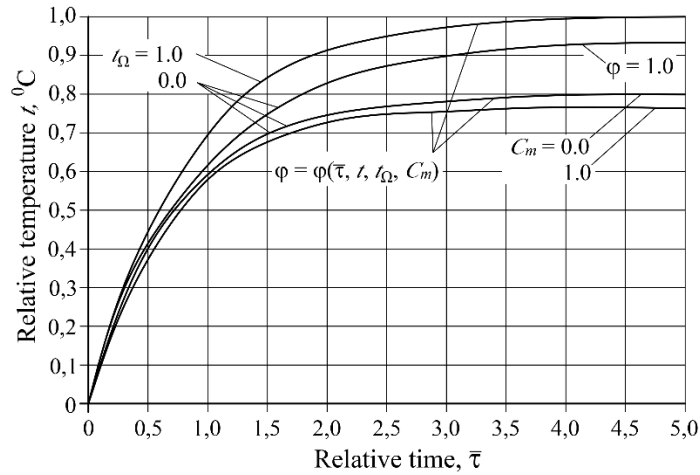


Fig. 8. Dynamics of the average air temperature in the fire source, taking into account humidity and methane content [10]

The analysis of numerical modeling results demonstrated that the dynamics of air temperature, under conditions where density functionally depends on other physical variables $\phi = \phi(\bar{\tau}, t, t_\Omega, C_m)$, significantly differ from the standard solution (40) with constant density ($\phi = 1.0$). In particular, when rock heating is not considered ($t_\Omega = 0$), the temperature values according to the standard solution are always higher. In this case, differences exceed 10% after three cycles of air flow passing through the fire source. As the wall temperature increases, the air at the fire source heats up more intensely, and the temperature dynamics always outpace the standard solution when $t_\Omega \rightarrow 1.0$. The effects of humidity and methane content on temperature are less significant compared to their impact on air density and heat capacity.

This is explained by the fact that the reduction in air density due to the presence of gas impurities is compensated by an increase in its heat capacity. As a result, even with 100% methane content in the air, the temperature decreases by only 5% (curve $C_m = 1.0$ in Fig. 8) compared to the case of air temperature determination without impurities ($C_m = 0.0$). The key parameters affecting air temperature at the fire source are the intensity of heat exchange (value S_f) and the temperature of the excavation walls (t_Ω). The dependence of t on these parameters, across their entire variation range in isolated mine workings, is presented in Fig. 9, taking into account the decrease in air density with increasing temperature.

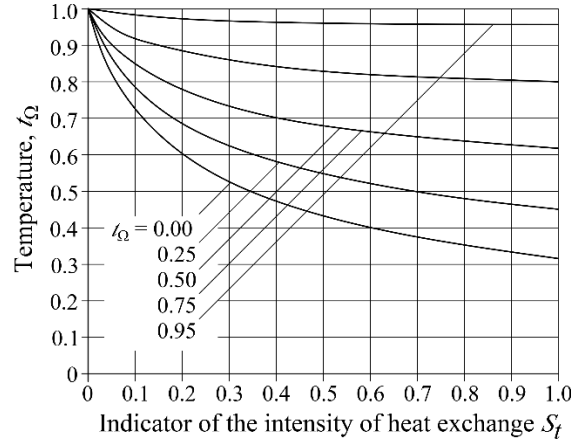


Fig. 9. The dynamics of the average temperature at the fire source depending on the intensity of heat exchange (S_f) and the wall temperature (t_Ω) [4]

Thus, when calculating the average air temperature at the fire source, it becomes necessary to determine the temperature of the excavation walls. In complex fires lasting from several hours to days or even months, the temperature of the surrounding rocks, as well as the airflow, increases. Ignoring the impact of this dynamic on the formation of thermal depression in isolated workings is unacceptable.

In mine heat calculations, the temperature dynamics of rocks are determined using either analytical or numerical solutions of standard heating (cooling) problems for a homogeneous solid body of cylindrical shape with infinite transverse dimensions. In this study on thermal depression in isolated mine workings (IBY), an approximate method is applied, based on the finite volume method by Patankar S. [5]. The problem is formulated under the following assumptions.

The rock mass is represented as a cylindrical layer with a thickness of d_r . The coordinate r , measured in meters, is counted from the axis of the excavation O_x into the depth of the rock. The value of d_r is determined based on the standard cooling curve of a solid body [104] or, with sufficient accuracy, using the following relationship:

$$dr \approx \sqrt{a_n \cdot \tau_g}, \quad (41)$$

where a_n – thermal diffusivity of rocks, m^2/s ; τ_g – burnout time of the fire load or cessation of flaming combustion at the fire source, s.

Only the part of the array within the volume of the fire source is considered. As a result of the simulation of heat conductivity, the heat conductivity of the rock mass is reduced to simulating the heat conductivity of its control volume V_p (in m^3), limited by the cross-sectional cuts of the excavation at $x = 0$ and $x = l$, the walls of the excavation, and the surface of the cylinder with a base radius $r = 0,5D + dr$ [6].

The temperature of the rocks is characterized by the average value T_p , K, within the volume V_p . Under these assumptions, $T_{st} = T_p$.

To determine the temperature of the rocks, a heat balance equation is formulated for the volume V_p . Based on the law of energy conservation, the amount of heat $d\Theta_p$, J, gained (lost) by the control volume V_p during the time interval $d\tau$, s, is equal to the amount of heat transferred (gained) by the air in the volume V_{vo} :

$$\frac{d\Theta_n}{d\tau} = -c_{p_n}\rho_n V_n \frac{dT_n}{d\tau} = \alpha_m \Omega l (T_n - T_{fs}), \quad (42)$$

where c_{p_s} – The heat capacity of rocks, J/(kg·K); ρ_p – Density of rocks, kg/m³.

In dimensionless variables $\bar{\tau}$ and \hat{t} [22]:

$$\hat{t} = \frac{T_n - T_0}{\Delta T_{op}}, \quad (43)$$

equation (42) is then presented in the following form:

$$\begin{aligned} \frac{d\hat{t}}{d\bar{\tau}} &= \Psi \cdot St \cdot (t - \hat{t}), \\ \psi &= \frac{1}{(1 + 2dr/D)^2 - 1} \frac{c_{p_a}\rho_0}{c_{p_n}\rho_n} \end{aligned} \quad (44)$$

where Ψ – the ratio between the heat capacity of the air volume at the fire source and the control volume of rocks.

Further, heat capacity is considered as the amount of thermal energy in Joules that can be received or transferred. Then, the dynamics of air temperature in the fire source, taking into account (37) and (44), are modeled by a system of first-order differential equations.

$$\frac{dt}{d\bar{\tau}} = i - t - \phi \cdot St \cdot (t - \hat{t}), \quad (45)$$

$$\frac{d\hat{t}}{d\bar{\tau}} = \Psi \cdot St \cdot (t - \hat{t}), \quad (46)$$

where $i = i(\bar{\tau})$ is the heat source function, which equals 1 during the burning period of the materials at the fire source τ_g , and 0 after the combustion ceases, during the cooling period of the rocks ($\tau > \tau_g$). The boundary conditions for the system of equations (45), (46) are the values of temperature at the initial moment $\tau = 0$:

$$T_{Bo} = T_n = T_{ct} = T_0 \text{ or } t = \hat{t} = 0, \quad (47)$$

After the combustion ceases, the cooling of the rock volume V_p моделюється тою ж системою рівнянь, is modeled by the same system of equations, but the initial values are taken as the solution obtained at the end of the combustion period τ_g :

$$\tilde{T}_{fs}(0) = T_{fs}(\tau_g); \quad \tilde{T}_n(0) = T_s(\tau_g) \text{ or } \tilde{t}(0) = t(\bar{\tau}_g); \quad \hat{t}_o(0) = \hat{t}(\bar{\tau}_g), \quad (48)$$

where $\bar{\tau}_g = \tau_g/\tau_0$ – is the relative value of the fire burning period; $\tilde{T}_{fs}(\tilde{\tau})$, $\tilde{t}(\tilde{\tau}_o)$ and $\tilde{T}(\tilde{\tau})_s, \tau_o(\tilde{\tau}_o)$ are the temperatures of the air and rocks after the fire source has stopped burning; $\tilde{\tau} = \tau - \tau_g$ is the time since the fire source stopped burning, in seconds; $\tilde{\tau}_o = \bar{\tau} - \bar{\tau}_g$ is the relative time since the fire source stopped burning.-

If we assume that the air density is constant ($\phi = \text{const}$), then the system of equations (45), (46) reduces to a single second-order differential equation

$$t'' + a_1 \cdot t' + a_0 \cdot t = i\psi, \quad (49)$$

where $a_1 = 1 + (\phi + \psi)St$ and $a_0 = \psi St$ – constants.

Together with the boundary conditions (47), (48), equation (49) is supplemented with constraints on the derivatives:

$$\begin{aligned} T'_{fs}(0) &= \Delta T_{op}; & \widetilde{T}'_{fs}(0) &= T'_{bo}(\tau_r) - \Delta T_{op}; \\ \text{or } t'(0) &= i; & \widetilde{t}'(0) &= t'(\bar{\tau}_r) - i. \end{aligned} \quad (50)$$

The temperature of the rocks is related to the air temperature by the following relationships:

$$\hat{t} = t - \frac{1}{\phi St} \cdot (1 - t - t'); \quad \hat{t}_o = \tilde{t} + \frac{1}{\phi St} \cdot (\tilde{t} + t), \quad (51)$$

The solution (49) with boundary conditions (47), (48), and (50) is

$$t = \begin{cases} 1 + t_1 e^{m_1 \bar{\tau}} + t_2 e^{m_2 \bar{\tau}}, & \bar{\tau} \leq \bar{\tau}_c; \\ \tilde{t}_1 e^{m_1 \bar{\tau}} + \tilde{t}_2 e^{m_2 \bar{\tau}}, & \bar{\tau} > \bar{\tau}_c, \end{cases} \quad (52)$$

where $m_{1,2} = -\frac{1}{2}a_1 \cdot (1 \mp \sqrt{1 - 4a_0/a_1^2})$ – the rate indicator of air heating (cooling) in the fire source; $t_1, t_2, \tilde{t}_1, \tilde{t}_2$ – integration constants, determined according to the boundary conditions:

$$t_1 = \frac{1 + m_2}{m_1 - m_2}; \quad t_2 = \frac{1 + m_1}{m_2 - m_1}; \quad \tilde{t}_1 = \frac{\tilde{t}'(0) - m_2 \tilde{t}(0)}{m_1 - m_2}; \quad \tilde{t}_2 = \frac{\tilde{t}'(0) - m_1 \tilde{t}(0)}{m_2 - m_1}, \quad (53)$$

Thus, according to (52) and (53), the dynamics of air temperature in the fire source are determined by the following factors: the heat release power during material combustion in the source (parameter ΔT_{op}); the power of convective heat transfer (parameter $\bar{\tau}$); the thermal resistance of the rock (parameter S_i); and the ratio ψ between the thermal capacity of the gas and solid medium in the volume V_{fs} and V_p , respectively.

Figure 10 presents graphs of the dynamics of air and rock temperature in the fire source, obtained based on equations (52) and (51) with standard air density, and through the numerical solution of the system of equations (45) and (46), considering the dependence of density on temperature. From this, it follows that neglecting the density-temperature relationship in modeling the thermal regime of an isolated ventilation district (IVD) leads to significant errors, especially during the fire development stage and the initial cooling phase of the rocks. However, for predicting rock temperature by the end of the isolation period, the analytical calculation method can be used.

Thermal calculations using the numerical method are valid for any values of the air flow rate that differ from G_0 . When the air supply to the section changes at a known moment in time, it is sufficient to determine the values of the right-hand sides of equations (45) and (46) at $G_0 = \tilde{G}_0$.

One of the calculation scenarios, where the air supply initially decreases continuously following a sinusoidal law and then, according to the same law, returns to its initial value, is presented in Figure 11. In this case, the arbitrarily chosen air supply variation allows for a significant reduction in rock temperature both during the combustion of materials at the fire source and during the cooling period. Consequently, such a ventilation regime in the IVU helps shorten the isolation period of the section. During the calculations, no restrictions were imposed on the nature of air supply variations. In particular, its regulation can be abrupt.

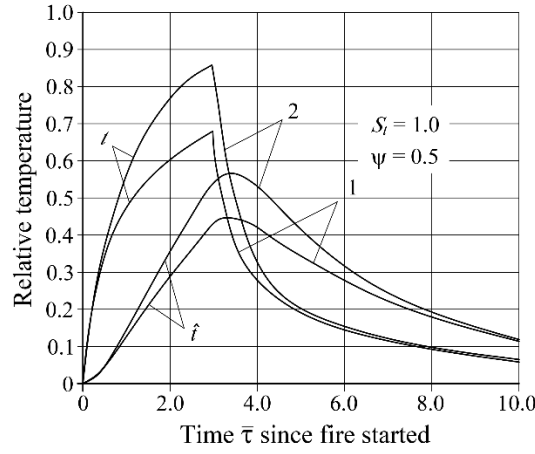


Fig. 10. Dynamics of air and rock temperature according to the analytical (1) and numerical (2) solutions of the problem [10]

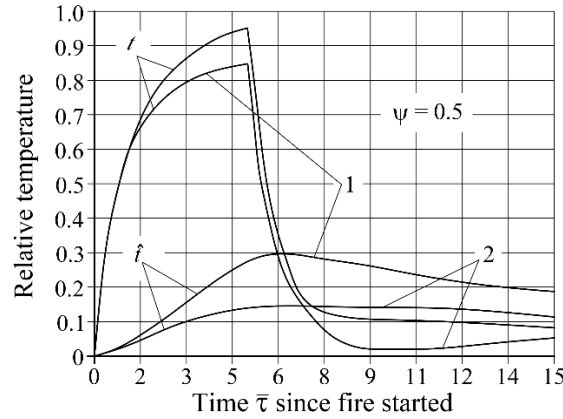


Fig. 11. Dynamics of air and rock temperature in the IVU under constant (1) and variable (2) air supply

The analytical expressions for temperature calculation (40), (51), and (52), derived under the assumption of constant air density, can be used equally with numerical methods. As numerical modeling of temperature dynamics has shown, the application of both methods over a wide range of S_t and ψ numbers allows for obtaining equivalent results, provided that the analytical calculation is performed twice: initially with $\varphi = 1$, and then after adjusting this parameter according to the obtained temperature value.

Furthermore, one of the options for analytical calculation is its sequential execution with a time step close to τ_0 . It should be noted that the objective of this research did not include determining the maximum temperature in the isolated section, which is necessary for assessing the timing of its reopening.

Thus, as a result of the conducted research, a mathematical model of the air and rock temperature dynamics at the fire source throughout the entire isolation period has been developed. This model represents a system of equations (45), (46) with boundary conditions (47), (48), and (50). The application of this model makes it possible to analyze the dependence of air and rock temperatures on the heat release capacity of burning materials, the ventilation parameters of the isolated ventilation unit (IVU), and the thermophysical properties of the surrounding rock. The obtained analytical or numerical expressions for temperature can be used to predict the impact of the IVU ventilation regime on its thermal conditions.

It was established a comprehensive mathematical model describing the dynamics of air and rock temperatures at a fire source within isolated mine workings. The model incorporates key factors such as the heat release rate of combustible materials, convective heat transfer, and thermal interactions with surrounding rock masses. By formulating the problem as a system of first-order differential equations with appropriate boundary conditions, both analytical and numerical solutions can be applied to simulate temperature variations throughout all phases of a mine fire, from ignition to cooling.

Analysis of the model demonstrates that the thermal behavior of the air and surrounding rock is highly sensitive to ventilation conditions, the heat release capacity of materials, and the thermophysical properties of the environment. The results indicate that accounting for temperature-dependent air density, humidity, and methane content is crucial for accurately predicting the evolution of the thermal regime. Neglecting these dependencies, especially during the development stage of a fire and the initial cooling phase, can lead to significant errors in temperature estimations.

The proposed modeling approach provides a practical tool for predicting the thermal conditions of isolated ventilation units in mines under varying airflow regimes. The numerical and analytical solutions allow for the evaluation of different ventilation strategies, including variable air supply, to optimize fire safety and shorten the isolation period. Consequently, the methodology offers a reliable basis for assessing fire risk, planning emergency responses, and managing thermal conditions in mine workings during and after combustion events.

5. Thermal depression of a fire in isolated extraction areas

The magnitude of the thermal depression of a fire can be determined from the equation of airflow movement along the workings of an isolated section. For an elementary air volume $dV = S \cdot dx$, m³, according to the calculation scheme [10], and taking into account the forces acting on it, the equation is formulated as follows:

$$-\rho u \frac{du}{dx} = \frac{dp}{dx} + \frac{\lambda_{tp}}{2 \cdot D_s} \rho u^2 + \left(\frac{d\rho}{dx} \cdot \delta \cdot \cos \beta + \rho \cdot \sin \beta \right) \cdot g, \quad (54)$$

where λ_{tp} – Friction coefficient, which depends on the roughness of the workings' walls [1, 7]:

$$\frac{\lambda_{tp} \rho_0}{D_s} = \frac{\lambda_{tp} \gamma_0 \cdot \Omega}{8 \cdot g \cdot S} = \alpha_{tp} \frac{\Omega}{S}, \quad (55)$$

$D_s = 4S/\Omega$ – diameter of the airflow cross-section, equivalent to a circular cross-section, m;
 α_{tp} – aerodynamic resistance coefficient of mine workings, used in mine aerology, (kg·s²)/m⁷ = 9.81 kg/m³;
 $\delta = 0,5D_s$ – radius of the cross-section of the working, equivalent to a circular cross-section, m.

Unlike the classical equation of air flow motion used in mine aerology [5], equation (54) represents gravitational forces with two components. The first, $p_{x1} = (d\rho/dx) \cdot \delta \cdot g \cdot \cos \beta$, N/m³, represents the pressure forces per unit volume that arise due to changes in air density along the direction of airflow. These forces are formed by the projection of the horizontal component \vec{p}_{cr} of the static pressure vector \vec{p}_{st} onto the x-direction. The second component, $p_{x2} = \rho \cdot g \cdot \sin \beta$, N/m³, is determined by the influence of the vertical component \vec{p}_{ca} of the static pressure \vec{p}_{st} vector in the same direction $p_{st} = \sqrt{p_{xg}^2 + p_{xa}^2}$.

The magnitude of the module p_{st} of the horizontal component of the static pressure vector does not exceed the pressure of an air column with a height equal to half the height of the workings' cross-section. Under constant air density within the workings, this component is absent. Therefore, this pressure is sometimes referred to as local and is usually disregarded due to its insignificance compared to barometric or leveling pressure (the vertical component of static pressure). Under normal ventilation conditions, this assumption is entirely valid, as the air density within the workings remains practically unchanged. However, during a fire, especially in horizontal workings, local pressure plays a crucial role, as it causes the stratification of the airflow into two opposite layers: a warm layer near the roof and a cold layer near the floor. In this case, the magnitude of p_{xh} characterizes the Archimedean forces responsible for the buoyancy of heated air masses within the cross-section of the working. The resulting thermal depression, denoted as h_{tl} , Pa, is referred to as local thermal depression. Meanwhile, the well-known fire-induced thermal depression in emergency ventilation [10, 23], which is caused by the vertical component of static pressure, is denoted by the commonly accepted symbol h_t , Pa, and is referred to as global thermal depression.

In vertical workings, the pressure of the air column in the cross-section degenerates (the average density across the cross-section is considered), and the entire volume of the working transforms into a vertical air column, whose static pressure fully corresponds to the barometric pressure. In this case, local thermal depression is absent.

The content of the other components included in (54) is as follows. The left-hand side of the equation represents the inertial force, under the influence of which the units of the elemental air volume in the working, with mass ρ , acquire an acceleration $u(du/dx)$, m/s². The right-hand side consists of the components of this force per unit volume. These include: the surface hydrodynamic pressure forces in the cross-section of the flow p , Pa; friction forces proportional to the kinetic energy of the flow, with a proportionality coefficient λ_{tr} (or α_{tr}); and gravitational forces in two projections, p_{xg} and p_{xv} .

Equation (54) is considered for each of the four characteristic sections of the ventilation scheme mentioned in [6]. The depression of the working along an arbitrary (not necessarily infinitesimally small) segment l is determined under the following assumptions.

It is assumed that air transfers or mass sources occur only at the boundaries of the segment: $x = 0$ and $x = l$. If a longwall section is considered, it is divided into three distinct parts: the fire source zone Z_o , with a length of l , and the adjacent zones Z_c (on the side of the ventilation stream entering the source) and Z_i (on the side of the stream exiting the source), respectively [6]. Within each section, the air density is characterized by an average value over the volume of the section, which is determined by taking into account the temperature, humidity, and methane content in the air, as described in equations (18) and (19).

Due to the adopted assumptions, the occurrence of local thermal depression is possible only in zones Z_c , Z_i , and in the sections of the roadways. In the fire source, due to the centralization of temperature and air density over its volume, only thermal depression h_t is possible. In the adopted ventilation connection scheme of the IVD (Fig. 4), local thermal sources are introduced into branches 4, 2, 6, and 7, while thermal depression (the global source of airflow) is modeled in branch 2 of the longwall, where the fire source is located. To determine the magnitudes of these airflow sources, equation (54) is solved through the following transformations.

Air is considered an incompressible gas in the hydrodynamic sense (i.e., its density does not depend on pressure within the velocity range of mine ventilation airflows) but thermally deformable. These conditions are modeled by the continuity equation and the density-temperature dependencies obtained in [2, 6, 10, etc.]:

$$\rho u = \rho_0 u_0 = \text{const}; \quad f_\rho = \frac{\rho}{\rho_0} = 0,758 \cdot (1 - 0,446 \cdot C_m) \frac{T_0}{T}, \quad (56)$$

where ρ_0 , u_0 , T_0 – the density, velocity, and temperature of the air at the inlet cross-section of the airflow $x = 0$, taking into account humidity and methane content.

According to (56), equation (54) is presented in the following form:

$$\rho_0 u_0^2 \frac{1}{f_\rho^2} \frac{df_\rho}{dx} = \frac{dp}{dx} + \alpha_{tr} \frac{\Omega}{S} \frac{1}{f_\rho} u_0^2 + \rho_0 g \left[\delta \frac{df_\rho}{dx} \cos \beta + f_\rho \sin \beta \right], \quad (57)$$

then, as a result of integrating equation (57) with respect to x over the range $x \in [0, l]$, the following equation is obtained (analogous to the Bernoulli equation):

$$h = p_0 - p_l = \left[\frac{\rho_0}{RS^2} \left(\frac{1}{f_{\rho l}} - 1 \right) + \tilde{f}_\rho \right] RQ_0^2 + \rho_0 g [\delta(1 - f_{\rho l}) \cos \beta + l(1 - \bar{f}_\rho) \sin \beta], \quad (58)$$

$$\tilde{f}_\rho = \frac{1}{l} \int_0^l \frac{dx}{f_\rho}, \quad \bar{f}_\rho = \frac{1}{l} \int_0^l f_\rho dx, \quad R = \alpha_{tr} \frac{\Omega l}{S^3}$$

where indexes «0» and «l» – indicate the values of the variables at the initial and final cross-sections of the section of the excavation, respectively; \tilde{f}_ρ – the harmonic mean value of the density function over the section of the excavation.;

\bar{f}_ρ – the average value of the density function over the section of the excavation.; R – aerodynamic resistance of the section of the excavation, $\text{Pa} \cdot \text{s}^2/\text{m}^6 = \text{kg}/\text{m}^7$; $\rho_0 g l \sin \beta$ – increase in static (barometric) pressure along the section of the excavation, Pa.

The analytical expressions that appear on the right-hand side of (58) have the following physical meaning:

$$k_u = \xi \left(\frac{1}{f_{\rho l}} - 1 \right), \quad (59)$$

- the resistance coefficient, proportional to the inertial forces of the moving air flow;

$\xi = \rho_0/RS^2$ – the proportionality coefficient; \tilde{f}_ρ – the coefficient that allows for accounting the change in aerodynamic resistance due to the expansion of air volumes when heated;

$$k_m = k_i + \tilde{f}_\rho, \quad (60)$$

- the thermal resistance coefficient, caused by the change in thermophysical properties of air after the onset of a fire;

$$h_{mi} = \rho_0 g \delta (1 - f_{\rho l}) \cos \beta; \quad h_m = \rho_0 g l (1 - \tilde{f}_\rho) \sin \beta, \quad (61)$$

- fire thermal depression, both local and global, Pa.

The analytical expressions for thermal resistance (59), (60), and the thermal thrust sources (61) include the value of air flow density $\rho_0 \neq \rho_n$ at the initial section of the excavation. For sections of the ventilation scheme (zone Z_c) approaching the fire source, the temperature at the initial section of the air flows is lower than at the final section, where $\rho < \rho_0$. Therefore, the coefficient k_i is positive, which physically corresponds to the fact that the aerodynamic resistance of the section increases due to the inertial forces. For air flows (zone Z_i) exiting from the fire source, the opposite tendency is observed: as the distance from the source increases, the flow velocity decreases (density increases) according to the continuity equation, thus reducing the frictional forces.

The second component of the thermal resistance coefficient \tilde{f}_ρ , in the case of warm air entering the section, is always greater than 1, since the expansion of the air volumes, with constant mass, contributes to an increase in aerodynamic resistance to their motion.

Thus, the aerodynamic resistance of the excavation section after the onset of a fire can either increase or decrease along the path of the air flow. The degree of these changes depends on the temperature, air content, and the ratio between the values of k_i and \tilde{f}_ρ , which respectively characterize the inertial forces and thermal expansion of the air volumes.

The value of the local thermal depression h_{li} , according to (61), has a positive value for air flows exiting from the fire source ($f_{\rho l} < 1$) and a negative value for those entering the source. This condition models the fact that the local thermal depression in zone Z_c , under the roof of the excavation, and in zone Z_i , near the ground, is directed against the depression of the fan. On the other hand, the air flow near the ground of the excavation, from the fresh ventilation stream, and under the roof, from the exit side, is influenced by both the fan and the local thermal depression. Therefore, the obtained analytical expression for local thermal depression corresponds to the processes of local recirculation of fire gases (natural convection) occurring in the zones adjacent to the fire source [2, 10, 16, 17, 18].

Expression (61) for the global thermal depression h_t is valid only for the case of downward ventilation of the section, where gravitational forces increase with depth, since the integration in (57) was performed without considering the sign of the projections of these forces on the Ox axis. To apply this formula for any type of ventilation, the increase in depth along the section $\Delta z = l \sin \beta$ is expressed through the height markings at its ends z , in meters, by the well-known relationship: $\Delta z = l \sin \beta = (z_0 - z_i)$. As a result, the value of h_t is positive for downward ventilation ($\tilde{f}_\rho < 1$) and negative for upward ventilation ($\tilde{f}_\rho > 1$) of the section.

In the accepted definitions (59-61), expression (58) for the depression of the section of the excavation is presented in the form of:

$$h = k_m R Q_0^2 + h_{mi} + h_m, \quad (62)$$

As a result, to model the airflow distribution in the VET at a given moment in time, it is necessary to calculate the average air temperature at specific sections of the ventilation scheme, and then determine the values of the density function corresponding to this temperature.

Analytical and numerical methods for calculating the values of the average temperature, which are necessary for determining k_i and h_t at the source section, are presented in [2, 10, 27]. The average air temperature at the sections adjacent to the source can be determined based on the results already obtained. The heat balance equation for the zones Z_c and Z_i , at a given moment in time, is represented by the iterative dependence on the time step τ_0 as follows:

$$c_{pa}\rho_0 V_z \frac{(T_z - T_n)}{\tau_0} = c_{pa}G_0(T^* - T_n) + \alpha_m \Omega l(T_0 - T_z), \quad (63)$$

where T_z – the average, over the volume of the zone $V_z = l_z \Omega_z S_z$, air temperature; T_n – temperature in the zone at the previous time step; $T^* = T_{fs}(\tau^*)$ – average air temperature at the fire source at the current moment in time τ^* .

In formulating this equation, the assumption was made that the average temperature of the air ascending from the fire source does not depend on its dynamics in the region downstream of the gas flow [2], and the choice of the time interval τ_0 allows for accounting the non-stationarity of heat transfer in the zones adjacent to the fire source.

The variables $\xi = x/l_z$ and $t_z = (T_z - T_0)/\Delta T_{op}$ (63) transform into the following form:

$$t_z - t_n = t^* - t_n - St_z \cdot t_z, \quad (64)$$

where $St_z = \alpha_{tz} \Omega_z l_z / c_{pa} G_0$ – Stanton number for the zones Z_c , Z_i , and the variables t with indices represent the relative values of the variables T with the same indices.

It follows from equation (64) that

$$t_z = \frac{t^*}{1 + St_z}, \quad (65)$$

The obtained analytical expression for temperature through the cooling rate exponent S_t does not contradict the well-known formulas of thermal calculations [2, 10, 17, 23].

According to equation (65), the average air temperature in the zones adjacent to the fire source, given that their volumes are approximately equal to the volume of the fire source $V_z \approx V_{vo}$, cannot exceed the value $(T_{vo} - T_0)/(1 + St_z)$. The values of t_z are determined for the moment in time when the temperature at the fire source T_{vo} is specified. In the general case, $V_z \neq V_{vo}$, and the Stanton numbers St for zones Z_c and Z_i differ from the value for the fire source volume. Therefore, according to equation (65), the average temperature in zones Z_c and Z_i is inversely proportional to their sizes, which aligns with the physical meaning of the problem's solution.

The calculation of temperature values T_z can be performed using numerical methods based on the system of equations (45) and (46), similar to the calculation of T_{vo} . However, the right-hand sides of the equations are determined at $i = 0$ with $\Delta T_{op} = T_{vo} - T_0$, meaning that the calculation is conducted without a heat source and with the incoming air temperature equal to the average air temperature in the fire source zone.

As a result, to calculate the thermal regime of the IVU, it is sufficient to determine the temperature dynamics at the fire source, and using similarity coefficients $k_a = 1/(1 + St_z)$ or by numerical methods – the temperature dynamics in the adjacent zones.

For the purpose of mathematical modeling of the relationship between thermal sources of draft, thermal resistance, and aerodynamic parameters of the IVU, the physical variables included in equation (58) are represented as relative values by dividing both sides of the equation by the characteristic depression $h_H = RQ_H^2$, Pa (Q_H – airflow rate in the ventilation scheme section before the fire occurrence, m^3/s):

$$\bar{h} = k_m q^2 + Fr(\bar{h}_{tl} + \bar{h}_m), \quad (66)$$

where $\bar{h} = (p_0 - p_l)/RQ_H^2$ – the relative magnitude of the depression of the ventilation scheme section, which can be expressed through parameters h_{sp} , Pa and b_{sp} , kg/m^7 , the characteristics of the fan, reduced to the section of the ventilation scheme, are expressed as follows:

$$\bar{h} = Ej - \bar{r} \cdot q^2, \quad (67)$$

where $Ej = h_{sp}/RQ_H^2$ – Euler number for mining workings conditions; $\bar{r} = b_{sp}/R$ – the relative value of the

conditional aerodynamic resistance of the mine ventilation network, b_{kp} , to which the considered section of the IVU ventilation scheme is connected.; $q = Q_0/Q_n$ – the ratio of the air flow rate in the section to its value before the fire occurred; $Fr = (\rho_0 g / R Q_0^2) \Delta z$ – Froude number for the conditions of mine workings in underground mines; $\bar{h}_{tl} = (\delta \cos \beta / \Delta z)(1 - \tilde{f}_\rho)$ – relative magnitude of local thermal depression; $\bar{h}_g = 1 - \bar{f}_\rho$ – relative magnitude of global thermal depression.

Before the fire occurs, $\tilde{f}_\rho = \bar{f}_\rho = 1$; $k_m = 1$; $\bar{h}_m = \bar{h}_{tl} = 0$, and the relative depression of the section is equal to one. Thus, the impact of fire thermal factors – such as the thermal resistance coefficient and thermal depression – on the ventilation of the isolated extraction area (IEA) is characterized by the degree of deviation of \bar{h} from 1. Therefore, the value of $\Delta_m = (\bar{h} - 1) \cdot 100, \%$; which represents the positive, negative, or zero increment of the section's depression within the ventilation scheme (expressed as a percentage of the depression of the same section before the fire), is justifiably referred to as the thermal depression of the section. This distinguishes it from the commonly accepted value h_t , which is only one of the components of this depression.

Based on the conducted study of thermal depression in specific sections of the ventilation scheme of an isolated extraction area (IEA), it has been determined that predicting the reverse impact of fire thermal factors on the ventilation regime should be carried out based on the following functional dependence of air flow rate on thermal parameters:

$$q \cdot |q| = \frac{1}{k_m + \tilde{r}} [Ej - Fr(\bar{h}_{tl} + \bar{h}_m)], \quad (68)$$

Thus, the presented analytical expressions for air temperature in terms of the aerodynamic parameters of the ventilation scheme section, as well as the dependence of air consumption on the thermal parameters of this section, make it possible to determine both the effect of ventilation mode on the thermal regime of the isolated working unit (IWU) and the reverse impact of fire-related thermal factors on air consumption. By applying dimensionless physical parameter complexes Ej , St , Fr , ψ , k_t , h_{tl} , h_t , t , \hat{t} , τ_0 , mathematical modeling of the interaction between fire thermal energy and the mechanical energy of ventilation systems becomes feasible for various scenarios of isolated mining sections. These scenarios differ in geometric dimensions, thermophysical properties of rocks, and isolation periods, while also considering humidity and methane content in the air. The results of these studies were used to develop a methodology for calculating the thermal regime of IWU depending on the ventilation methods applied to the fire source.

6. Forecast of maximum temperature dynamics at the fire source

During the application of various ventilation control methods to the fire source, the velocity of the ventilation airflow may change both in magnitude and direction. The duration of the fire isolation period is measured in months. As a result of inertization, the composition and physical properties of the gas environment within the isolated volume undergo significant changes [28-30]. It is worth noting that particularly interesting results were obtained by the authors of studies [29-32] in modeling the processes of heating and ignition of coal particles in methane-air mixtures near the fire source, as well as in their application for methane emission management during the mitigation of methane-air explosion consequences in mines. These methods were tested during the shaft isolation process in the course of the accident elimination at the "Novodonetska" mine [30-31]. Predicting the impact of all these factors on the timeframe for accident mitigation is only possible through mathematical modeling using modern computational tools.

The maximum temperature is considered to be the surface temperature of the rock mass in the combustion zone of the fire. The temperature calculation is performed using a numerical method by solving the system of equations for convective-diffusive heat transfer in both the gaseous and solid media. The initial data for the calculations include:

T_{0a} and T_{0r} – air and rock temperature before the fire outbreak, °C;

G – mass flow rate of the gas stream through the fire source, kg/s;

L – total length of workings in the isolated section, m;

L_0 – distance to the fire source from bulkhead P_1 on the side of the incoming ventilation stream, m;

τ – specified forecast time, in hours or days;

τ_n – the duration of the period from isolation to the start of the ventilation influence method, in hours or days;

τ_c – the duration of the free development period of the fire, in hours or days;

τ_p – the duration of the period of application of the ventilation impact method, in hours or days;

S – the cross-sectional area of the workings in the isolated section, m²;

The gas flow rate may be a function of time, depending on the presence of impurities in the air or representing the flow rate of inert gases being supplied. The cross-section of the workings is defined for each characteristic section: the haulage drift, the longwall, and the ventilation drift. Figure 12 presents the computational scheme of the isolated section.

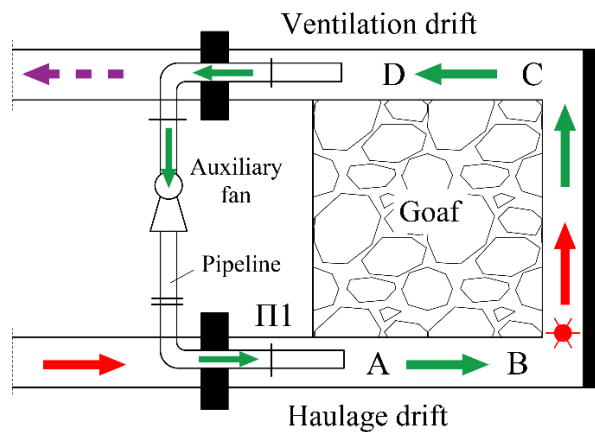


Fig. 12. Computational scheme of the isolated section

At the time step $(n + 1)$, the calculation is performed using the following formulas:

$$t_j^{n+1} = (1 + R_e + \frac{S_t}{1 + N_u})^{-1} \left[R_e \cdot t_{j-1}^{n+1} + \hat{F}_x \cdot (t_{j+1}^n + t_{j-1}^n) + (1 - \hat{F}_x) \cdot t_j^n + \frac{S_t}{1 + N_u} t_{\Omega j}^{n+1} \right], \quad (71)$$

$$t_{ij}^{n+1} = F_x \cdot (t_{i,j+1}^n + t_{i,j-1}^n) + (1 - 2 \cdot F_x - 2 \cdot F_r) \cdot t_{ij}^n + F_r \cdot (t_{i+1,j}^n + t_{i-1,j}^n), \quad (72)$$

$$t_{\Omega j}^{n+1} = \frac{\hat{t}_{1j}^{n+1} + N_u \cdot t_j^{n+1}}{1 + N_u}, \quad (73)$$

де $F_x = \frac{a \cdot \Delta \tau}{\Delta x^2}$, $\hat{F}_x = \frac{\hat{a} \cdot \Delta \tau}{\Delta x^2}$, $F_r = \frac{a \cdot \Delta \tau}{\Delta r^2}$, $\hat{F}_r = \frac{\hat{a} \cdot \Delta \tau}{\Delta r^2}$ – Grid Fourier numbers

$R_e = \frac{u_0 \cdot \Delta \tau}{\Delta x}$, $N_u = \frac{\alpha \cdot \Delta r}{\lambda}$ and $S_t = \frac{\alpha \cdot \Omega \cdot \Delta \tau}{\rho_0 \cdot c_p \cdot S}$ – discrete Reynolds, Nusselt, and Stanton numbers; $t_{ij} = \frac{T_{ij} - T_{0g}}{\Delta T_{op}}$, $\hat{t}_{ij} = \frac{\hat{T}_{ij} - T_{0n}}{\Delta T_{op}}$, $t_{\Omega j} = \frac{T_{\Omega j} - T_{0a}}{\Delta T_{op}}$ – Relative temperature values of the gas environment at the nodal points i, j of the computational grid, as well as of the rock mass and the surface of the mining excavation walls; T_{ij} , \hat{T}_{ij} , $T_{\Omega j}$ – current temperature of the gas environment, rock mass, and excavation walls, K; ΔT_{op} – maximum temperature increase at the fire source, K; $\Delta \tau$ and Δx , Δr – calculation grid steps in time and direction: along the mine workings, into the depth of the rock mass, s and m, respectively; a and \hat{a} – thermal diffusivity of the gas medium and rock mass, m^2/s ; u_0 – characteristic velocity of the gas flow (at the inlet of the ventilation stream into the section), m/s; α – heat transfer coefficient between the gas flow and the rock mass, $W/(m^2 \cdot s)$; Ω – perimeter of the mine workings: $\Omega \approx 2\sqrt{\pi S}$, m; ρ_0 – density of the gas medium, kg/m^3 ; c_p – heat capacity of the gas medium, $J/(kg \cdot K)$. Considering the one-dimensional formulation of the problem for the temperature of the gas medium, the heat source function was specified at the boundary between the air and the rock mass with corresponding temperature values within the combustion zone.

Figure 13 presents the results of modeling the temperature of the rock mass and the gas environment over the course of one month from the onset of the fire. The graph illustrates how heat distribution evolves within the isolated section, considering both conductive and convective heat transfer processes. These results provide insights into the long-term thermal behavior of the affected area, which is crucial for assessing ventilation strategies and fire suppression methods.

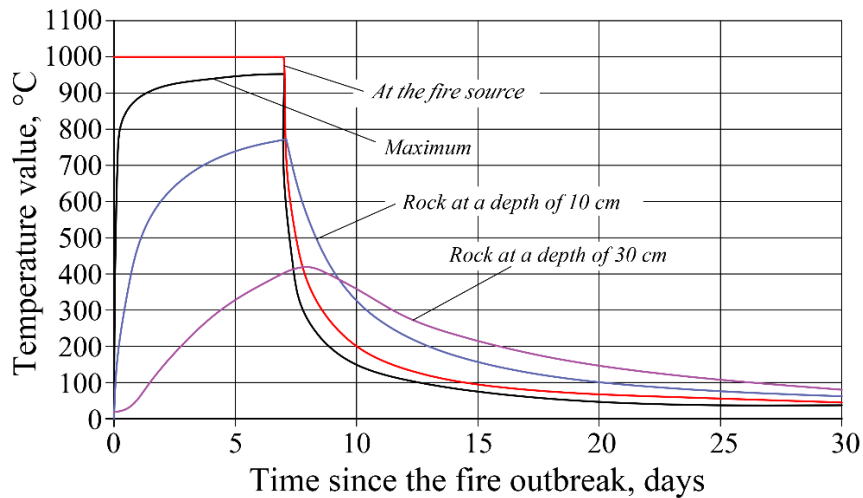


Fig. 13. Results of the monthly forecast of the thermal regime of the isolated section

The proposed models for forecasting maximum temperature dynamics at the fire source are applicable across a range of ventilation conditions commonly encountered in mine operations. Specifically, the models remain reliable when the airflow velocity through the isolated section varies between 0.5 and 5.0 m/s, reflecting typical natural and controlled ventilation scenarios. They can accommodate changes in both the magnitude and direction of the airflow, as well as variations in gas composition due to the presence of methane, humidity, or inertization processes. However, the accuracy of predictions decreases if extreme ventilation conditions occur – for example, very low airflow rates that significantly reduce convective heat transfer, or abrupt flow reversals that create localized turbulence not captured by the one-dimensional formulation. Within the defined limits, the models provide a robust tool for assessing the thermal regime, optimizing ventilation strategies, and supporting fire mitigation measures over isolation periods ranging from hours to several months.

During the modeling process, data from a real mine fire were used. Two days after the fire started, the longwall and sections of the haulage and ventilation roadways, each 40 meters long, were isolated. Then, over the next five days, work was carried out to install equipment for recirculation. The recirculation process was implemented on the seventh day.

Since each method of ventilation influence is characterized by a specific dynamic of mass flow rate, it is possible to predict the impact of any of them on the thermal regime of the isolated section. This allows for a comparative assessment of the effectiveness of each method and the selection of the optimal one based on the thermal factor.

7. The methodology for forecasting temperature in the fire source

During fire extinguishing operations in coal mines and assessing the development process of fires in mines, great importance is placed on forecasting the temperature indicators in the fire's center. These indicators are crucial for the actual evaluation of the environment in the fire's extinguishing area, as they serve as control parameters for determining the cooling of the rock mass and, ultimately, indirectly assess the extinguishment of the fire. Therefore, the issues related to temperature evaluation are highly relevant. In this article, the authors attempt to use known dependencies to prepare a justification for forecasting the temperature in the fire zone, with a view to further developing new and improving existing methods. Recently, many studies have been conducted by various authors on this topic. Without diminishing the results and merits of other authors, we will reference only one of the comprehensive works [2, 10].

As is known, when considering the heating and cooling of the rock mass, the anisotropy of its thermophysical properties is taken into account, as these properties are not uniform in different directions, both along the coal seams and the host rocks, as well as along the cleat or perpendicular to it. The processes in the rock mass are also significantly influenced by the type of combustion source: point, linear, or volumetric. For instance, with a point combustion source (such as methane or coal in the mined space), regardless of the duration of combustion, it is preferable, if possible, to consider the cooling process of the rock mass in three dimensions, whereas with a linear combustion source (such as wood or conveyor belts in mining operations), it should be considered in two or one dimension, depending on the specific emergency situation.

As noted [10], the cooling process of the rock mass begins once combustion ceases (flaming combustion when the oxygen concentration is below 10%, smoldering combustion when the oxygen concentration is 2-3%). The size of the fire's center, and therefore the type of combustion source, is determined based on reconnaissance data, laboratory analysis of air samples, etc. The duration of combustion is established from the moment the fire begins until its extinguishment, whether through active firefighting methods or by isolation techniques using ventilation influence: through pressure equalization, recirculation of fire gases, or multiple local reversals of ventilation streams.

The total amount of heat released by the fire into the rock mass is determined using well-known methods, based on data on air flow or its escape through an isolated section, as well as data from the analysis of the air composition at the outgoing ventilation stream. Based on the above, we will consider the following methodology. It will examine the cooling process of the rock mass with anisotropic thermophysical properties in an n -dimensional space, described by the equation presented below [10, 12, 33]:

$$\frac{\partial T}{\partial \tau} = \sum_{i=1}^n a_i \frac{\partial^2 T}{\partial x_i^2}, \quad (74)$$

where T – rocks temperature, K;

a_i – thermal conductivity coefficient of rocks depending on the direction, m^2/s ;

τ – time from the moment of fire cessation, s;

x_i – spatial coordinate, m;

n – загальне число взаємно перпендикулярних напрямків або координат ($i = 1, 2, \dots, n$).

In the case of three directions ($n = 3$) in an isotropic medium ($a_1 = a_2 = a_3 = a$), we obtain the commonly used heat conduction equation:

$$\frac{\partial T}{\partial \tau} = a \left(\frac{\partial^2 T}{\partial x_1^2} + \frac{\partial^2 T}{\partial x_2^2} + \frac{\partial^2 T}{\partial x_3^2} \right), \quad (75)$$

which, similar to (74), can be represented as:

$$\frac{\partial T}{\partial \tau} = a \sum_{i=1}^3 a_i \frac{\partial^2 T}{\partial x_i^2}, \quad (76)$$

The solution to equation (74), without specifying boundary conditions at this stage, will be sought using the source function [2]. Thus, the particular solution to equation (74) will take the form:

$$T = \frac{A}{\tau^{n/2}} \exp \left[- \sum_{i=1}^n \frac{(x_i - x_i^0)^2}{4a_i\tau} \right], \quad (77)$$

where x_i^0 – the distance from the origin along the i -th direction to the epicenter of the combustion zone, m. A – the constant to be determined., $K/s^{n/2}$.

After a series of transformations and considering the fire power, we obtain the solution of equation (74) in the following form:

$$T = \frac{T_1 - T_0}{(4\pi\tau)^{n/2}} \prod_{i=1}^n \left(\frac{\ell_i}{a_i^{1/2}} \right) \exp \left[- \sum_{i=1}^n \frac{(x_i - x_i^0)^2}{4a_i\tau} \right], \quad (78)$$

T_1 – Temperature in the fire cell, K;

T_0 – Temperature of the surrounding rocks, K;

\prod – Product symbol;

λ_i – Dimensions of the fire cell along the coordinates, m.

Let's check whether the amount of heat given by the fire cell to the mass is conserved in the anisotropic space. To do this, we will integrate the solution (5) in all directions for x_i from $-\infty$ to $+\infty$, and we will obtain:

$$\int_{-\infty}^{\infty} T dx_1 dx_2 \dots dx_n = (T_1 - T_0) \prod_{i=1}^n \ell_i \prod_{i=1}^n \frac{1}{2\sqrt{\pi a_i \tau}} \int_{-\infty}^{\infty} \exp \left[- \frac{(x_i - x_i^0)^2}{4a_i\tau} \right] dx_i, \quad (79)$$

Since all the integrals on the right-hand side of equation (79) equal one under the product symbol \prod , the amount of heat given by the fire cell is conserved in the anisotropic space and equals the initial value:

$$\int_{-\infty}^{\infty} T dx_1 dx_2 \dots dx_n = (T_1 - T_0) \prod_{i=1}^n \ell_i, \quad (80)$$

Let's show that by using the fundamental solution (78), we can combine them to satisfy not only equation (74) but also the boundary conditions. Next, we consider the heat conduction problem in a half-space, where the coordinate x_1 changes from 0 to $+\infty$. Then, at the boundary (when $x_1=0$), certain conditions can be specified. These conditions will be:

- Equality of temperature on the array walls and in the surrounding air:

$$T|_{x_1=0} = T_0, \quad (81)$$

- Thermal insulation of the rockmass

$$\left. \frac{\partial T}{\partial x_1} \right| = 0, \quad (82)$$

- Equality of heat fluxes at the contact between the array and the air:

$$\lambda_1 \left. \frac{\partial T}{\partial x_1} \right|_{x_1=0} = \alpha_1 (T|_{x_1=0} - T_0), \quad (83)$$

where λ_1 – thermal conductivity coefficient of the rock mass in the direction of the x_1 coordinate, $W/(m \cdot K)$;

α_1 – heat transfer coefficient between air and the rock mass, $W/(m^2 \cdot K)$;

T_0 - air temperature in contact with the rock mass, K.

Obviously, boundary condition (83) is the most general. Thus, in the case of intensive heat exchange between air and the rock mass ($\alpha_i \rightarrow \infty$), we obtain the first boundary condition (81), and in the absence of heat exchange ($\alpha_i = 0$) – the second boundary condition (82).

Let us consider the problem of heating and cooling of the rock mass first for one dimension ($n = 1$), with a subsequent generalization of the obtained results to an n-dimensional space.

During combustion, the air temperature T_p is assumed to be equal to the combustion temperature T_1 , and instead of condition (81), we have:

$$T(0, \tau) = T_1, \quad (84)$$

The initial temperature of the rock mass or the rocks surrounding the air is assumed to be:

$$T(x_1, 0) = T_0, \quad (85)$$

The solution of equation (74) for $n = 1$ and boundary conditions (84) and (87) is given by [5]:

$$T(x_1, \tau) = T_1 - (T_1 - T_0)\Phi\left(\frac{x_1}{2\sqrt{a_1\tau}}\right), \quad (86)$$

where the function Φ represents the probability integral:

$$\Phi\left(\frac{x_1}{2\sqrt{a_1\tau}}\right) = \frac{2}{\sqrt{\pi}} \int_0^{\frac{x_1}{2\sqrt{a_1\tau}}} e^{-r^2} dr, \quad (87)$$

After the combustion ends, the temperature distribution in the rock is described by expression (86) at $\tau = \tau_g$:

$$f(x_1) = T(x_1, \tau_g) = T_1 - (T_1 - T_0)\Phi\left(\frac{x_1}{2\sqrt{a_1\tau_g}}\right), \quad (88)$$

This temperature distribution in the rock mass is the initial condition for solving equation (74) for the cooling period of the rock mass for $n = 1$: $T(x_1, 0) = f(x_1)$.

In practice, the cooling of rock mass is of particular interest not at the initial but rather at the subsequent and final stages of fire extinction, so it is important to know not the initial temperature distribution after combustion, but the total amount of heat absorbed by the rock mass.

The total amount of heat accumulated during the combustion time $\tau = \tau_g$ with temperature $(T_1 - T_0)$ over a section of length:

$$\ell_1 = 2\sqrt{\frac{a_1\tau_g}{\pi}}, \quad (89)$$

Let us apply a heat impulse equal to Gg at the center of this section:

$$x_1^0 = 2\sqrt{\frac{a_1\tau_g}{\pi}}, \quad (90)$$

After a series of transformations, considering that for maximum heat exchange ($\alpha_i \rightarrow \infty$), we have from (83) the condition (81) and $B = -1$, and for no heat exchange ($\alpha_i = 0$), we have from (83) the condition (82) and $B = 1$, we obtain:

$$T(x_1, \tau) = T_0 + \frac{(T_1 - T_0)\ell_1}{2\sqrt{\pi a_1\tau}} \left\{ \exp\left(-\frac{(x_1 - x_1^0)^2}{4a_1\tau}\right) + B \cdot \exp\left(-\frac{(x_1 + x_1^0)^2}{4a_1\tau}\right) \right\}, \quad (91)$$

where B is the coefficient that defines the heat exchange conditions between air and rock mass.

Let us verify how accurately solution (91) describes the temperature distribution in the rock mass during its cooling. For this, we use the known solution of equation (74) for $n = 1$, given the initial condition of heating the rock mass to a depth ℓ_1 :

$$\begin{aligned} T(x_1, 0) &= T_1, & \text{if } 0 \leq x \leq \ell_1 \\ T(x_1, 0) &= T_0, & \text{if } x > \ell_1 \end{aligned} \quad (92)$$

The solution of equation (74) with initial condition (92) and boundary condition (82) is [5]:

$$T(x_1, \tau) = T_0 + \frac{T_1 - T_0}{2} \left[\Phi \left(\frac{x_1 + \ell_1}{2\sqrt{a_1\tau}} \right) - \Phi \left(\frac{x_1 - \ell_1}{2\sqrt{a_1\tau}} \right) \right], \quad (93)$$

Comparing two solutions – (91) for $B = 1$ and (93) using data from Table 1 – we conclude that formula (97) describes the cooling process of the rock mass with a heat source concentrated in the center of the section $x_i^0 = 0,5\ell_1$ with sufficient accuracy (error not exceeding 5%).

Dynamics of rock mass cooling at its contact with air

Table 1.

$\sqrt{a_1\tau}/\ell_1$	0,5	0,75	1,0	1,5	2,0	2,5	Calculation data according to formulas
$\frac{T - T_0}{T_1 - T_0}$	0,843	0,650	0,520	0,359	0,276	0,223	(93)
	0,879	0,673	0,530	0,366	0,278	0,223	(91) for $B = 1$

From Table 1, it follows that, starting from a certain cooling time $\tau \geq \ell_1^2/4a_1$, the calculation data obtained using formula (91) with $B = 1$ practically do not differ from those derived using formula (93). This allows the method of heat-emission sources to be employed for predicting the temperature at the fire center.

Let us now extend the obtained results to the case of an n -dimensional anisotropic space. If heat propagation occurs only in one direction, the boundary conditions (81)–(83) are applied at the point $x_1 = 0$. When two coordinates, x_1 and x_2 , are defined, the heat spreads over a plane, and the boundary conditions are imposed along the line $x_1 = 0$. Finally, for three-dimensional space, the boundary conditions are applied over the plane $x_1 = 0$. Using solution (78) of equation (74), we satisfy conditions (81)–(83) and obtain a solution to equation (74) analogous to (91), valid for n -dimensional anisotropic space. In the special case where $n = 1$, expression

$$\exp\left(-\frac{x_1 x_1^0}{a_1 \tau}\right) \cdot \exp\left(-\frac{(x_1 - x_1^0)^2}{4a_1 \tau}\right) = \exp\left(-\frac{(x_1 + x_1^0)^2}{4a_1 \tau}\right)$$

can be transformed into a more convenient form:

$$T = T_0 + \frac{T_1 - T_0}{(4\pi\tau)^{n/2}} \prod_{i=1}^n \left(\frac{\ell_i}{a_i^{1/2}} \right) \left[1 + B \cdot \exp\left(-\frac{x_1 x_1^0}{a_1 \tau}\right) \cdot \exp\left(-\sum_{i=1}^n \frac{(x_i - x_i^0)^2}{4a_i \tau}\right) \right], \quad (94)$$

It is known that, at the epicenter of heat release – i.e., at the point with coordinates $x_i = x_i^0$ – the temperature of the rocks during their cooling can be determined using equation (94), which yields:

$$T = T_0 + \frac{T_1 - T_0}{(4\pi\tau)^{n/2}} \prod_{i=1}^n \left(\frac{\ell_i}{a_i^{1/2}} \right) \left[1 + B \cdot \exp \left(-\frac{x_1^{02}}{a_1\tau} \right) \right], \quad (95)$$

The length of the burning zone along the coordinate axis x_i as in (89), equals:

$$\ell_i = 2 \sqrt{\frac{a_i \tau_g}{\pi}}, \quad (96)$$

Thus, formula (95), considering (90), takes the form:

$$T = T_0 + \frac{T_1 - T_0}{(4\pi\tau)^{n/2}} \prod_{i=1}^n \left(\frac{\ell_i}{a_i^{1/2}} \right) \left[1 + B \cdot \exp \left(-\frac{x_1^{02}}{a_1\tau} \right) \right], \quad (97)$$

According to references [2, 40], the heat transfer coefficient α depends on the Reynolds number, $Re = ud/\nu$, where u is the air velocity at its contact with the rockmass (m/s), d is the equivalent diameter of the excavation or actively ventilated zone of the mined-out area (m), and ν is the kinematic viscosity of air (m²/s).

Typically, instead of air velocity, data on air flow rate through the excavation or leakage into the goaf are used (Q , m³/s), and instead of diameter, the ratio of cross-sectional area (S , m²) to the perimeter (P) of the ventilation stream is applied, i.e., $d = 4S/P$. Thus, the dependence of the coefficient B on the Reynolds number resembles its dependence on the ratio Q/P , leading to:

$$B = f(Q/P), \quad (98)$$

The comparison between the calculation data from formulas (94) and (97) for $n = 1$ and the results of numerical experiments modeling thermal processes using equation (74) with condition (83) showed that the relationship (98) takes the form:

$$B = \frac{1 - 6 Q/P}{1 + 20 Q/P}$$

It has been established that the obtained relationship, together with (88), can be used – with a sufficient degree of accuracy – to predict the temperature at the fire center from the moment combustion ceases ($\tau \geq \tau_g$). As previously [10, 12, 35], the temperature for an exogenous fire in the excavation is assumed to be $T_1 = 1000^\circ\text{C}$, and for an endogenous fire, $T_1 = 1200^\circ\text{C}$.

Based on the above theoretical reasoning, a methodology is proposed for determining the temperature at the center of an isolated fire. The following input data are used:

Q – flow rate of the gas-air mixture through the isolated section (m³/s);

S – average cross-sectional area of the excavation (m²);

τ_g – combustion time from ignition to complete extinction (days);

τ – time since combustion ceased (days);

m – thickness of the mined seam (m);

x_0 – width of the actively ventilated zone of the goaf (approximately 20 m);

T_0 – native rock temperature ($^\circ\text{C}$).

Calculation procedure can be provided as follows.

1. Determine perimeter P (m) of the actively ventilated goaf using: $P = 2(x_0 + m)$. For exogenous fires, use: $P = 4\sqrt{S}$.
2. Determine parameter I (m²/s), equivalent to the Reynolds number: $I = 4Q/P$.
3. Determine the heat exchange coefficient B between the air and surrounding rockmass: $B = (1 - 1,5I)/(1 + 1,5I)$.
4. Determine relative time $\bar{\tau}$ from the moment combustion ceased, $\bar{\tau} = \tau/\tau_g$
5. Determine relative temperature \bar{T} at the fire center using:

$$\bar{T} = \frac{1 + B \exp\left(-\frac{1}{\pi\bar{\tau}}\right)}{\pi\sqrt{\bar{\tau}}}.$$

Using the obtained data, determine the temperature T (°C) at the fire center:

$$T = T_1 + (T_1 - T_0) \cdot \bar{T}.$$

This formulated method for determining the temperature at the center of an isolated fire can be used in conjunction with other temperature estimation methods, such as those based on unsaturated hydrocarbons. Such methods are recommended in standards by VNIGD “Respirator” and other institutions [36, 37]. For example, in works conducted by the Ukrainian mine rescue service (DVHRS) in cooperation with the Institute of Geotechnical Mechanics (IGTM) of the NAS of Ukraine, improved evaluation techniques for rockmass conditions during fire suppression are proposed [37–40]. One improvement suggests, for greater measurement accuracy, collecting ethylene samples near the roof and acetylene samples near the excavation floor, considering statistically sufficient air sample quantities [38].

When applying the method for assessing the temperature in the fire zone, measurements are taken in the workings from the fire side. Initially, measurements should be conducted on the intake side of the ventilation flow in the surrounding rocks at an accessible distance. After the construction of isolation seals, the stabilized air temperature near the seal is periodically measured. The final temperature assessment is recommended to be performed using the following formula:

$$T_i = \frac{t_i}{t_1 \cdot T_1},$$

where: T_i – estimated temperature of the rock mass near the fire center, °C; T_1 – initial temperature of the rock near the fire, measured at the beginning, °C; t_1 – initial air temperature near the stopping, measured at the beginning, °C; t_i – air temperature near the stopping, measured at intervals over time, °C.

Under laboratory conditions, as a predictive measure, it is proposed to take coal samples in advance, before a fire occurs, as part of preventive measures during the identification of indicator gases and the assessment of their dynamics. These samples are gradually heated in muffle furnaces until coal ignition, allowing for the evaluation of gas dynamics through laboratory experiments. Subsequently, by analyzing the actual measured changes in indicator gases, the real state of the fire can be determined. Clearly, these proposals are not regulatory, require further refinement, industrial verification, and discussion.

8. Methods for detecting the development of underground fires

Methods for detecting the initial stage of exogenous fires. Methods and approaches for forecasting, preventing, and extinguishing underground fires have been developed by many scientists and specialists [2, 7, 34, 35, 37]. The necessity of developing effective methods for detecting underground fires at an early stage is evident. It is also clear that the use of any fire detection method should be complemented by other measures that ensure an overall increase in the fire safety level of a coal mine. In recent years, several fundamental approaches (methods) have been proposed for forecasting (detecting) the initial stage of exogenous fire development. These methods are presented in Table 2.

Methods for fire detection

Table 2.

Fire Detection Method	Essence of the Detection Method
1. Physiological Method	<p>This is the simplest and least accurate method. It is based on identifying signs of fire through human sensory perception and is divided into visual signs and those that directly affect a person.</p> <p>Visually, fire can be detected through increased air humidity (fog and condensation), the appearance of fire-related odors (in coal mines – the smell of burning, kerosene, gasoline, or tar from dry coal distillation).</p> <p>Fire anticipation may also be felt due to the effect of CO on the human body, which causes gradual poisoning. Symptoms include sweating, drowsiness, fatigue, and a depressed state.</p>
2. Thermal Method (Physical)	<p>This method relies on the operation of thermal detectors. These detectors are designed to send a signal when the air temperature at the detector's location exceeds a preset threshold.</p>
3. Smoke Detection (Physical)	<p>During combustion of organic substances, small particles of burned and unburned material (ash) rise with fire gases into the air, forming an aerosol cloud – smoke. Smoke can appear even during the heating stage, making this method effective for early fire detection. Smoke detectors are used for this purpose.</p>
4. Chemical-Analytical Method (Gas Composition Monitoring)	<p>This method is based on measuring the gas composition in the mine atmosphere and analyzing its condition. Key gases for monitoring include carbon oxides (CO and CO_2), nitrogen oxides, and oxygen (O_2). Changes in these concentrations are typical in early stages of mine fires.</p> <p>Carbon monoxide (CO) and hydrogen (H_2) are the main gases indicating fire presence. This principle underlies the chemical-analytical method, commonly used in coal mines. This method also includes analyzing specific fire coefficients.</p>
5. Methane Emission Forecasting Method	<p>This method allows detection of endogenous fires by observing a sharp increase in gas emissions in a section compared to normal conditions. It is based on increased airflow to the fire source during oxidation, which may in turn raise methane levels. More reliable indicators include methane surges on non-working days when no coal extraction (and thus no extra methane release) occurs.</p>

6. Mineralogical Method	This method is based on the formation of new mineral compounds in mine water during a fire. The chemical composition of water flowing from mined-out areas depends on the mineralogical composition of rocks and the ongoing chemical processes. For example, at elevated temperatures, the water shows increased oxidation and higher sulfuric acid content along with various minerals.
7. Statistical Method	This method involves processing available fire occurrence data using multiple correlation equations.

To significantly improve the level of fire safety, it is necessary to optimize the resources related to mine ventilation management. For this purpose, the following measures are applied [34, 35, 37]:

- 1) Collection and monitoring of information about the state of mine atmosphere parameters and technical equipment (sensors, communication channels, regulators, etc.);
- 2) Analysis of the mine atmosphere state, current fire situation by areas; forecasting the situation and calculating its impact on the ventilation system;
- 3) Display of information about the state of the atmosphere, its parameters, and the probability of fire and accidents by sections; display of system performance data;
- 4) Processing of control actions of technical equipment.

The first group of functions includes the following measures:

- Monitoring methane concentration and air velocity in mine workings, as defined by the “Safety Regulations...” [2];
- Monitoring the operating mode of the main ventilation fan (MVF) – its air supply and pressure drop;
- Monitoring the condition of air flow regulators (AFRs).

The second group of functions includes:

- Preliminary processing and recording of operational information;
- Analysis of deviations of mine atmosphere parameters from nominal values;
- Creation of records on the state of the mine atmosphere: timestamp, carbon monoxide and methane concentrations in sections, air velocity and temperature, presence of smoke, air density, and others;
- Forecasting emergency and fire conditions by sections and selecting control modes;
- Calculating control actions on MVF and AFR;
- Forecasting the aero-gas conditions in the mine based on the implemented control actions and displaying the corresponding information on the dispatcher’s screen.

The third group of functions includes:

- Displaying information about the aero-gas situation in the mine;
- Issuing warning alerts about emergency conditions in controlled parameters and technical equipment failures;
- Printing reports on the overall fire and aero-gas situation (upon dispatcher request).

The fourth group of functions involves:

- Processing control actions by the main ventilation fan regulator and AFR drive.

Thus, the entire set of tools required for registering the early signs of fires emerging in mine workings constitutes a system for detecting the initial stage of underground fires.

Analysis of statistical data shows [2, 10] that the vast majority of exogenous fires develop from micro- or mini-heat sources introduced into a combustible environment from outside.

Open flame sources are typically caused by:

- Short circuits and sparking in electrical cables and equipment;
- Ignition of surfaces exposed to friction (frictional pairs);
- Blasting operations;
- Ignition of air-methane mixtures due to heated surfaces, sparks, and other causes [28, 33, 34].

In general, the process of material ignition development can conditionally be divided into *four phases* (according to the classification of NDIHS "Respirator"):

- *First phase* – Heat absorption process (endothermic reaction), accompanied by intense oxidative decomposition. During this phase, visible and invisible smoke is released, which in mixture with air forms an aerosol. The dispersed phase of this aerosol consists of solid particles of varying sizes generated during thermal decomposition. The temperature of the surrounding gas medium remains nearly constant.
- *Second phase* – The rate of oxidation increases. This leads to heat accumulation – a disruption in the balance between the rate of heat release and the rate of heat dissipation from the oxidation zone. An exothermic reaction occurs without ignition. The local temperature in the oxidation zone rises to 200–280°C. During these reactions, in addition to intense smoke release (due to thermal decomposition), chemical decomposition occurs, releasing key indicator gases – carbon monoxide and carbon dioxide, as well as water vapor. The temperature of the surrounding gas increases slightly.
- *Third phase* – Active pyrolysis of the material occurs with the release and local ignition of thermal decomposition products (gases and aerosols). The local temperature in the pyrolysis zone reaches 280–500°C. At this phase, the temperature of the surrounding gas medium near the ignition zone begins to rise. Convective air flows begin to form and warm up.
- *Fourth phase* – The local material temperature in the ignition zone reaches 500°C, and the flame engulfs the entire area. New zones are actively being prepared for spontaneous combustion. The flame front begins to move across the material surface. The area covered by the flame expands. An exponential increase in the temperature of the surrounding gas environment begins. Convective airflows are formed and intensify, further heating the air.

The described ignition process represents the early development stage of a fire source. As ignition progresses, this stage transforms into the initial fire stage, characterized by a non-stationary development process. Analysis of the dynamics of underground fire development has allowed the identification of key features for detecting the initial stage, considering additional proposed informational parameters (Fig. 14), which can be divided into two major groups:

- Parameters related to technological and design features;
- Parameters related to physical properties [2].

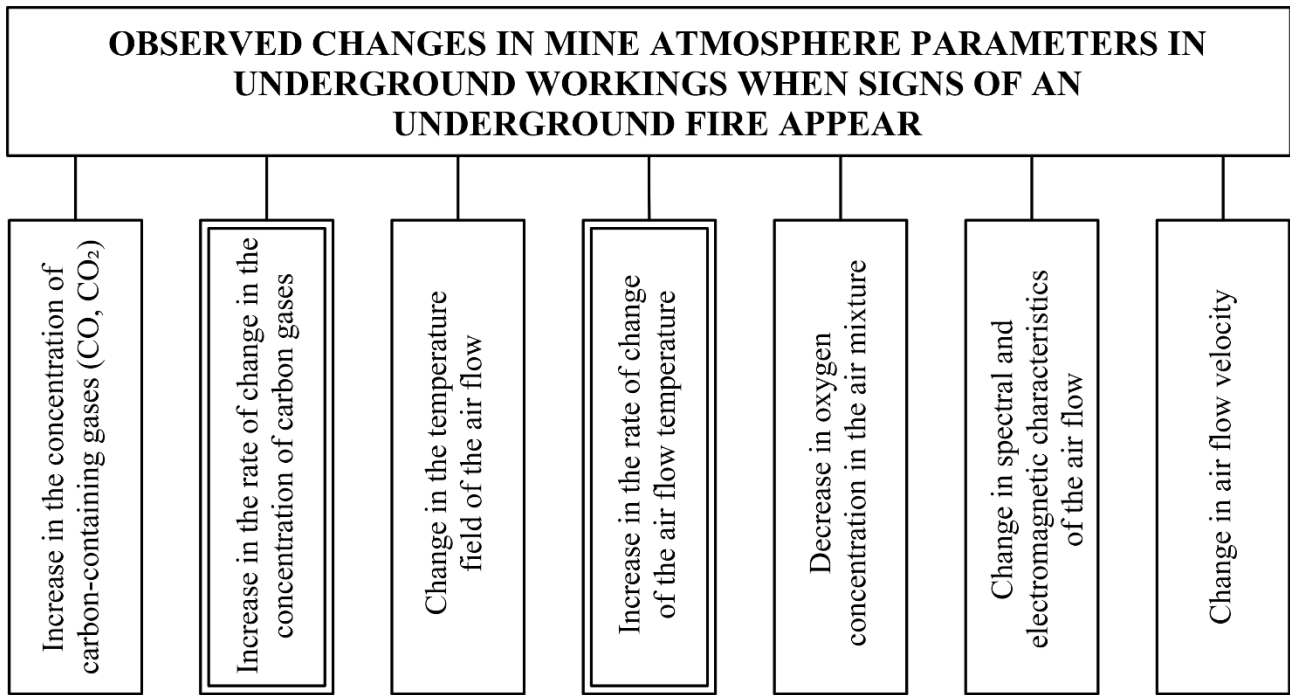


Fig. 14. Main characteristics in detecting the initial stage of an underground fire [2]

The main features of detecting an underground fire include: the large extent and branching of underground workings, the complexity of the ventilation system; physical parameters of the air stream related to heat and mass transfer (flow velocity, temperature field magnitude, gas concentrations, and overall gas composition); and physical parameters not related to heat and mass transfer (spectral characteristics, air density or illuminance, electromagnetic characteristics). The most significant interest in terms of detecting underground fires lies in these physical characteristics. It has been established that the most effective additional emergency criteria for early detection of an underground fire are the rate of air temperature rise and the rate of increase in carbon monoxide concentration.

The most commonly used devices for detecting signs of fire [3] are instruments for recording the ambient air temperature, smoke aerosols, and carbon-containing oxides, mainly carbon monoxide and hydrogen. Works [2, 34, 37] present a relatively simple formula (99) for determining the temperature in a horizontal working after the occurrence of an exogenous fire:

$$T = T_n + (T_{fg} - T_p) \frac{\alpha V}{eGC} (L - V_p \tau), \quad (99)$$

where T – temperature of fire gases behind the source, K; T_p – rock temperature at depth, K; T_{fg} – temperature of fire gases in the combustion zone, K; L – distance from the initial fire source point, m; V – perimeter of the working, m; τ – fire duration, s; h – heat penetration coefficient through the working walls, darcy; G – air mass flow rate, kg/h; V_p – fire front movement speed, m/h.

The speed of the fire front movement is determined by formula (100) [2, 11, 38]:

$$V_n = \frac{V}{0,011 + 0,009 \cdot V}, \quad (100)$$

where V – ventilation flow velocity, m/s; V_p – fire front movement speed, m/s.

According to work [2], the distance L satisfies the inequality $L \leq V_p \cdot \tau$ behind the fire source, and $L > V_p \cdot \tau$ ahead of the fire source.

Study of temperature field changes during an endogenous fire. If ignition has moved from the fourth phase to the initial combustion stage, a rapid temperature increase is observed at the fire source. At the same time, all atmospheric parameters, without exception, change actively. The temperature field in and near the source at this fire development stage is defined by the dependence described in [19, 35], while in [7], a relationship is provided for the temperature change during the endogenous ignition process, taking into account the evaporation of initial moisture and the oxygen sorption rate. Below is the formula (101) for determining the temperature at the self-ignition source:

$$T = \frac{E}{\ln \left(\frac{(1-m) \left(\rho_1 c_1 \frac{\delta T}{\delta \tau} - \lambda \frac{\delta^2 T}{\delta x^2} \right) + \rho_2 c_2 V \frac{\delta T}{\delta x} + Q_w \rho_3 \frac{dW}{d\tau}}{\rho_1 C q_c k (1-m)} \right) R}, \quad (101)$$

where m – porosity of the coal accumulation, %; E – activation energy of coal, J/mol; ρ – ρ – coal density, kg/m³; c_1 – heat capacity of the coal accumulation, J/(kg·K); T – temperature, K; τ – time, s; λ – thermal conductivity coefficient of coal, W/(m·K); C – oxygen (O₂) concentration, %; q_c – heat effect of the oxidation reaction, J/mol; R – universal gas constant, J/(mol·K); k – oxidation rate constant, m³/(kg·s); ρ_2 – gas density, kg/m³; C_2 – heat capacity of the gas, J/(kg·K); V – gas flow velocity, m/h; Q_w – specific heat of water evaporation, J/kg; ρ_3 – water density, kg/m³; W – coal moisture content.

Methods for detecting endogenous fires To prevent and extinguish underground endogenous fires, determining the stages of coal self-ignition is of primary importance. The earlier an endogenous fire is detected, the fewer resources and efforts are required to eliminate it. The main signs of the initial stages of coal self-ignition include [9, 33, 39]: an increase in the temperature of coal, air, and water (above the natural values for the given mine working); a steady increase in the specific content of carbon monoxide in the mine atmosphere, hydrogen, saturated and unsaturated hydrocarbons above their background levels.

Additional indicators include a decrease in the oxygen content, an increase in the carbon dioxide content, the appearance of the smell of sublimation products of coal in the mine workings, and an increase in mine air humidity. Typically, the following underground sites are subject to monitoring: coal accumulations formed due to sudden outbursts of coal and gas or other gas-dynamic events; protective coal pillars in mine workings, as well as coal pillars in longwalls and barrier pillars at the borders of mine extraction areas; goafs of active and abandoned panels; old unsealed workings; geological fault zones; accumulations of loosened coal in voids behind mine supports and near isolation stoppings; areas where coal seams or interlayers are exposed above; roof collapses and floor heaving in longwalls; isolated sections and workings, isolation stoppings; and return airflows from sections and mine wings.

Method for determining coal temperature based on the ratio of unsaturated hydrocarbons. It is well known that coal self-heating is accompanied by its thermal decomposition and desorption of syngenetic gases. Among the gases released during decomposition and desorption are ethylene and acetylene. In the absence of coal self-heating, the background volumetric content of these gases is approximately 10⁻⁷...10⁻⁶%, and their ratio is close to one. Typically, with increasing temperature during coal self-heating, the release of ethylene and acetylene increases. It is considered that in the self-heating and early self-ignition stages – up to the ignition temperature of volatile matter – the volumetric increase of ethylene outpaces that of acetylene, causing their ratio to increase systematically [2, 9, 10, 37].

After the ignition temperature is reached, depending on the coal mass undergoing self-ignition and the amount of incoming air, the ethylene-to-acetylene ratio may continue increasing or sharply drop to values typical of subcritical temperatures, accompanied by a simultaneous rise in acetylene content. Therefore, we believe that by observing changes in the volumetric content of ethylene and acetylene and their ratio, one can identify the development stage of an endogenous fire and estimate the coal temperature before ignition occurs [9, 10, 37].

Monitoring coal temperature in inaccessible areas, and the stage of the self-ignition process via the ethylene-to-acetylene ratio, should be conducted in zones of high endogenous fire risk. This provides additional information to assess the probability of methane-air mixture explosions and the effectiveness of implemented safety measures. Other operational monitoring methods may also be used to increase the reliability of forecasting.

To determine coal temperature using the ethylene-to-acetylene ratio at the monitored site, gas samples must be collected from at least two locations: one from the incoming airflow, and the other along the path of the air stream after it passes through areas with the highest likelihood of coal heating. Care should be taken to minimize dilution of gaseous products by fresh air. The interval between sampling during early-stage self-heating (or self-ignition) monitoring should be approximately half of the coal's self-ignition incubation period, but no more than 10 days [37]. Once the combustion stage is confirmed, subsequent gas sampling for determining coal temperature using the ethylene-acetylene ratio should only be conducted after fire-extinguishing measures have been implemented.

Let us now consider the *main stages of endogenous fire development and their characteristics*. As is well known, the effectiveness of endogenous fire suppression largely depends on accurate identification of the development stage. These stages are primarily determined based on mine air composition. However, the volume of information obtained from traditional mine air composition monitoring may not always provide a scientifically sound basis for choosing the most appropriate and safe tactical suppression measures.

Therefore, monitoring coal self-heating and interpreting it is best done not only through indirect indicators (such as carbon monoxide presence or smell of burning), but directly – by determining the actual temperature of heated coal. In inaccessible areas, coal temperature should be inferred from the ratio of unsaturated hydrocarbons. The high sensitivity of this method has, for the first time in mining practice, made it technically feasible to monitor coal self-heating at temperatures below the critical ignition point.

In this context, it is reasonable to distinguish four stages in the development of an endogenous fire (Figure 15):

- Coal self-heating;
- Initial stage of coal self-ignition (endogenous fire);
- Combustion;

Coal cooling.

The coal self-heating stage occurs within a temperature range from the quasi-stationary value (20–50 °C) to the critical value (Table 3), at which point a rapid temperature increase begins, leading to coal self-ignition [2, 9, 37].

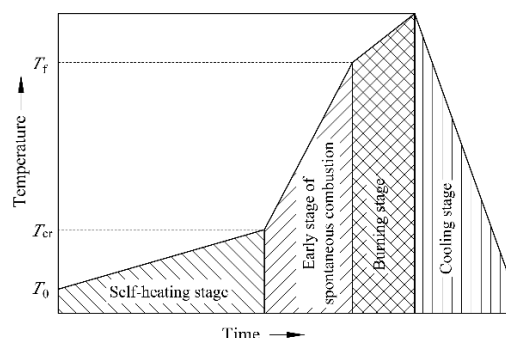


Fig. 15. Dynamics of the coal spontaneous combustion process [2]

T_0 – initial temperature of the coal; T_{cr} – critical ignition temperature of coal;
 T_f – flash point temperature of volatile substances

Table 3.

Type of Coal	Critical self-ignition temperature, T_{kp} , °C	Ignition temperature, T_b , °C
Lignite (brown coal)	70- 90	150- 200 (smoldering)
Bituminous coal ($V^{daf} > 20\%$)	90- 120	300-350
Lean coal ($V^{daf} < 20\%$)	120- 140	600-700

The heating of coal begins as soon as favorable conditions for the accumulation of oxidation heat are created, meaning when the amount of heat generated as a result of coal oxidation exceeds the total amount of heat spent on heating it, convective heat loss through the air, and heat transfer to the surrounding rocks.

As the temperature rises, heat accumulation in the coal deposits and the evaporation of moisture accelerate the oxidation process. If, during the development of spontaneous combustion, external factors change (e.g., a rapid increase in convective heat loss), thermal equilibrium may occur, and the heating of the coal deposit stops. If the heat release exceeds the heat dissipation to the external environment, the coal temperature gradually increases until it reaches a critical level.

At this stage, the self-heating of coal is monitored using the following indicators: an increase in the coal temperature beyond a set quasi-stationary value, determined by the ratio of ethylene and acetylene in mine air samples; an increase in the volumetric share of carbon monoxide, hydrogen, and both limited and unlimited hydrocarbons over time above background levels.

It is easier to prevent an endogenous fire if signs of its emergence are detected at the self-heating stage of the coal. This stage is spread over time, and its duration is determined by the incubation period of spontaneous combustion, which should be established through laboratory studies of coal samples. Carbon monoxide is typically not detected at this stage. Data on the duration of the incubation period are usually used when choosing measures to prevent endogenous fires. Due to the possibility of determining the self-heating temperature of coal based on the ratio of unlimited hydrocarbons, these data are also essential for selecting the most effective methods for extinguishing sources of coal self-heating.

The early stage of coal spontaneous combustion (the early stage of an endogenous fire) is characterized by a temperature range from the critical temperature to the ignition temperature of volatile substances emitted from the coal (Table 3). Upon reaching the critical temperature, the self-heating process accelerates sharply, oxygen consumption increases, and temperature rises, leading to heat accumulation.

Traditional control methods for detecting early signs of spontaneous combustion of coal include gas analysis to determine the volumetric share of carbon monoxide, oxygen, hydrogen, methane and its homologs, and carbon dioxide, as well as measuring the temperature of water and air. However, traditional methods do not always allow differentiation between the initial stage of coal spontaneous combustion and the combustion stage. For instance, the appearance of a carbon monoxide volumetric share in the mine air of the order of thousandths of a percent is typically associated with an increase in coal temperature beyond a critical value. However, depending on the relative location of the self-heating source and the gas sampling points, air leaks, and the physico-chemical properties of coal, this volumetric share of CO could indicate either the initial stage of spontaneous combustion or the combustion stage. On the other hand, with slow cleaning work and large exposed surfaces of coal that oxidizes easily, the appearance of small carbon monoxide volumetric shares in the mine air may not be linked to self-heating or combustion. Therefore, after detecting traditional signs of

coal self-heating at the initial stage (increased CO volumetric share, appearance of H_2 and other gases), the actual development stage of the process must be clarified by the maximum coal temperature in the deposit, which is determined from the ratio of ethylene and acetylene in the gas samples. Detecting signs of endogenous fires at the initial stage of coal self-heating is of great practical importance. The earlier the self-heating of coal is detected, the less heat will be accumulated by the coal and surrounding rocks, making it easier to extinguish the endogenous fire. The specifics of extinguishing endogenous fires depend on their development stage, primarily due to the ignition and explosion potential of methane-air mixtures.

The greatest safety for mine rescue operations can be ensured during the extinguishing of endogenous fires at the initial stage of development. However, in most cases, traditional control methods cannot distinguish the early stage of a fire in an inaccessible location from the combustion stage. Therefore, when carbon monoxide is present in mining workings and there is a risk of forming an explosive methane volumetric share, the endogenous fire is usually localized within a limited volume using explosion-resistant barriers. The method of determining temperature by the ratio of unlimited hydrocarbons allows for determining the maximum coal temperature in the developed space or in another inaccessible mine location, distinguishing the combustion stage from the initial stage of coal spontaneous combustion. This information is necessary but insufficient for ensuring safety during active fire extinguishing methods for endogenous fires.

The specificity in this case is that for the safe extinguishing of a fire, it is necessary to know the time during which coal self-heating can transition into the combustion stage. This time can be determined for the most dangerous situations, which arise when the oxidation heat is completely spent on heating the coal. For coal from the Donetsk basin of various grades, average values for the time to ignition of the coal (τ_i) are determined depending on the coal temperature (Figure 16).

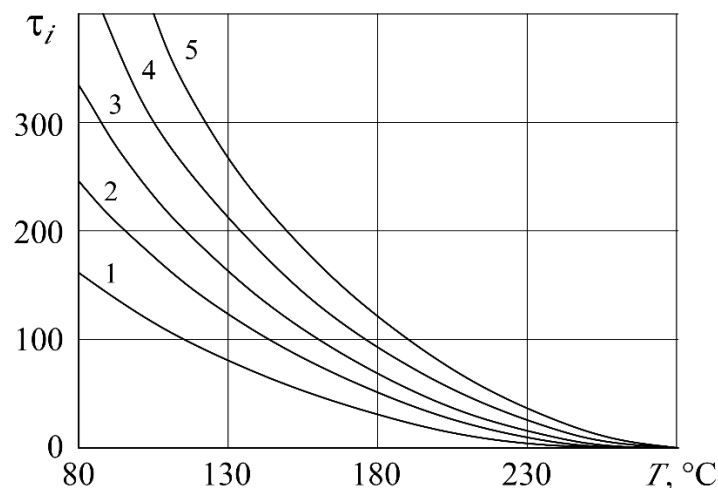


Fig. 16. Dependency of the ignition time of coal on its temperature for coal grades:
1 – Long-flame coal; 2 – Gas coal; 3 – Coking coal, Fat coking coal; 4 – Lean caking coal;
5 – Lean coal [35, 43]

The use of the method for determining the ignition time of coal in combination with the temperature control method based on the ratio of non-limiting hydrocarbons allows for improving the efficiency and safety of operations when mitigating the consequences of endogenous fires.

The coal combustion stage is characterized by temperatures exceeding the ignition temperature of volatile substances. The control over the development and extinguishing of endogenous fires is carried out through the collection, processing, and interpretation of information obtained from the following: observations of external signs of endogenous fires (temperature of coal, rocks, air, water; presence of flames, smoke, fog, condensation on the surface of mine workings, smell of burning and sublimation products); determination of coal temperature in areas inaccessible for direct observation in the mine, based on the ratio of micro-dollars of ethylene and acetylene; gas analysis to determine the volume fraction of CO , CO_2 , H_2 , CH_4 and O_2 in the mine workings.

The presence of at least one of the following signs indicates an underground endogenous fire: open flame, glowing coal, smoke, smell of burning or sublimation products of coal in the mine workings; steady increase in the volume fraction of hydrogen and carbon monoxide in air samples taken from the areas most likely to have a fire; heating or condensation on the external surface of the coal block or the walls of the mine workings; coal reaching the self-heating temperature (determined by the ratio of non-limiting hydrocarbons), close to the ignition temperature of volatile substances.

During the period of extinguishing the endogenous fire, the control over its development and extinguishing is organized by the head of mine rescue operations together with the responsible person in charge of the accident liquidation work. The organization of control includes: selection of air sampling locations; establishing the frequency of air sampling; monitoring compliance with the established air sampling schedule in mine workings, timely delivery of samples to the laboratory, and obtaining reports on the analysis results; assessing the operational situation based on analysis results.

From the moment of detection until the completion of extinguishing the endogenous fire, regular monitoring of the gas composition in the fire zone must be conducted through air sample collection and analysis to determine the volume fraction of O_2 , CO_2 , CO , CH_4 , H_2 , as well as the coal temperature in areas inaccessible for observation, which is determined by the ratio of non-limiting hydrocarbons.

In the first 10 days after detecting the endogenous fire, air samples must be taken to determine the volume fraction of oxygen, carbon monoxide, carbon dioxide, hydrogen, and methane at least once a day. The frequency of subsequent air sampling to determine these components and the frequency of sampling for determining the coal temperature in inaccessible areas based on the ratio of non-limiting hydrocarbons (ethylene and acetylene) are set depending on the activity of the fire.

The cooling stage of coal is characterized by a temperature range from the ignition temperature to a temperature below the critical value. The ability to determine the coal temperature at this stage allows for scientifically justified decisions regarding the possibility of classifying endogenous fires as extinguished and uncovering isolated fire zones to mine additional coal reserves.

In our opinion, attention should be paid to the curves presented in the work [2, 35], comparing different data on the development time of endogenous and exogenous fires in underground workings (Fig. 17).

The signs of an extinguished fire are as follows: the absence of carbon monoxide in air samples taken from the fire zone, or its volumetric fraction being lower than the background value for a specific mining area (excavation); a decrease in the temperature of the water draining from the isolated fire zone to a value characteristic for this particular mine workings; the temperature of the coal, determined by the ratio of non-bound hydrocarbons, being below the critical spontaneous ignition value.

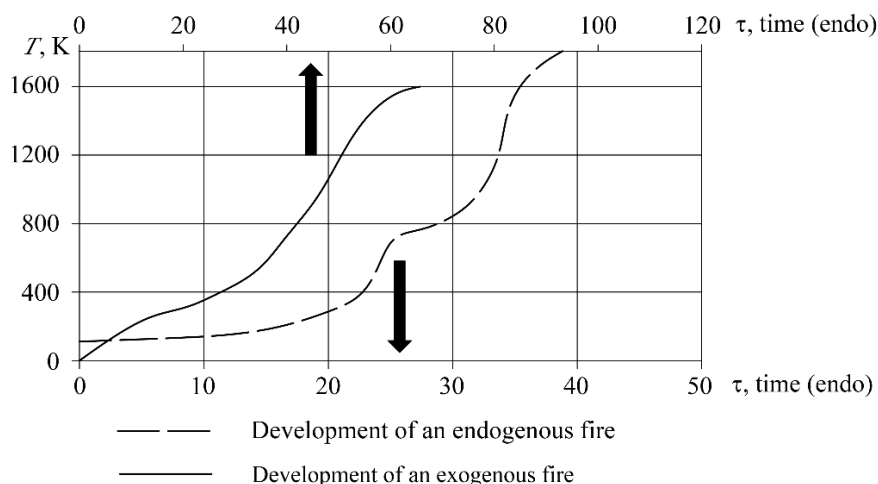


Fig. 17. Dependencies of the time development of endogenous and exogenous fires

After the fire is extinguished, isolating crosscuts are opened, and the mine workings of the fire zone are ventilated, the fire service units conduct reconnaissance. Only after the reconnaissance of the mine workings in the fire zone, control observations of the air gas composition for 5 – 10 days, and the absence of signs of coal self-ignition, can the isolating fire zone crosscuts be dismantled and the construction and restoration work carried out.

In our future research, we plan to implement modern IoT (Internet of Things) systems combined with thermal imaging (thermal cameras) for practical applications in coal mines. IoT represents a technological framework in which physical objects are equipped with sensors, communication devices, and software, enabling them to collect, transmit, and exchange data over the internet without direct human intervention. Key components of IoT systems include sensors and devices (“things”), communication networks such as Wi-Fi, LTE/5G, and LPWAN technologies (e.g., LoRaWAN, NB-IoT), cloud-based or local platforms for data storage and processing, and analytical tools including AI and machine learning for automated decision-making. These capabilities allow continuous monitoring of mine environments and real-time assessment of critical parameters such as temperature, gas concentrations, and equipment status.

The integration of IoT systems with thermal imaging technologies offers significant potential for improving fire detection and safety in underground coal mines. Thermal cameras can capture heat signatures of combustible materials and fire sources, while IoT networks transmit these data to centralized or cloud-based platforms for immediate analysis. This combination allows for rapid identification of abnormal temperature increases or fire hazards, enabling mine operators to implement preventive measures before incidents escalate. By providing real-time monitoring and automated alerts, these technologies enhance operational efficiency, reduce response times, and minimize risks associated with delayed detection of fires.

The practical application of IoT and thermal imaging in mines, where traditional fire detection systems may be limited, represents a promising direction for future research and safety management. Implementing such systems can help optimize ventilation strategies, support predictive maintenance of equipment, and improve overall mine safety. Moreover, this approach contributes to the broader goals of digital transformation and modernization in the mining sector, providing a foundation for data-driven decision-making and advanced monitoring solutions that can be adapted to other industrial or hazardous environments.

9. Methodology for monitoring ignition and fire development

Chapter 9 discusses the main methods and approaches to monitoring and controlling fires in coal mines, which is one of the key issues in ensuring industrial safety. In particular, the causes of coal self-ignition and the spread of fire in mining conditions are analyzed. The use of modern technologies, such as thermal cameras, gas analyzers, and early detection systems, is outlined for prompt response to emergencies.

Innovative approaches to modeling the processes of ignition and fire spread using mathematical algorithms and computer simulations are proposed. The focus is on creating integrated control and forecasting systems, as well as solutions such as: monitoring coal ignition; key concepts about the mechanism and causes of coal self-heating; characteristics of the coal oxidation rate; features of ethylene and acetylene release during coal heating; release of indicator gases and their background values that characterize the development of the coal self-ignition process; methodology for determining the incubation period of coal self-ignition and determining coal temperature based on the ratio of unsaturated hydrocarbons. These solutions are aimed at reducing risks to miners' lives, optimizing fire prevention measures, and improving safety management efficiency in enterprises.

9.1. Control of coal ignition

To prevent and extinguish underground endogenous fires, determining the stages of coal self-heating development is of paramount importance. The earlier an endogenous or exogenous fire is detected, the fewer resources and efforts are required to extinguish it.

The control of coal self-heating is based on a gas analysis method, which involves measuring the volumetric concentration of carbon monoxide, as well as the temperature of the air, surrounding rocks, and water in the mine workings of the fire section. Additionally, the volumetric concentration of carbon dioxide, methane, oxygen, and hydrogen is also monitored.

The gas analysis method, which involves periodic sampling of air in controlled areas and analyzing it with laboratory instruments, is labor-intensive. Therefore, to increase the efficiency of monitoring coal self-heating at early stages, automatic gas analyzers should be used.

The main signs of the early stages of coal ignition are considered to be:

- An increase in the temperature of the coal, air, and water (higher than natural values for the specific mine workings);
- A steady increase in the volumetric concentration of carbon monoxide, hydrogen, aliphatic and unsaturated hydrocarbons, observed in the mine workings, exceeding their background values.

Additional signs include:

- The decrease in the volumetric concentration of O_2 ;
- An increase in the volumetric concentration of CO_2 ;
- The appearance of the smell of sublimation products of coal in the mine workings;
- An increase in the humidity of the mine air.

It is recommended that the following objects be monitored:

- Accumulations of coal formed due to sudden coal and gas outbursts or other gas-dynamic phenomena;
- Protective pillars of mine workings, as well as coal pillars in faces, barrier pillars at the boundaries of mining extraction fields;
- Produced spaces of active and worked-out mining sections;
- Old unextinguished mine workings;
- Locations of geological disturbances;

- Accumulations of loose coal in cavities behind mine supports and near isolating crosscuts;
- Exposed coal seams and layers, roof collapses, and ground slippage in the faces;
- Isolated areas and workings (isolating crosscuts);
- Outgoing ventilation streams from sections and wings of the mine.

If a degassing system is available in the area, regardless of the coal's susceptibility to self-ignition, the background volumetric concentration of the mentioned gases is determined for the degassing wells. After this, it is necessary to monitor that the volumetric concentration of these gases in the mine air and degassing wells does not exceed their background value.

If the volumetric concentration of carbon monoxide or hydrogen in the mine workings exceeds the background value, it is necessary to assess the dynamics of the indicator gases' changes. To do this, a series of measurements of CO , H_2 , O_2 , CO_2 , CH_4 , C_2H_2 , C_2H_4 concentrations should be taken daily for three days at any fixed location of the emergency area.

If the volumetric concentration of CO in the mine workings of the controlled section exceeds 0.0017%, work in the section must be stopped, people should be evacuated to fresh air, and measures should be taken to locate and eliminate the source of CO emissions. A steady increase in the volumetric concentration of carbon monoxide, hydrogen, and unsaturated hydrocarbons indicates the presence of a coal ignition hotspot, i.e., the beginning of a fire.

9.2. Fundamental concepts on the mechanism and causes of coal self-heating and spontaneous combustion

The analysis of the mechanisms and causes of coal self-heating and spontaneous combustion conducted by P.S. Pashkovsky [11] indicates that the nature of these complex processes is not yet fully understood. Scientists and specialists from many countries, where coal mining has been developing since the early 19th century, continue to search for solutions to prevent endogenous fires.

Extensive research conducted in various countries does not provide a definitive answer as to why some coal seams are more prone to spontaneous combustion than others composed of similar coal and mined under nearly identical conditions. Coal is a complex heterogeneous substance whose properties are not solely determined by its chemical composition. To comprehensively describe coal properties, including its tendency to self-ignite, a combination of chemical, physical, and mechanical characteristics must be analyzed.

Different petrographic components of coal play varying and sometimes ambiguous roles in oxidation and spontaneous combustion processes. Research conducted both domestically [45, 46, 50] and abroad has yielded contradictory results. According to Professor V.S. Veselovskyi, the most significant factor in this regard is the relationship between petrographic structure, porosity, and the diffusion permeability of coal matter for oxygen [48, 49].

There is also no consensus among scientists regarding the effect of mineral impurities on coal's propensity for spontaneous combustion. Many researchers believe that mineral impurities have only a secondary influence on the development of the self-ignition process. However, alternative hypotheses suggest that sulfuric acid and other compounds formed during pyrite oxidation in humid conditions affect coal by promoting the formation of sulfo-products, which, together with iron ions, act as catalysts for low-temperature oxidation. It is generally recognized that pyrite, particularly in its amorphous form, contributes to spontaneous combustion by causing fracturing of the coal mass. Other mineral impurities (such as silicon and clay minerals) typically reduce chemical activity by increasing coal's overall ash content.

Moisture content plays a crucial role in coal's self-ignition process. Unfortunately, there is no unified perspective on either the quantitative or qualitative assessment of this factor. Some researchers argue that moisture slows down the self-ignition process, while others claim that it accelerates oxidation and increases coal's chemical activity. A third group suggests that moisture has no significant impact on unoxidized coal [41, 43, 44].

The size of oxidizing coal particles – i.e., its strength and structural properties, which determine the degree of

coal fragmentation – significantly influences the development of self-ignition processes. Foreign researchers previously assumed, without sufficient justification, that reducing coal particle size increases the risk of spontaneous combustion. However, it is now recognized that the total void volume in coal accumulations must be considered, as it affects oxygen access to coal particles. Research conducted by the Respirator Research Institute (NII GD) has shown that oxidation rates increase only when particle sizes are reduced to a certain threshold. Beyond this point, further reduction in coal fraction size leads to an increased oxidation rate, with the critical particle size depending not only on experimental conditions but also on internal surface area, porosity, and oxidation degree.

A critical factor in coal self-heating and spontaneous combustion is the rate of heat accumulation within coal accumulations. This depends on the specific heat of oxygen sorption as well as the heat capacity and thermal conductivity of coal. According to Professor V.S. Veselovsky, the specific heat of coal oxidation remains virtually unchanged as temperature increases and is independent of coal metamorphism and absorbed oxygen levels. Experimental studies by V. Olpinsky indicate that the specific heat of coal oxidation in the 293–373 K temperature range is 12.6×10^6 J/m³. Other experiments suggest that low-thermal-conductivity coal is more prone to spontaneous combustion. In this context, coal and surrounding rock moisture levels can also play a role, as increasing moisture content raises their heat capacity, thermal conductivity, and temperature diffusivity.

In the late 1960s, methane concentration in coal began to be considered an important factor in assessing endogenous fire hazards. Methane has a multifaceted role in inhibiting coal oxidation. On the one hand, coal that slowly releases methane also oxidizes slowly, undergoing gradual deactivation (leading to the hypothesis that coal with high residual methane content is less prone to spontaneous combustion). On the other hand, high gas content in mined areas facilitates the rapid formation of an oxygen-free environment. Both domestic and international practices include experiments on artificially gasifying isolated mining areas to prevent coal self-ignition [11, 34].

To date, approximately 20 theories explaining coal spontaneous combustion have been proposed based on various perspectives on the process and its influencing factors. The most widely accepted theories include the pyrite, bacterial, phenolic, and "coal-oxygen complex" theories [11, 50].

The **pyrite theory**, one of the earliest, was formulated in 1866 to explain the causes of coal self-ignition. According to this theory, spontaneous combustion occurs due to the interaction of pyrite present in coal with oxygen and water. The oxidation of pyrite releases heat, and if this heat accumulates within a coal pile, spontaneous ignition occurs. Proponents of the pyrite theory justified its role in self-ignition by demonstrating that pyrite oxidation releases between 13.82 and 17.16 J of heat per milliliter of oxygen consumed, compared to 8.79 to 13.82 J of heat released by coal oxidation without pyrite inclusions.

Further experimental studies and analysis of the conditions leading to endogenous fires in coal seams with very low pyrite concentrations have undermined the validity of the **pyrite theory** of coal spontaneous combustion. Researchers of this process have concluded that the presence of sulfur in coal is not the primary cause of its self-ignition. It is known that coal from the coal basin with a low sulfur content (less than 1%), is highly prone to spontaneous combustion, whereas Donbas coal, with a sulfur content of up to 5%, does not always exhibit this tendency. Experimental studies have shown that pyrite behaves differently during oxidation depending on grain size, structure, and the physical conditions under which the reaction occurs. In its pure form, pyrite oxidizes relatively slowly but reacts more actively with oxygen in the presence of the organic mass of coal. While pyrite oxidation by oxygen cannot be considered the sole cause of coal self-ignition, it does contribute to the development of this process. The oxidation of pyrite in the presence of moisture leads to the release of sulfuric acid and iron sulfate, which act as catalysts in the progression of coal self-ignition. Sulfuric acid, formed during pyrite oxidation under mining conditions, reacts with magnesium and calcium carbonates present in some coals as veins. This process results in coal cracking, exposing new reactive surfaces to oxygen.

The **bacterial theory** was proposed in the first half of the 20th century by W. Potter. According to this theory, microorganisms, particularly thiobacteria, multiply in moist coal. Their metabolic activity generates heat, which, due to the poor thermal conductivity of coal, accumulates, increasing the temperature within the coal mass. When the temperature reaches 343 K, the microorganisms die, but chemical reactions between coal and

oxygen intensify in the heated material. However, specialized research at the Institute of Microbiology investigating the role of microorganisms in coal self-heating during storage has shown that while bacteria may play a role in coal oxidation, their contribution is so negligible that it cannot even trigger the initial stages of self-heating.

The **phenolic theory** was proposed by V.V. Tronov in 1940. According to this theory, spontaneous combustion occurs due to the presence of phenolic atomic groups in coal, which actively absorb oxygen upon contact with air, leading to exothermic oxidation reactions. It is believed that monoatomic and polyatomic phenols in coal are relatively inert to molecular oxygen, and their oxidation does not exhibit autocatalytic behavior. In contrast, aldehydes, olefins, alkyl-substituted aromatic hydrocarbons, as well as naphthenic and paraffinic hydrocarbons, undergo autocatalytic self-oxidation. The oxidation potential of coal is determined by the proportion of phenolic hydroxyl groups, but no single chemical component of coal alone can fully explain its oxidation behavior.

The **coal-oxygen complex theory** was proposed by R.V. Wheeler in the mid-20th century and was further developed by domestic researchers such as N.M. Karavaev, V.F. Oreshko, and V.S. Veselovsky. This theory is the most widely accepted today. Its proponents argue that the primary cause of coal spontaneous combustion is its interaction with oxygen.

Initially, coal adsorbs oxygen, forming unstable oxygen-containing complexes such as peroxides on its surface. The formation of these peroxide compounds releases heat. If heat dissipation is limited, the rate of coal-oxygen interaction increases. The adsorption process transitions into chemisorption, followed by the decomposition of unstable oxygen-containing compounds, leading to the formation of more complex carbon-oxygen structures [25, 48, 49]. As the process accelerates, heat and gaseous oxidation products – carbon dioxide, carbon monoxide, and water – are released. Eventually, the process becomes self-sustaining, resulting in coal ignition.

Practical evidence supports the coal-oxygen complex theory: coal isolated from oxygen exposure does not self-ignite. Reducing airflow to coal slows oxidation reactions, forming the basis of modern strategies for preventing endogenous fires.

9.3. The rate of coal oxidation

The rate of coal oxidation at low temperatures generates both scientific and practical interest, as the correct solution to this issue determines the choice of methods and means for preventing, localizing, and extinguishing endogenous fires. The existence of conflicting views on the mechanism of coal oxidation has led to the need for experimental verification of these viewpoints.

V.S. Veselovskiy, based on the uneven oxidation of a coal sample by molecular oxygen, concluded that the limiting stage of the low-temperature oxidation rate is not the chemical reaction but the rate of oxygen diffusion to the internal surface of the coal particle [48, 49]. This perspective on the oxidation mechanism provides a convincing argument in favor of the proposed concept.

According to the principles of diffusion kinetics and sorption [2, 25, 26], chemical reactions occurring in the diffusion zone should have the following characteristics:

- The direct proportionality between the reaction rate and the effective concentration of the reactant (first-order reaction);
- The relatively weak dependence of the reaction rate constant on temperature;
- The dependence of the reaction rate constant on the rate of reactant flow;
- The reaction rate should not depend on the total pressure in the system when the composition and flow rate remain constant, since with a change in total pressure, the volumetric share of oxygen changes directly proportional, while the diffusion coefficient is inversely proportional to pressure.

Experimental studies should establish whether these characteristics, typical of the diffusion mechanism of the oxidation process, correspond to reality. It is known that the rate of chemisorption of molecular oxygen in bituminous coals largely determines their activity during oxidation. However, the traditional volumetric

method is a long and costly process [25, 26, 47, 48]. Since the determinations using this method are performed under static conditions, diffusion processes of oxygen from the core of the flow through the boundary layer to the internal surface of the coal particle, as well as desorption of oxidation products, significantly affect the kinetics of oxidation.

In this regard, a new method has been developed to determine the oxygen sorption rate constants, which is based on the capabilities of gas chromatography. The essence of the method is that oxygen is pulse-injected into the carrier gas stream, and as it moves along the chromatographic column with the investigated coal, it interacts with the coal.

9.4. Kinetics of ethylene and acetylene emission during coal heating

The study of the kinetics of ethylene and acetylene emission during coal heating holds significant scientific and practical interest, especially in the context of fire prevention, localization, and extinguishing in mines [11].

The air filtration rate is largely determined by the volumetric fraction of oxygen. With oxygen deficiency and when coal temperature rises to 523–573 K, the volumetric fraction of acetylene in the gaseous oxidation products sharply decreases, while the ethylene-to-acetylene ratio continues to increase (Figure 18). With sufficient oxygen, the opposite situation may occur: a rise in the acetylene fraction suddenly reduces the ratio of the indicator components due to the increase in acetylene concentration (Figure 19, curve 2) [11]. Both cases are observed under real mining conditions, indicating that the air filtration rate through the reactor should be optimal.

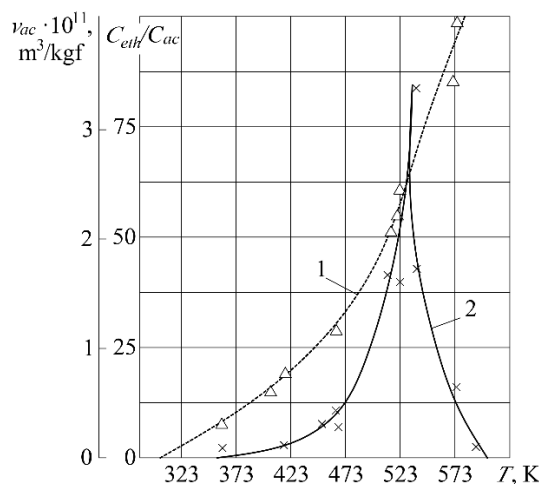


Fig. 18. Temperature dependence of the ethylene-to-acetylene ratio C_{eth}/C_{ac} and specific volumetric rate of acetylene formation v_{ac} during thermal oxidative destruction of coal of the KZh grade [11]:
1 – ratio C_{eth}/C_{ac} ; 2 – specific rate of acetylene formation v_{ac}

When studying the temperature dependence of ethylene and acetylene formation, it is important to consider the mass of the coal and the shape of the reaction vessel. The coal sample should be sized such that, upon heating, the ethylene and acetylene concentrations in the gas phase remain within the sensitivity range of the measuring equipment.

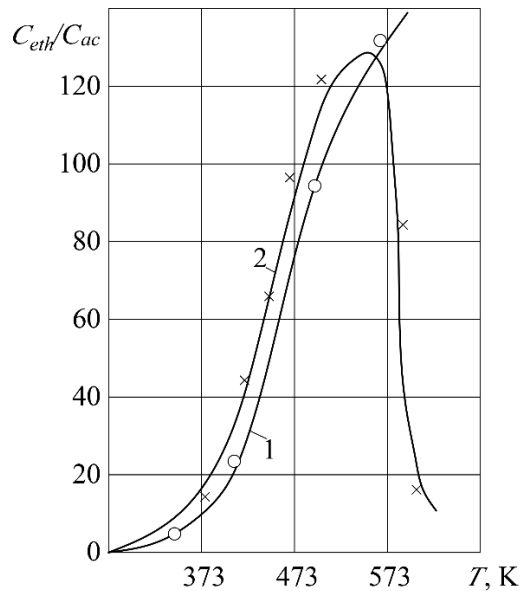


Fig. 19. Temperature dependence of the ethylene-to-acetylene volumetric ratio $C_{\text{eth}}/C_{\text{ac}}$ during heating of coal of the D grade [11]:

1 – air filtration rate $6 \times 10^{-3} \text{ m}^3/(\text{m}^2 \cdot \text{s})$; 2 – air filtration rate $8 \times 10^{-2} \text{ m}^3/(\text{m}^2 \cdot \text{s})$:

The formation of unsaturated hydrocarbons during coal heating is a chain reaction. Therefore, the contact conditions of radicals in the gas phase with the reactor walls may influence secondary reactions, which also lead to the formation of ethylene and acetylene, especially at temperatures close to the ignition point of coal. Thus, the geometric parameters of the reactor were chosen such that the gas-dynamic regime in natural conditions is similar to that in the reactor, and the relative number of radicals in the coal seam space near the surrounding rock approximately matches the number in contact with the reactor walls.

9.5. Background values of indicator gases characterizing the development of coal spontaneous combustion

The most informative indicator gases that characterize the development of coal self-heating are carbon monoxide and hydrogen. This is due to their physicochemical properties, particularly the fact that they are hardly adsorbed by coal and surrounding rocks, are not soluble in water, and create a so-called "background" level.

The "background value" refers to the volumetric fraction of indicator gases in mine workings that is consistently observed in the absence of coal self-heating (spontaneous combustion) under specific mining-geological conditions and established technological modes of coal extraction, roof control, and ventilation of the working face.

The presence of background indicator gases in mine workings is caused by their constant release from coal and host rocks, low-temperature coal oxidation, operation of mine machinery and mechanisms, as well as emissions from industrial enterprises and vehicles (if mines are located near industrially developed areas and busy roads). Monitoring the background concentrations of indicator gases is necessary in all mining areas working coal seams prone to self-ignition. This significantly increases the efficiency of early detection and control of spontaneous combustion.

In mines, to determine the background concentration of carbon monoxide and hydrogen, air samples should be taken from the mine atmosphere in airflow streams entering and exiting the working face. If the area is equipped with a degasification system, samples should also be taken from degasification boreholes and pipelines. Sampling methods are specified in relevant regulatory documents [2, 23, 35].

In mining sections using the room-and-pillar method to extract gently dipping seams (Figure 20a), samples must be collected from the incoming air stream (point 1) and the outgoing air streams (points 2 and 3). In the case of a return-ventilation scheme with auxiliary fresh air to the exhaust stream (Figure 20b), samples should

be taken from the incoming air (point 1), the auxiliary fresh stream (point 2), and the outgoing streams (points 3, 4).

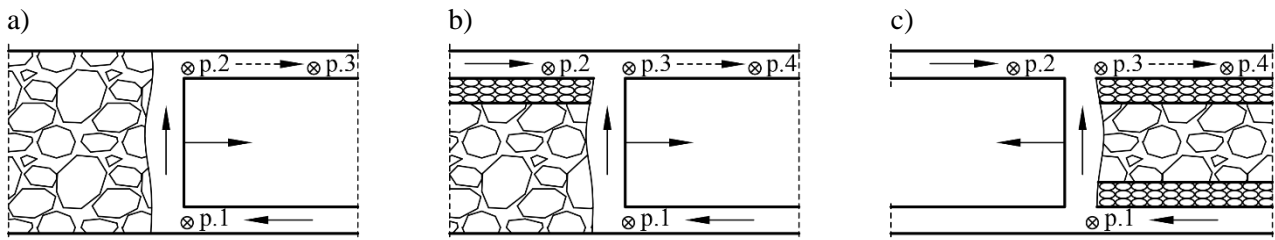


Fig. 20. Schemes for gas sampling locations: (a) return-flow ventilation to the coal seam; (b) with auxiliary fresh air to the coal seam; (c) with auxiliary fresh air to goaf: ⊗ – gas sampling point; —→ – fresh airflow; - - -→ – outgoing airflow

In full extraction and return-ventilation schemes with auxiliary air to the goaf (Figure 20c), one sampling point should be located at the incoming air stream (point 1), with the others in the auxiliary air (point 2) and the outgoing air streams of the section.

For extracting seams by advancing or retreating strips (Figure 21), samples must be collected from the incoming air (point 1), auxiliary fresh air (point 2), and outgoing air streams. Additional sampling points are recommended where gas carryover is likely due to thermal depression. In advancing extraction (Figure 21a), such a location may be near the working face close to the ventilation roadway (point 5). In retreating extraction (Figure 21b), this includes the ventilation crosscut (point 5) and isolated workings on the ventilation roadway (point 6).

Samples should be collected during different shifts (preparation, production), at least 3 hours after technological operations that generate increased CO emissions (blasting, shearer cutting). At each sampling point, at least three air samples should be collected at 30 – 60-minute intervals. Samples are collected in elastic gas-tight containers, such as rubber bags or chambers. They must be analyzed in a gas analysis lab within 12 hours of collection.

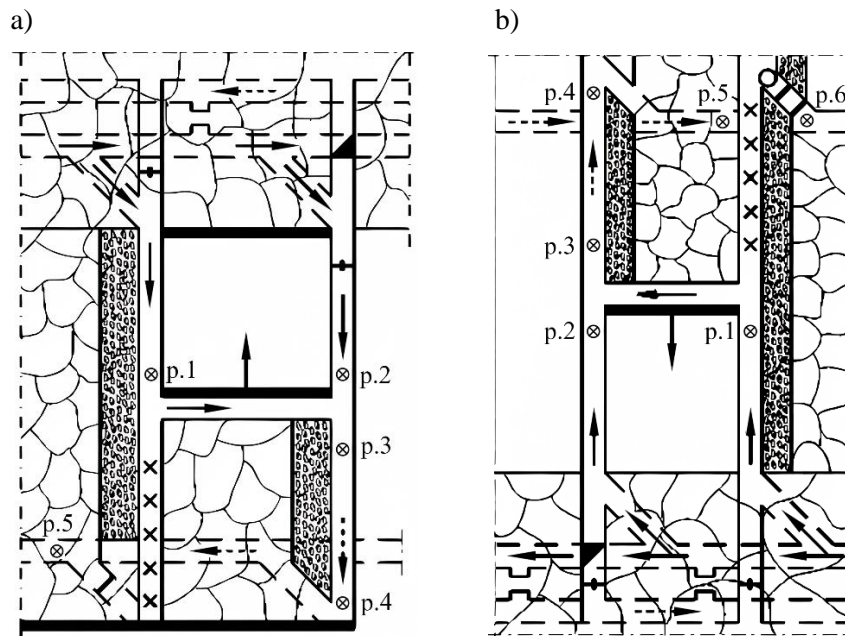


Fig. 21. Gas sampling location schemes during extraction of gently dipping seams: (a) advancing method; (b) retreating method

After determining the volumetric fraction of carbon monoxide and hydrogen from three samples, their average values for each sampling point are calculated using the following formulas:

$$(C_{CO}^i)^{av} = \frac{\sum_{i=1}^3 C_{CO}^i}{3} \text{ and } (C_{H_2}^i)^{av} = \frac{\sum_{i=1}^3 C_{H_2}^i}{3} \quad (102)$$

where C_{CO}^i and $C_{H_2}^i$ are the volumetric fractions of carbon monoxide and hydrogen in the i -th sample, respectively, in %.

Sampling is carried out three times at intervals of 4 to 5 days. Each time, the average values of the volumetric fraction of carbon monoxide and hydrogen at the sampling point are calculated. The background values are considered to be the maximum of the obtained average volumetric fractions of carbon monoxide and hydrogen. During the sampling process, it should be remembered that in the case of a sharp change in the air flow rate at the controlled section (by more than 25%), sampling must be repeated no sooner than 3 hours after the stabilization of the air flow rate.

If the volumetric fraction of carbon monoxide and hydrogen changes (in at least three samples) by more than 25% in either direction, the background volumetric fractions of carbon monoxide and hydrogen must be redefined. Since the volumetric fractions of indicator components depend on their dilution, when determining the background, it is necessary to take into account the air flow entering the section. Therefore, in determining the early stages of coal self-heating, if possible, one should use not the absolute values of the background but rather their product with the volume of air passing through the sampling point. This value represents the amount of indicator component produced per unit time at the controlled section, or the background flow of the indicator component:

$$\Phi = C_{av}Q/100 \quad (103)$$

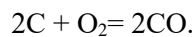
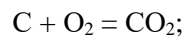
where Φ – background flow of the indicator component, m³/s; C_{av} – volumetric fraction of the indicator component, %; Q – air flow rate entering the controlled section, m³/s.

9.6. Emission of indicator gases during combustion of disintegrated coal mass

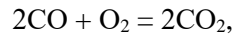
Below, we consider the emission of indicator gases during the combustion of disintegrated coal mass, for example, located in the mined-out space of a mine [1, 2]. It should be remembered that when analyzing coal combustion, there are two temperature regimes of self-heating and seam combustion:

- Low-temperature slow oxidation, where sorption processes play a predominant role and must be considered in calculations (e.g., fuel oxidation during long-term storage);
- High-temperature combustion, where the rate of adsorption and desorption is so high that the unsteadiness related to sorption processes can be neglected.

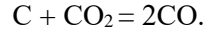
In these conditions, the main gases reacting with the carbon in coal are oxygen, carbon dioxide, and water vapor. It has been experimentally established [39] that regardless of the oxidation mechanism of carbon, the primary combustion products are carbon dioxide and carbon monoxide. With high humidity in the combusted coal, the combustion products may contain a significant amount of water vapor, or, in the case of oxidation of carbon by water vapor (as in “wet” gasification), hydrogen and methane may appear in the primary products. There is also the possibility of carbon interacting with multiple oxidizing agents if they are in contact with the carbon surface. Thus, the main result of the chemical transformation of carbon at high temperatures is the formation of carbon-oxygen compounds through primary reactions [55]:



In addition to these, on the surface of a carbon particle (fragment), secondary reactions may occur involving the formed carbon monoxide and oxygen diffusing through the mined-out space:



and the reduction of the formed carbon dioxide on the coal surface:



It should be noted that, under certain conditions, either the primary or secondary reactions may play the main role in the process under consideration. Taking the above into account, during the heating and combustion of coal in the mined-out space, the following summary reactions occur [5, 39, 54, 55] (Fig. 22), which can be described by the following equations:

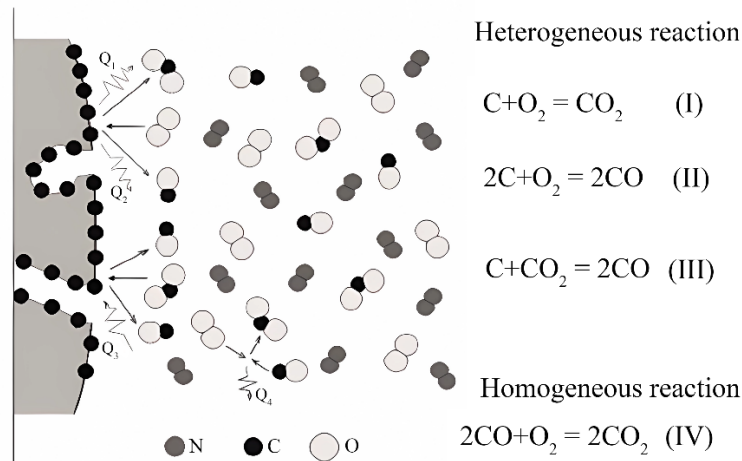
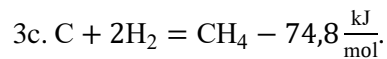
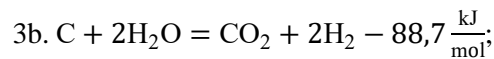
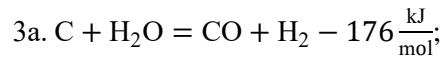
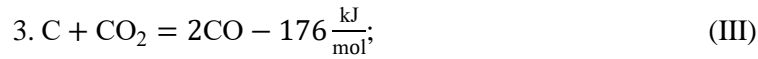
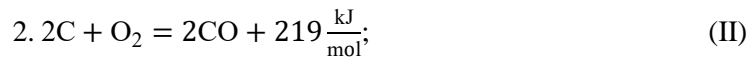
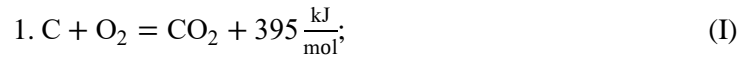


Fig. 22. Main reactions during coal oxidation in dry air [39]

The significant variation in activation energies even for the same type of coal is caused not only by the heterogeneity of carbon materials but also by the insufficiently accurate accounting of diffusion effects.

During the study of oxygen interaction with spherical carbon balls made of electrode coal (diameter 5–6 mm) at 400–500°C, it was established that the activation energy for electrode carbon at oxygen concentrations above

10% is 168 kJ/mol; with reduced oxygen levels, the energy increases, and at 2% it reaches 218 kJ/mol (Fig. 23). This change is likely due to a change in the oxidation mechanism and the simultaneous occurrence of multiple reactions.

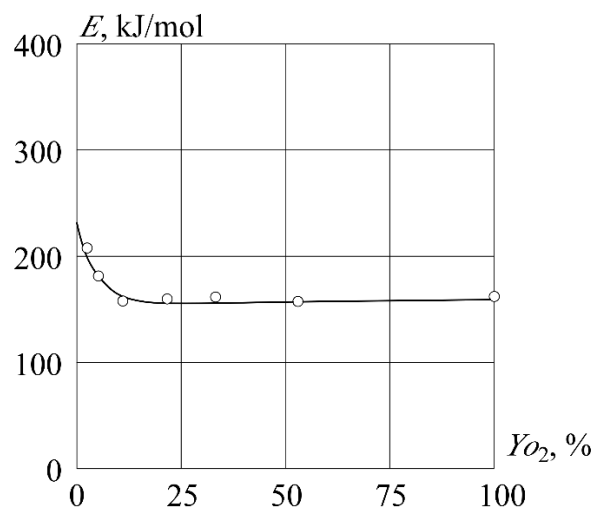


Fig. 23. Dependence of activation energy of electrode carbon on oxygen content in the oxidative zone

Processing of experimental data on the kinetics of coal interaction with gases shows [2] that the plots of the logarithm of the reaction rate constant versus the inverse temperature converge as temperature increases. This allows for the assumption of the existence of a conditional point – a pole. This makes it possible to express the reaction rate constant [1, 4, 39], knowing only the activation energy, through the coordinates of the pole k_* and T_* using the formula:

$$k_i = k_* \exp \left[-\frac{E_i}{RT} \left(1 - \frac{T}{T_*} \right) \right] = k_* \exp \left[\frac{E_i(T - T_*)}{RTT_*} \right].$$

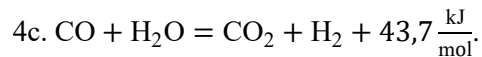
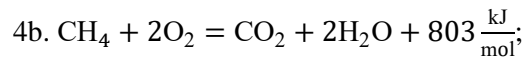
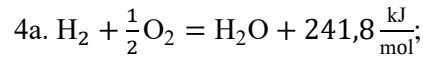
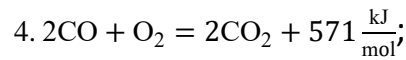
Analysis of experimental material leads to the conclusion that the pole should be located in the zone of fairly high temperatures. As the temperature rises, the lines of reaction rate constants converge and, starting from a temperature close to the sublimation temperature of carbon, they should merge into one line, as the differences due to the structure and lattice of individual coals disappear. One possible example of such a pole is the one proposed by S.G. Shestakov, with coordinates: $k_* = 100 \text{ m/s}$ and $T_* = 2600 \text{ K}$.

Activation energy values for the reaction $2C + O_2 = CO_2$ for different types of fuel [1, 55]

Table 4.

Coal grade	Activation energy, kJ/mol
Peat	83,6 – 85
Lignite (Brown coal)	90 – 105
Bituminous coal	115 – 135
Lean coal and Anthracite	140 – 146
Electrode coal	167

Thus, by knowing the activation energy of only one carbon reaction, the rate constants of other reactions can easily be obtained (Table 4). Under conditions of counter diffusion – where products of its incomplete conversion move from the surface of the carbon mass into the oxidizer flow, which in turn diffuses toward them from the surrounding volume – inevitable interactions occur near the carbon surface through the following reactions:



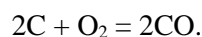
In general, the rate of homogeneous combustion reactions can depend on the concentrations of both components involved. However, experimental data show that the chemical conversion rate of CO, H₂, and CH₄ with oxygen is primarily determined by the content of these components in the mixture, following first-order reaction kinetics. Only at low oxygen concentrations does the reaction rate begin to depend significantly on the oxygen content as well.

The tendency of various chemical reactions to proceed spontaneously is compared under standard conditions of the initial mixture. It is under these conditions that the equilibrium constant at different temperatures is usually determined. In this case, the equation of the chemical reaction isotherm may be expressed in atmospheres:

$$\Delta G_T = -RT \ln K_p \text{ or } K_p = \exp\left(-\frac{\Delta G_T}{RT}\right)$$

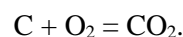
With this equation for the standard Gibbs free energy change [25, 26, 39] for reactions in the carbon-oxygen system, one can conduct a thermodynamic analysis.

Line AB corresponds to the reaction of incomplete chemical conversion of carbon:



It is easy to see that the standard chemical affinity of solid carbon for oxygen during the formation of carbon monoxide significantly increases with temperature, as AB decreases at higher temperatures.

Line CD expresses the temperature dependence of the standard Gibbs energy change for the complete carbon oxidation reaction:



This line is nearly horizontal in Figure 24, indicating that the standard chemical affinity of carbon for oxygen to form carbon dioxide is also very high, but it remains nearly unchanged over the 600–3000 K temperature range.

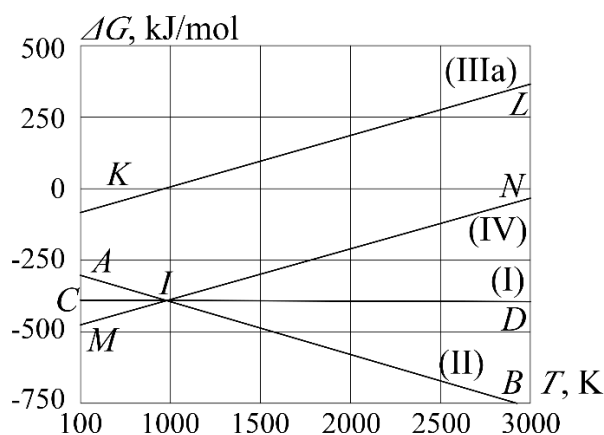
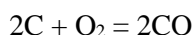
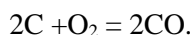


Fig. 24. Temperature dependence of the standard Gibbs free energy change for reactions in the carbon–oxygen system

Lines AB and CD intersect at point 1. To the right of point 1, line AB lies below line CD. Therefore, at high temperatures ($T > 1000$ K), the reaction:

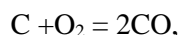


has a more negative Gibbs energy change than:

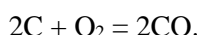


This indicates that under such conditions, carbon monoxide is a more thermodynamically stable compound than carbon dioxide.

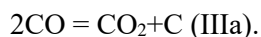
At lower temperatures ($T < 1000$ K), line AB lies above line CD, meaning that the Gibbs energy change is more negative for the reaction:



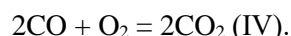
than for:



Rising line KL characterizes the temperature dependence of the standard Gibbs energy change for the decomposition of carbon monoxide:



Line MN establishes the functional dependence of Gibbs energy on temperature for the chemical conversion of carbon monoxide:



In the low-temperature region ($T < 1000$ K), the standard Gibbs energy change for reaction (IIIa)—equal to the negative value of reaction (III)—becomes less than zero (line KL). This means that the decomposition of carbon monoxide according to reaction (IIIa) is thermodynamically probable under these conditions and may occur in the CO–C–CO₂ system. Hence, at low temperatures ($T < 1000$ K), CO₂ is the more stable gas in the equilibrium CO–C–CO₂ system.

In the higher temperature range ($T > 1000$ K), i.e., to the right of point 1, the standard Gibbs energy change of reaction (IIIa) is positive, indicating low (or rather zero) probability of carbon monoxide decomposition via reaction (IIIa). Therefore, at high temperatures ($T > 1000$ K), CO is the more thermodynamically stable compound in the CO–C–CO₂ system. In practical scenarios, carbon and oxygen interact either under oxygen-

rich conditions or in the presence of excess solid carbon fuel.

In summary, carbon monoxide (CO) is more stable than carbon dioxide (CO₂) at high temperatures. Conversely, CO₂ is more stable than CO at lower temperatures.

9.7. Method and means for determining coal temperature based on the ratio of unsaturated hydrocarbons

Self-heating of coal is accompanied by its thermal decomposition and desorption of syngenetic gases [2, 11, 23, 39]. Among the decomposition and desorption products – along with other gases – ethylene and acetylene are present. Under normal temperatures, i.e., when self-heating does not occur, the background volumetric concentrations of these components range from 10⁻⁷...10⁻⁶%, and their ratio is close to one.

As is known [2, 11], with increasing temperature during coal self-heating, the release of ethylene and acetylene rises. At the heating stage and the early stages of ignition – up to the temperature at which volatile substances ignite – the increase in ethylene concentration outpaces that of acetylene, which causes their ratio to increase. Upon reaching ignition temperature, depending on the mass of the coal accumulation undergoing spontaneous combustion and the amount of air available to it, the ethylene/acetylene ratio may either continue to rise or suddenly drop to values typical of subcritical temperatures, accompanied by a simultaneous increase in acetylene concentration.

Thus, by tracking changes in the volumetric fractions of ethylene and acetylene and their ratio, it is possible to identify the stages of endogenous fire development and approximately determine coal temperature before ignition.

Coal temperature at the self-heating center can be determined using the following expression:

$$T_y = T \left(1 + \frac{\Delta T_n}{100} \right) \cdot k_{H_2} \cdot k_{H_2O} \cdot k + T_0, \quad (104)$$

where T_y – coal temperature at the self-heating center, °C;

T – temperature rise of the coal relative to the surrounding rock, °C;

T_0 – temperature of the host rocks, °C;

ΔT_n – maximum error in determining the coal's temperature rise relative to the host rock, % (Table 5);

k_{H_2} – coefficient accounting for hydrogen concentration change in air samples taken from the fire area, $k_{H_2} \approx 0,85 - 0,95$;

k_{H_2O} – coefficient accounting for changes in water temperature and air humidity from the isolated emergency area, $k_{H_2O} \approx 0,9 - 1$.

The coefficients k_{H_2} and k_{H_2O} re determined according to the methodology of the Institute of Geotechnical Mechanics of the National Academy of Sciences of Ukraine (IGTM).

Possible maximum errors in determining coal temperature based on the ethylene-to-acetylene ratio arising from the mass transfer of indicator components

Table 5.

Scheme No. (see Figure 4)	Location of Coal Accumulation in Mined-Out Area	Maximum Error, %, Relative to Measurement Range	
		Up to 373 K	Up to 523 K
1	Along the haulage drift	10	15
2	Along the ventilation drift	10	15
3	Along the longwall face line	3	5
4	In the installation chamber	3	5
5	Along the haulage drift	12	16
6	Along the ventilation drift	15	20
7	Along the longwall face line	8	12
8	In the installation chamber	6	10
9	Along the haulage drift	15	25
10	Along the ventilation drift	15	25
11	Along the longwall face line	3	5
12	In the installation chamber	3	5

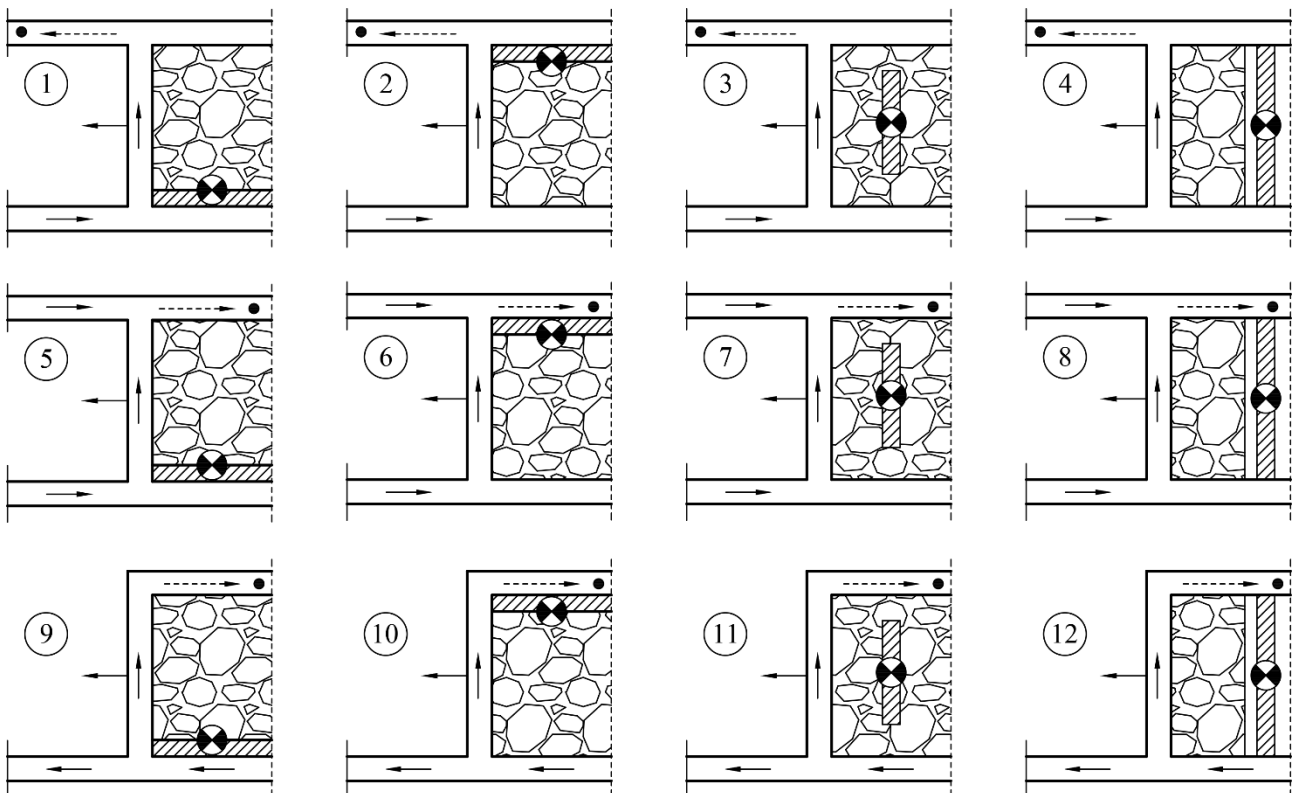


Fig. 25. Schemes for calculating possible errors in determining the maximum coal temperatures:

● – air sampling points; ⊗ – coal self-heating centers

The excess of coal temperature over the temperature of the surrounding rocks is determined based on the ratio of the actual volumetric fraction of ethylene to acetylene (C_{eth}/C_{ac}), released from the coal during self-heating at the monitored site. The experimentally established values of the dependencies $C_{eth}/C_{ac} = DT$ for different coal grades are presented in Table 6.

Values of the parameter T depending on the ratio of the volumetric share of ethylene and acetylene C_{eth}/C_{ac}

Table 6.

Temperature $T, ^\circ\text{C}$	The ratio of C_{eth}/C_{ac} for coal grades*									
	G	SS	GZ	Z	D	KZ	K	OS	T	A
20	1	1	-	-	-	-	-	-	-	-
30	4	2	1	1	1	-	-	-	-	-
40	7	3	2	2	2	1	1	1	-	-
50	11	6	3	3	3	2	2	2	-	-
60	15	9	5	4	4	3	3	3	-	-
70	19	12	9	6	5	4	4	4	1	-
80	25	18	12	9	6	5	5	5	2	-
90	32	23	17	13	10	8	6	6	3	-
100	39	29	23	18	14	11	9	7	4	-
110	47	36	28	23	19	15	12	8	5	1
120	57	45	36	30	24	19	15	9	6	2
130	67	53	45	37	30	23	19	10	8	3
140	80	64	53	45	38	29	22	11	10	4
150	93	75	64	55	46	35	27	13	13	6
160	110	87	76	65	55	42	32	17	16	9
170	125	102	88	76	65	50	37	21	21	12
180	145	116	102	88	76	57	43	26	25	15
190	165	132	116	102	88	66	49	30	30	18
200	188	150	132	115	102	75	56	35	35	22
210	210	170	145	128	113	92	63	41	41	25
220	230	180	160	142	125	96	70	48	47	29
230	252	207	175	155	138	107	79	63	54	33
240	273	236	190	170	150	118	88	70	61	38
250	295	245	205	182	163	128	96	78	69	42
260	315	264	220	196	177	140	105	86	77	47
270	340	283	235	210	190	150	114	94	84	52
280	360	302	250	223	202	161	124	103	92	57
290	380	320	265	237	215	172	133	112	100	63
300	400	340	280	250	228	182	143	121	110	70
400	-	-	-	-	-	-	-	-	215	140
500	-	-	-	-	-	-	-	-	340	240
600	-	-	-	-	-	-	-	-	480	360

*The coal classification presented here follows the standards adopted in Ukraine, which correspond to widely accepted international norms commonly cited in global technical literature: G – Gas coal; SS – Lignite / Soft

brown coal; GZ – Fat gas coal / High-volatile gas coal; Z – Fat coal / High-volatile bituminous coal; D – Coking coal / Blast-furnace coal; KZ – Fat coking coal / High-quality coking coal; OS – Semi-coking coal / Optimum coking coal; T – Thermal coal / Steam coal; A – Anthracite.

The temperature of the rocks surrounding the coal seam is determined using the following expression:

$$T_0 = T_g + \frac{H_{zp} - H_1}{g_r}, \quad (105)$$

where T_0 – Temperature of the surrounding rocks, °C;

T_g – Temperature of rocks in the constant temperature zone, °C (for Donbas mines: $H_1=30$ m; $g_r=9...10^\circ\text{C}$; $T_g = 33$ m/°C);

H_{zp} – Depth of mining operations, m;

H_1 – Depth of the constant annual temperature zone of rocks at a given location, m;

g_r – Average geothermal gradient for the given area, m/°C.

Control of coal temperature in areas inaccessible for observation and monitoring the stages of spontaneous combustion development based on the ethylene-to-acetylene ratio should be organized in zones with a high risk of endogenous fires. Monitoring coal temperature during the extinguishing of endogenous fires using the volumetric ratio of ethylene to acetylene provides additional information, allowing for the assessment of the potential explosion risk of the methane-air mixture and the effectiveness of the applied measures. This control should be implemented from the moment the fire occurs until its extinguishment, and in the case of fire isolation, until its official decommissioning. At the same time, the use of other types of operational monitoring is not excluded.

The organization of monitoring includes:

- Selecting air sampling locations and establishing sampling frequency;
- Collecting air samples;
- Determining the volumetric concentration of ethylene and acetylene;
- Identifying the stages of spontaneous combustion development based on coal temperature analysis.

To determine coal temperature using the ethylene-to-acetylene ratio, at least two gas samples must be taken from the monitored area. One sample should be collected from the incoming airflow, while the other should be taken from the airflow that has passed through the areas most likely to experience coal heating, ensuring that the dilution of exhaust gaseous products with fresh air is minimized.

Samples can be collected directly from mine workings, sampling tubes embedded in isolation seals, rubble strips, or directly from the goaf, as well as from boreholes drilled from underground workings or from the surface. The positioning of gas sampling points depends on the ventilation scheme and mining method. According to the ventilation schemes and mining methods shown in Figure 26, samples can be taken from tubes placed in the rubble strip near the ventilation roadway at intervals of 40-60 meters or near the location where air leaks from the goaf into the working area.

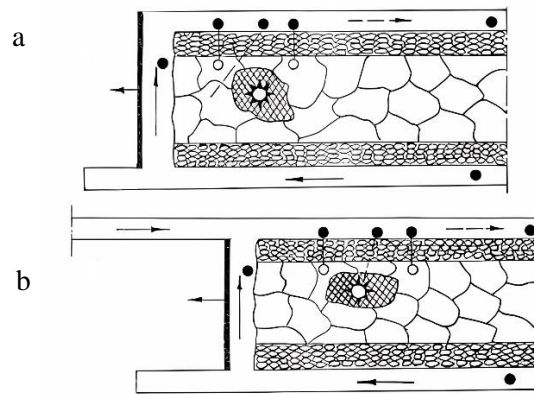








Fig. 26. Schemes of gas sampling point locations for determining the volumetric fraction of ethylene and

acetylene (for a full extraction system) under (a) a return-air ventilation scheme and (b) a partial fresh-air

supply to the goaf:  - fresh air stream;  - return air stream;  - coal self-heating (self-ignition) zone;  - gas sampling point;  - gas sampling tube;  - borehole for gas sampling

Under the room and pillar mining system (Figure 27), sampling must be provided near the locations of gas emission from the goaf (point 2 in Figure 27a and point 3 in Figure 27b), as well as from boreholes drilled into the caving dome (point 3 in Figure 27a and point 4 in Figure 27b). In addition, one of the mandatory sampling points must be located in the incoming air stream (point 4 in Figure 27a and point 5 in Figure 27b).

In the presence of a self-heating (spontaneous combustion) source in an isolated section (Figure 27c), samples from the outflowing streams originating from the combustion source must be taken either behind the air-exhausting stoppings (point 1) or in the general exhaust stream near these stoppings (point 2).

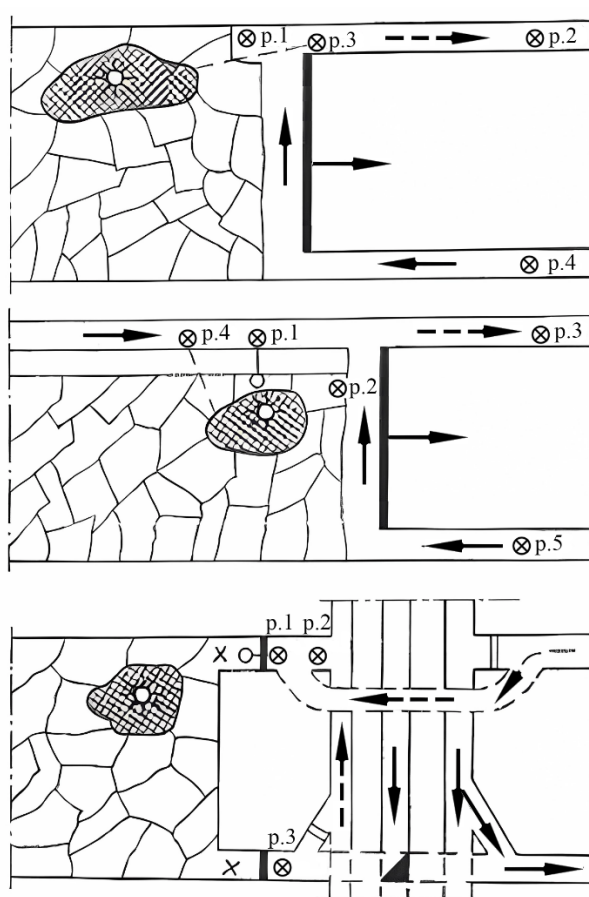


Fig. 27. Diagram of gas sampling points for determining ethylene and acetylene concentrations:
a – return air ventilation scheme; b – ventilation scheme with additional fresh air and exhaust stream directed to the pillar; c – isolated section

The interval between sample collections during monitoring for early signs of self-heating (spontaneous combustion) should be approximately half the incubation period of coal self-ignition, but no more than 10 days. The frequency of sampling during monitoring of extinguishing processes for endogenous fires is determined by the mine rescue operation manager, depending on the nature and stage of fire development. If it is determined that the self-ignition process has reached the combustion stage, further gas sampling to determine coal temperature based on the ethylene to acetylene volume ratio should only be carried out after implementing measures aimed at extinguishing the endogenous fire. Samples are collected for analysis by

pumping gas through a special *U*-shaped metal concentrating tube filled with a sorbent (Figure 28).

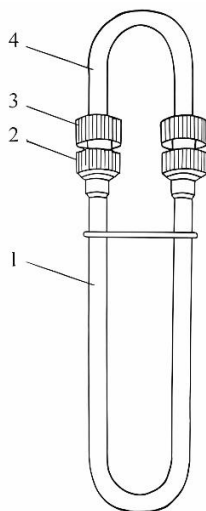


Fig. 28. Concentrating tube: 1 – tube with sorbent; 2 – nut; 3 – adapter; 4 – rubber tube

The length of the concentrating tube is 0.20 m, with an inner diameter of 4 mm. Activated carbon is used as the sorbent. When the analyzed gas passes through the concentrating tube, the sorbent absorbs micro-impurities of ethylene and acetylene. For further quantitative analysis of these micro-impurities, the minimum volume of gas passed through the tube must be sufficient to establish thermodynamic equilibrium between the sorbent and the impurity components. Under constant temperature, the amount of adsorbed impurity definitively determines its volume fraction in the gas phase. For a concentrating tube of the given dimensions, the volume of gas passed should be no less than $1 \cdot 10^{-3} \text{ m}^3$. Further increasing the volume of gas passed does not affect the sample size since it does not change the already established equilibrium.

The shelf life of the sample collected in the concentrating tube is practically unlimited under normal ambient temperatures. Desorption of micro-impurities from the sorbent in noticeable amounts occurs only if the concentrating tube is heated to temperatures significantly higher than ambient. The collected sample is delivered to a laboratory for analysis using a chromatograph with a highly sensitive flame ionization detector.

9.8. Methodology for determining the incubation period of coal self-ignition

As a rule, according to existing standard methods [1, 2, 40], the determination of the incubation period of coal self-ignition for specific seam conditions can be performed by calculation or using a computer. Below, these approaches are examined.

Determining the incubation period of coal self-ignition by calculation.

The incubation period of coal self-ignition, τ_{ihk} , in days, is calculated using the following formula:

$$\tau_{ihk} = \frac{C_s(T_{kp} - T_0) + 0,6\lambda W_0/100 + q_d X_0}{24\alpha K^{0,45} C_{O_2} q_{O_2}}, \quad (106)$$

where C_s – specific heat capacity of coal, J/(kg·°C);

T_{kp} – critical temperature of spontaneous combustion of coal, °C;

T_0 – initial temperature of coal accumulation, °C;

λ – rate of temperature change of coal accumulation per unit time, cal/g;

W_0 – initial moisture content of coal, %, determined as:

$$W_0 = 100 \cdot (m_1 - m_2)/m_0 \quad (107)$$

where m_1 – mass of the sample with the crucible after being held in the desiccator, g;

m_2 – mass of the sample with the crucible after drying, g;

m_0 – mass of coal sample, equilibrated in the desiccator, g.

To determine the initial moisture content of coal, two coal samples with a fraction size of 0.2 mm are placed in desiccators. In the first desiccator, the relative humidity over the coal is maintained at 98%, and in the second one – 100%.

q_o – specific heat of desorption of methane, cal/ml;

X_0 – natural methane content, ml/g;

α – coefficient of oxygen absorption from air;

K – oxygen sorption rate constant for coal, m³/(kg·s), determined as follows:

- Coal sample of fraction 1–3 mm, weighing from 50 to 120 g, is loaded into the sorption vessel at a temperature of 18–20°C;
- The initial oxygen concentration in the air above the coal in the sorption vessels is measured;
- The sorption vessels are sealed and placed in a thermostat at a temperature of 10–20°C;
- After one, three, and five days, the final oxygen concentration in the air above the coal is measured.

Based on these measurements, the oxygen sorption rate constant for coal is determined:

$$K = -\frac{V}{m \cdot \tau} \cdot \ln \frac{(100 - C_0)C_c}{C_0(100 - C_c)}, \quad (108)$$

where V – volume of air in the reaction vessel, m³;

m – mass of coal sample, kg;

τ – time of contact between air and coal, days;

C_0 – initial oxygen concentration in the air above the coal, %;

C_c – final oxygen concentration in the air above the coal, %;

C_{O_2} – oxygen concentration at the coal accumulation input, fractions of unit;

q_{O_2} – specific heat of oxygen sorption by coal, cal/ml.

Determination of the Incubation Period of Spontaneous Combustion of Coal Using Electronic Calculating Machines

The incubation period of spontaneous combustion of coal using electronic calculating machines is determined by the following formula:

$$\tau_{inh} = \sum \Delta\tau, \quad (109)$$

where $\Delta\tau$ – time interval, s.

The incubation period of spontaneous combustion of coal is equal to the total duration of the time intervals $\Delta\tau$, during which the total temperature change reaches the critical value for the spontaneous combustion temperature of coal:

$$\sum \Delta\tau = T_{cr}, \quad (110)$$

where T_{cr} – critical temperature of spontaneous combustion of coal, °C, ($T_{cr} = 90-130^\circ\text{C}$);

ΔT – temperature change of the coal accumulation during time intervals $\Delta\tau$, °C.

The total duration of time intervals is determined by:

$$\sum \Delta\tau = \sum \frac{\Delta T}{Q^{gen} - Q^{hle} - Q^{hle}}, \quad (111)$$

where Q^{gen} – rate of temperature change in the center due to heat generation during the interaction of oxygen with coal, °C/s, determined as:

$$Q^{gen} = \frac{V_v \gamma \Pi q K C_0 \nu}{(\nu + K V_v \Pi \gamma) \gamma C_c V_v \Pi}, \quad (112)$$

where V_v – volume of coal, m³;

γ – coal accumulation density, kg/m³;

Π – coal porosity, fractions of unit;

q – thermal effect of coal oxidation, J/m³;

ν – volumetric air combustion rate, m³/s;

C_c – specific heat capacity of coal, J/(kg·°C);

K – oxygen sorption rate constant for coal, m³/(kg·s), determined as:

$$K = K_0 \exp\left(-\frac{E}{R(T + \sum \Delta T)}\right) \tau^{-h} f(w), \quad (113)$$

where K_0 – initial oxygen sorption rate constant for coal, m³/(kg·s);

E – activation energy, J/mol, determined as:

$$E = -R \frac{\ln(K_{T_1}/K_{T_2})}{T_2/(T_1 - 1)}, \quad (114)$$

where R – universal gas constant;

K_{T_1} – oxygen sorption rate constant at temperature T_1 , m³/(kg·s);

K_{T_2} – oxygen sorption rate constant at temperature T_2 , m³/(kg·s);

T_1 – thermostat temperature, K, ($T_1 = 283 - 293$ K);

T_2 – thermostat temperature, K, ($T_2 = 313 - 333$ K);

h – rate of coal deactivation over time, fractions of unit, determined as:

$$h = -R \frac{\ln K - \ln K_0}{\ln \tau}, \quad (115)$$

$f(w)$ – activation index of the reaction rate constant at the critical moisture content, fractions of unit, determined as:

$$f(w) = 1,009 \exp \left[\frac{-\left(\frac{100W}{W_0} - 35\right)^2}{40} \right] + 1, \quad (116)$$

where W – moisture content of the studied coal sample dried at 105°C for 2 hours, %;

Q^{sun} – rate of temperature change in the center due to heat transfer by air, °C/s, determined as:

$$Q^{sun} = \frac{\nu C_a \rho_a (T + \sum \Delta T - T_a)}{\gamma C_v V_v \Pi}, \quad (117)$$

where C_a – specific heat capacity of air, J/(mol·°C);

ρ_a – air density, kg/m³;

T_a – initial temperature of the supplied air, °C;

Q^{hle} – rate of temperature change in the center due to heat loss by evaporation, °C/s, determined as:

$$Q^{hle} = \frac{\nu r \mu}{\gamma C_v V_v \Pi R (T + \sum \Delta T)} (P_v - \phi P_{H_2O}), \quad (118)$$

where r – latent heat of water evaporation, J/m³;

μ – molecular weight of water, kg/mol;

P_v – vapor pressure of water above coal, N/m²;

ϕ – humidity of the supplied air, fractions of unit;

P_{H_2O} – vapor pressure of water over water, N/m².

10. Passport of endogenous fire hazard of coal seams

The research conducted above has allowed the formulation of some principles for practical purposes in the extraction of coal seams or sections prone to spontaneous combustion. It has also led to the development of a passport for such seams. This passport should be included in the regulatory documents and must be mandatory for completion before the extraction of each seam. It should contain all necessary information and clarifications required when evaluating the self-heating process of the seam, the occurrence, and subsequent extinguishing of an endogenous fire. The content of such a passport is outlined below.

Let's consider the passport of fire hazard for coal seams prone to spontaneous combustion. Spontaneous ignition of coal, as a self-accelerating process, is caused by the accumulation of heat in the coal pile due to its oxidation by oxygen from the air, and it sequentially goes through three stages: self-heating (warming), early stage of spontaneous ignition, and combustion (endogenous fire) and smoldering (extinguishing).

The self-heating (warming) stage begins after conditions are created in the coal pile for heat accumulation and occurs within a temperature range from the natural temperature characteristic for the coal seam within the mine field (20–50°C) to the critical temperature. The critical temperature for lignite coal is between 70 and 90°C, for hard coal – from 90 to 120°C, and for poor-quality coal – from 120 to 140°C, depending on the coal properties.

Self-heating (warming) of coal is activated when air flows into a sufficient accumulation of loose coal masses with increased chemical activity. Self-heating is caused by the ability of coal to interact with oxygen. During the self-heating (warming) stage, moisture evaporates, which activates the oxidation process of coal, gradually increasing the temperature in the coal pile. In this process, micro-impurities of carbon monoxide and unsaturated hydrocarbons, such as ethylene and acetylene, appear in the surrounding air.

The duration of the self-heating (warming) stage depends on the natural temperature of the surrounding rocks, coal moisture, natural and residual gas content, coal porosity, volatile substance content, ash content, and other factors, and can range from several to 15–30 days.

When the critical temperature is reached in the coal pile, a sharp increase in the rate of coal oxidation begins. The early stage of coal spontaneous ignition occurs within a temperature range from the critical temperature to the ignition temperature of volatile substances, which for lignite coal is between 150–200°C, for hard coal – from 300 to 350°C, and for poor-quality coal – from 600 to 700°C.

In the early stage of coal spontaneous ignition, the moisture evaporation process is completed, and intensive oxidation of coal begins. The oxygen content in the air surrounding the coal pile decreases, and the emission of carbon monoxide and dioxide, hydrogen, and saturated and unsaturated hydrocarbons increases.

The duration of this stage, under favorable conditions, can range from several hours to 1–2 days. The following condition indicates these stages:

$$(\text{CO} - \text{CO}_f) / (\text{H}_2 - \text{H}_{2f}) > 10,$$

were

CO, H₂ – gas content in the mine air, %;

CO_f, H_{2f} – background gas content in the mine air, %.

The combustion (endogenous fire) stage is characterized by a temperature exceeding the ignition temperature of volatile substances. Signs of this stage include the smell of burning and sublimation products, the presence of smoke, glowing coal, and open flames.

The distinctive feature of this stage is the condition:

$$(\text{CO} - \text{CO}_f) / (\text{H}_2 - \text{H}_{2f}) < 10,$$

were

CO, H₂ – gas content in the mine air, %;

CO_f, H_{2f} – background gas content in the mine air, %.

During the self-heating and early stages of coal spontaneous ignition, the increase in ethylene content exceeds the increase in acetylene content in the surrounding atmosphere, which allows for the control of the temperature in the coal pile. At the combustion (endogenous fire) stage, depending on the mass of the coal pile, both the further increase in ethylene and acetylene content and their sharp decrease can occur, making it impossible to determine the temperature of the coal in the pile.

The purpose of the fire hazard passport for the coal seam is to determine the indicators that define the stages of coal spontaneous ignition during the extraction of the coal seam under specific mining and geological conditions. This will allow for the timely determination of measures to prevent the combustion stage (Table 7).

Indicators of the spontaneous combustion hazard of the coal seam

Table 7.

№	Indicator		Unit
1	Group of spontaneous combustion hazard of the coal seam		
2	Group of spontaneous combustion hazard of the coal seam in areas of geological faults		
3	Natural temperature characteristic of the coal seam within the mine field	–	T _n , °C
4	Critical temperature	–	T _{cr} , °C
5	Temperatures of ignition of volatile compounds	–	T _v , °C
6.	Content of volatile matter		V ^{daf} , %
7	Background concentration in mine air		
7.1	ethylene	–	C ₂ H _{4f} , %
7.2	acetylene	–	C ₂ H _{2f} , %
8	Induction period of coal spontaneous combustion	–	t _{in.} , days
9.	Thermal and physical properties of coal		
9.1	thermal conductivity	-	λ, W/m·K
9.2	thermal diffusivity	-	α, mm ² /s
9.3	specific heat capacity	-	c _p , J/kg·K

The coal seam endogenous fire hazard passport is an integral part of the technological design documentation. The indicators of the coal seam endogenous fire hazard passport are taken into account when determining the procedures, methods, and timing of fire prevention measures to prevent underground fires caused by coal spontaneous combustion, in accordance with NPAOP 10.0–1.01.

In the technological design documentation, the coal seam endogenous fire hazard passport is included in the form of an explanatory note containing the justification of the decisions made, measures for preventing underground fires from coal spontaneous combustion, their timing and frequency, safety measures, and indicators of the coal seam endogenous fire hazard, presented as shown in Table 8.

Parameters of the coal seam spontaneous combustion hazard

Table 8.

Indicators, Signs, Actions	Coal spontaneous combustion														
	Self-heating (warming-up) stage					Early stage of spontaneous combustion					Combustion stage (endogenous fire)				
Indicators															
T _n , °C	T _n						T _{cr}			T _v					
CO, %	CO _f														
H ₂ , %	H _{2f}														
O ₂ , %	≥ 20														
CO ₂ , %	≤ 1														
C ₂ H ₄ , %	C ₂ H _{4f}														
C ₂ H _{4f} , %	C ₂ H _{4f}														
t, days	0									t _{in.}					
Signs	(CO-CO φ)/(H ₂ - H ₂ φ) > 10										(CO-CO φ)/(H ₂ - H ₂ φ) < 10				
	Emergence of trace amounts of carbon monoxide and unsaturated hydrocarbons, such as ethylene and acetylene					Reduction of oxygen concentration accompanied by enhanced release of CO and CO ₂ , hydrogen, and saturated as well as unsaturated hydrocarbons					Detection of smoke odor and sublimation products, along with visible smoke, red-hot coal, and open flames				
Actions	Drafting a report on early indicators of coal spontaneous combustion, and planning and executing preventive measures against coal spontaneous combustion fires										Implementation of the Emergency Response Plan				

11. The issue of determining the lower explosion limits of coal dust, the release of volatile substances from the coal seam, and the norms of slagging *

The main factors determining the explosiveness of coal dust are the particle size distribution of the coal dust, the release of volatile substances, the ash content in coal, moisture, and others. As is well known, dust explosions involve particles starting from 0.75-1 microns in size, and the explosiveness of coal dust continuously increases with the increasing degree of dust dispersion [57, 61]. The spread of the explosion throughout the entire dust cloud is possible if it has sufficient density. The minimum concentration of the dust cloud, at which the dust is still capable of exploding, is called the lower explosion limit of suspended coal dust. For settled dust, the lower explosion limit refers to its minimum quantity, relative to a unit volume, at which the explosion can still spread across the dusted area.

Among all the hazards of mining operations and the accidents they cause, the most severe in terms of social and economic consequences are coal dust explosions [62]. For instance, as a result of an explosion at the O. F. Zasyadko mine (November 2007), the number of fatalities reached over one hundred.

11.1. The issue of preventing dust formation and dust protection in mines

The essential conditions for the initiation and propagation of coal dust explosions in mines include: a suspended cloud of coal dust with explosive properties at a concentration exceeding the lower explosive limit for that particular dust; and an ignition source with sufficient energy and duration of exposure to the dust cloud, exceeding the induction period for the explosion of suspended dust.

A necessary condition for the propagation of a dust explosion along mine workings is the presence of loose deposited coal dust on surfaces, which under certain conditions can become airborne, forming a dust cloud of explosive concentration. It should be noted that unlike gas explosions, where the explosive atmosphere forms as a result of diffusive mixing, dust explosions require additional energy to create a certain volume of suspended dust at explosive concentration. In industrial conditions, energy sources may include a gas explosion or flash, gas-dynamic phenomena, blasting operations, and other dynamic impacts on deposited dust. Although such a combination of time and space conditions required for the initiation and propagation of coal dust explosions is unlikely, explosions do occur in mines.

The main causes of coal dust explosions in mines are, on one hand, the unsatisfactory state of dust control measures during the main production processes of coal extraction and transportation, which are accompanied by high dust generation and intensive dust deposition throughout the mine workings; and on the other hand, gross violations of safety regulations regarding the maintenance of dust control regimes and effective monitoring of dust explosion safety. From a practical standpoint, the lower explosive limit of deposited coal dust is one of the most critical regulatory indicators that characterize the explosion hazard of mine workings.

As established in [60, 61], the main sources of dust generation and entry into the mine atmosphere are coal extraction and mine development processes. In the overall dust balance of a mine, these sources typically account for 85–90% of total dust emissions. The remaining 10–15% originates from coal (rock mass) transportation, loading/unloading processes, and other sources [62]. This distribution of source intensity defines the main directions for implementing existing and developing new methods and means of dust control in mines. These methods generally include:

1. Preventing dust formation during coal (rock mass) destruction by binding dust particles initially present in the pores and fractures of the rock through pre-wetting with liquid under high pressure (typically up to 30 MPa or more).
2. Reducing dust generation during the operation of mining machines by improving the design of cutting elements and optimizing rock destruction regimes to minimize the output of fine fractions, including dust.
3. Binding and settling of dust particles through the supply of spraying liquid (water, wetting agent solutions, emulsions, foams, etc.) to dust generation and emission zones during machine operations – i.e., dust suppression by irrigation. This is one of the most widespread and effective methods in coal mines.

4. Preventing the entry of unsettled suspended dust into the general ventilation flow by isolating the source of dust generation and directing it to dust collection devices – i.e., dust extraction systems.
5. Limiting the transverse spread of suspended dust in the area around the mining machine to improve the effectiveness of irrigation and dust extraction by isolating dust-laden airflows from direct influence of strong ventilation streams in zones of formation, movement, and interaction with dust control means. This method is considered the most promising, especially in high-productivity longwall mining.
6. Preventing (or reducing the intensity of) dust release into adjacent workings during main technological operations by cleaning outgoing ventilation airflows from dust using water (air-water) curtains or dust collection devices.

Water-air curtains are commonly used in mines but are less effective when ventilation airflow exceeds 2 m/s. Given that allowable airflow velocities in production workings can reach 6 m/s or more under certain conditions (including the use of dust trapping and air-cleaning devices), solving this issue is urgent.

Thus, the only widely used dust control method in mines is irrigation. Dust suppression systems have been developed and implemented for mining and development machines that supply water to each cutting pick for efficient dust suppression and ejector-based air-dust removal, while also providing protection against frictional ignition of coal dust-methane-air mixtures (CDMAM) near operating machines.

Operational experience shows that in many Ukrainian coal mines, mining and development machines are equipped with primitive, retrofitted irrigation devices that do not supply water to each pick. Moreover, contaminated (untreated) mine water is often used, significantly reducing system reliability and dust suppression efficiency. Devices for controlling dust suppression parameters and machine interlocks are often tampered with or disabled.

According to most researchers, priority areas for further R&D in dust control in mines include the development and creation of:

- Schemes and equipment for high-pressure irrigation, delivering water directly to the cutting zone of coal or rock to ensure effective protection against CDMAM frictional ignition.
- Highly reliable sprinklers that provide the most effective dust suppression parameters.
- Filtering devices to protect dust suppression systems from mechanical impurities larger than 200 μm , or over 50 μm when using high-pressure irrigation.
- Dust extraction systems for longwall and development workings that provide localized isolation and extraction of dust-laden flows away from the main working area.
- Effective methods and rational schemes of dust suppression for auxiliary technological processes, including transportation of mechanized support sections, loading/unloading operations, and cleaning dust from outgoing airflows.

Currently, the coal industry lacks reliable and operational methods and tools for objectively monitoring the quality of implemented coal dust explosion protection measures and the overall level of explosion safety in mine workings. Ongoing control of these measures is entrusted to mine personnel, while periodic inspections are carried out by specialists from the State Paramilitary Mine Rescue Service (SPMRS).

In deep mines, the most effective wet methods for preventing coal dust explosions are practically not used due to the potential deterioration of sanitary and hygienic conditions. However, this issue can be addressed by applying hygroscopic wetting and binding compounds, which provide a protective effect that lasts several times longer than traditional wet cleaning or dust spraying.

To protect areas of mine workings where conventional water or rock dust barriers cannot be installed (such as short preparatory workings, distribution stations, areas with concentrated electrical equipment, or junctions

between longwalls and roadways), automatic explosion protection systems of the SLVA and SVShA types have been developed. These systems are designed to localize and suppress explosions at the earliest stage of development.

Nevertheless, many mines continue to rely on film-based polyethylene container barriers (PBS type), which have proven to be insufficiently effective in localizing coal dust explosions. Investigations of past accidents have confirmed their limited efficiency.

In practice, mechanical rock dusters and self-propelled units for cleaning mine workings from dust and applying binding solutions are rarely used. Instead, these tasks are typically performed manually, which significantly increases labor intensity and compromises the quality of explosion prevention measures.

It is important to emphasize that coal dust explosions in mines can and should be completely eliminated through the systematic implementation of available explosion protection technologies and consistent monitoring of explosion safety conditions in mine workings.

11.2. Determination of volatile matter output from coal seam

The determination of volatile matter output from coal seams and the lower limits of coal dust explosiveness are conducted to assess the danger of coal seams to dust explosions and to develop methods and means for dust explosion protection. As is known, the most important characteristic of all types of solid combustible minerals is their ability to undergo thermal transformations when heated without access to air. All types of solid fuels contain combustible components and a significant amount of non-combustible material (ballast) (Figure 29) [67]. Determining the volatile matter output is a traditional method for coal analysis. In nearly all existing coal classifications, volatile matter output is one of the primary indicators.

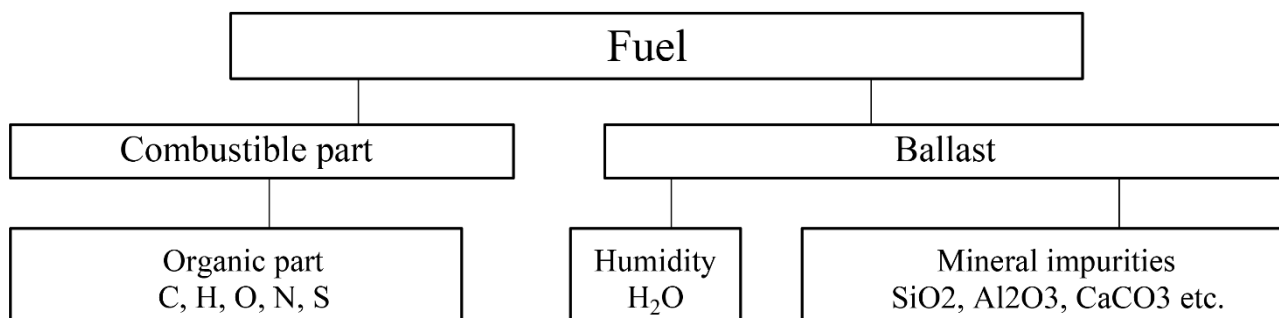


Fig. 29. Components of solid fuel

To determine the volatile matter output from coal seams in Ukrainian coal mines, the Institute of Geotechnical Mining Technology (IGTM) of the National Academy of Sciences of Ukraine has developed a regulatory guideline [56]. This guideline sets the procedure for determining volatile matter output for coal, the lower limits of coal dust explosiveness, and the methodology for correcting the norms of slaking. This guideline applies to all economic entities regardless of ownership form, whose activities are related to the design, construction, and operation of coal mines hazardous due to coal dust explosions. The following terms are used in this guideline with the following meanings:

- Analytical sample: A representative portion of a sample obtained from the laboratory sample, crushed to 0-0.2 mm, and intended for analysis;
- Analytical state of fuel (upper index a): A state of fuel characterized by sample preparation, including grinding to a particle size of less than 0.2 mm (or to a size specified by special analysis methods), and adjusting the moisture content of the fuel to an equilibrium state with the humidity of the laboratory

environment;

- Brown coal: Coal of lower carbonification, formed from peat as a result of diagenesis;
- Hard coal: Coal of medium carbonification, formed from brown coal as a result of metamorphism;
- Laboratory sample: A representative portion of the sample obtained by processing the combined sample to a particle size of 0-3 mm, and intended for laboratory tests and preparation of analytical samples;
- Weighing: The precisely weighed amount of substance for chemical reaction or analysis;
- Combined sample: A sample consisting of a required number of spot samples taken directly from the batch of fuel and characterizing its average quality;
- Dry ash-free state of fuel (upper index daf): A conditional state of fuel that contains no moisture or ash.

It is important to note that to clarify the essence of the method for determining volatile matter output, we will examine the scheme of processes occurring during the heating of coal. Coal contains various types of water: external, hygroscopic, constitutional, and hydrous (in mineral impurities). It is considered that during heating, coal primarily releases occluded gases, external moisture, and hygroscopic moisture. This release begins at relatively low temperatures, up to 100°C. Other types of moisture (not to be confused with decomposition water or pyrogenic water) are released at much higher temperatures than 100°C.

Simultaneously with the release of moisture, humic acids in young coals begin to decompose, releasing CO₂. In peat, this decomposition begins at 105°C, water release begins at 120°C, and tar begins to be released at 200°C. In brown coal, the decomposition processes occur at higher temperatures. Between 280–340°C, CO₂, oxygen, and hydrogen sulfide are released. In all coals, between 350–500°C, primary tar and primary gas are released, including H₂, CO, CO₂, CH₄, and others. At 500–600°C, primary product release ends, and at 700–800°C, coking occurs, releasing coke tar and coke gas. However, volatile matter release does not stop here. At 800–850°C, carbonates decompose, releasing CO₂. At 1000°C, the solid residue (coke) contains about 0.5% hydrogen and about 3% oxygen.

During volatile matter determination, all these processes occur vigorously, and during moisture evaporation, a significant amount of heat is absorbed (about 600 cal per 1g of water). Many secondary decomposition processes of the released liquid and gaseous products are also endothermic, meaning they absorb heat. The space (furnace or flames) around the crucible cools when introducing a cold crucible and during the violent release of volatiles, which slows down the coal decomposition process and volatile release. However, since the thermal power of the burner flame or electric furnace is relatively significant compared to the crucible size, the temperature quickly restores, and volatile release continues. For the same coal, the higher the temperature and the longer the heating time, the more volatile products are released. Therefore, all methods for determining volatile matter involve setting the heating time and temperature to obtain comparative results. Thus, taking into account the above, volatile substances in solid fuel minerals are understood as a mixture of gaseous and vaporous products formed during their heating without air access. The solid residue obtained in this process represents the product of thermal transformations of organic and mineral substances in solid fuel minerals, which in the case of the solidified product is called crucible coke or coal tar.

The volatile matter output and the characteristics of the solid residue are part of various scientific and technological classifications of solid fuel minerals. These indicators depend on the degree of metamorphism and the parent materials of solid fuel minerals.

Thus, despite its apparent simplicity and ease, determining the volatile matter output is a complex process of coal decomposition and is therefore an extremely sensitive analysis. To obtain fully comparable results, standard conditions for determination must be strictly followed, as even the slightest deviation from these conditions can significantly distort the analysis results. The general principle for determining volatile matter output is established for all types of solid mineral fuels, while the conditions for determination differ for the group of hard coal (hard coal, anthracite, bituminous shales, coal briquettes, beneficiation products) and for the group of brown coal (lignites, brown coal, brown coal briquettes, processing products).

Sampling of coal in the mine. When developing coal seams with volatile matter output of less than 15% (except anthracites) and when opening new coal seams, samples should be taken and sent to the laboratory for testing their dust explosiveness and determining the lower limits and slaking norms. The coal sampling for testing is carried out by the technical control department worker in the presence of the ventilation and safety manager (or their deputy or assistant) and the representative of the state mine rescue service (DVRG). Samples are taken from the working face by striking a 10-20 cm wide strip of coal from the roof to the floor along the entire seam thickness to a depth of 10-20 cm.

For thick seams developed using a layer separation system, samples are taken from the entire thickness of the extracted layer. When it is not possible to sample directly from the face, sampling from the wagons is allowed. In this case, samples are taken from several (but no fewer than three) wagons. To do this, 1 kg of coal is taken in turn from the following locations along the length of the wagon: from the middle of the first half, from the center, and from the middle of the second half. From the collected sample (primary), visible rock is discarded. The sample is crushed on a metal sheet or a wooden shelf covered with roofing iron to a grain size of no more than 10 mm, then it is mixed using the cone method and reduced by quartering to 1 kg. After that, the sample is placed in two jars of 0.5 kg each. The jars with the samples are labeled with the required information as specified in the form provided in Appendix A of this guideline. Other label copies are wrapped in paper and placed in the sample jars. After filling the jars with coal dust, they are tightly closed, and for hermetic sealing, the lid's cut area is wrapped with insulating tape in three or four layers. One jar with the sample is sent to the laboratory of a specialized (profile) institution for dust explosiveness testing, and the other – the control sample – is stored at the mine until test results are received. Samples sent for testing to the IGTM NASU laboratory are accompanied by a letter signed by the chief engineer of the mine. The laboratory conducts testing within 15 days of receiving the samples and sends the test results to the mine (enrichment plant).

Sample Processing. The initial sample can weigh from 0.5 to 3 kilograms. For analysis, the sample mass should not exceed 0.5 - 2 grams, so the sample needs to be reduced. The processing of initial samples consists of the following operations: crushing, mixing, and reducing. The primary sample is first crushed, with larger pieces being manually broken down. Then, the processing of the combined sample with pieces up to 150 mm is carried out in two stages. The first stage is crushing the fuel from its initial size to 0 - 3 mm or 0 - 10 mm for preparing the laboratory sample. The second stage is crushing from this size to the final size of 0 - 0.2 mm — an analytical sample for performing subsequent analyses. Laboratory samples are taken to determine the content of working or laboratory moisture, after which laboratory samples are processed into analytical samples. The analytical fuel sample is used to determine the physical and chemical quality indicators of the fuel. Moisture determination in the analytical sample is necessary for recalculating the indicators to dry and other states of the fuel, as well as to make corrections to the results of determining such indicators as volatile matter content.

There are two methods for preparing analytical samples of brown and hard coal: the conventional and accelerated methods. They differ in the drying regimes of the samples. In both cases, a coal sample weighing about 500 grams is poured onto a metal sheet in a layer no more than 10 mm thick.

In the conventional method, the weighed metal sheet with the sample is placed in a pre-heated electric drying oven (50 ± 5)°C and dried to an air-dry state. Drying time for brown coal and combustible shales is 4 - 5 hours, for hard coal - 3 hours, and for anthracite – 2 - 3 hours. During drying, the sample is mixed every 30 minutes.

In the accelerated method for preparing the analytical sample, the laboratory sample is dried at a temperature of (130 ± 5) °C for 15 minutes.

After drying and cooling to room temperature, the laboratory sample is ground in a mill or crushed in a porcelain mortar to a size of no more than 200 microns. The ground sample is left on a metal sheet at room temperature for at least 12 hours, after which it is thoroughly mixed, leveled, and an analytical sample of no less than 100 - 125 grams is taken from various spots. The sample is placed in a jar, labeled, tightly closed with a lid, and sent for analysis.

Determining Volatile Matter. The sample is heated without access to air at 900°C for 7 minutes. The volatile matter yield, in percent, is calculated based on the mass loss of the sample, subtracting the mass loss due to the moisture content of the sample. A muffle furnace with electric heating and a constant temperature zone

$(900 \pm 5)^{\circ}\text{C}$ is used for laboratory testing. The temperature of 900°C should be maintained as precisely as possible. An acceptable deviation of $\pm 5^{\circ}\text{C}$ includes measurement errors and temperature distribution inhomogeneity. If the temperature fluctuates in the muffle furnace by more than $\pm 10^{\circ}\text{C}$, the volatile matter output values exceed the established limits. To meet these requirements, the furnace must have a zone with a stable temperature, controlled by a thermocouple (Figure 30).

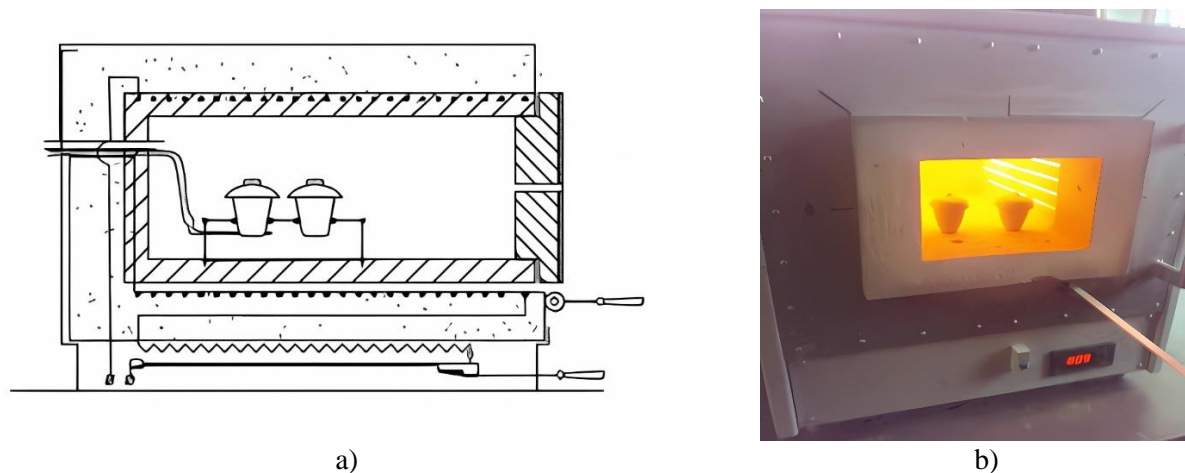


Fig. 30. Muffle Furnace: a) general view; b) during testing

The thermal power of the muffle furnace should be such that after placing a cold stand with crucibles inside, the temperature inside the furnace should reach 900°C within no more than 4 minutes. If not, the test is repeated. The stand with the crucibles is placed in the furnace's stable temperature zone and this position is used for all determinations.

Crucibles for volatile matter determination. Porcelain or quartz conical crucibles with ground lids are used, which allow the free removal of volatile matter but prevent oxygen from penetrating. The mass of the crucible with the lid should be between 10 and 14 grams. The lid must fit tightly on the crucible, with a horizontal gap of no more than 0.5 mm. The lid is ground to the crucible using mechanical rotation, forming a groove on the inner surface of the lid.

The fitting of lids to porcelain crucibles is carried out mechanically by rotating the lid until a groove forms on its inner surface. This process ensures that the lid seats properly, providing a tight and secure fit with the crucible. For accurate and reliable analysis, it is crucial that the lid adheres closely to the crucible, preventing any gas or material leakage during the experiment. Therefore, the fit of the lid must be carefully checked each time before commencing the procedure, as shown in Figure 31.

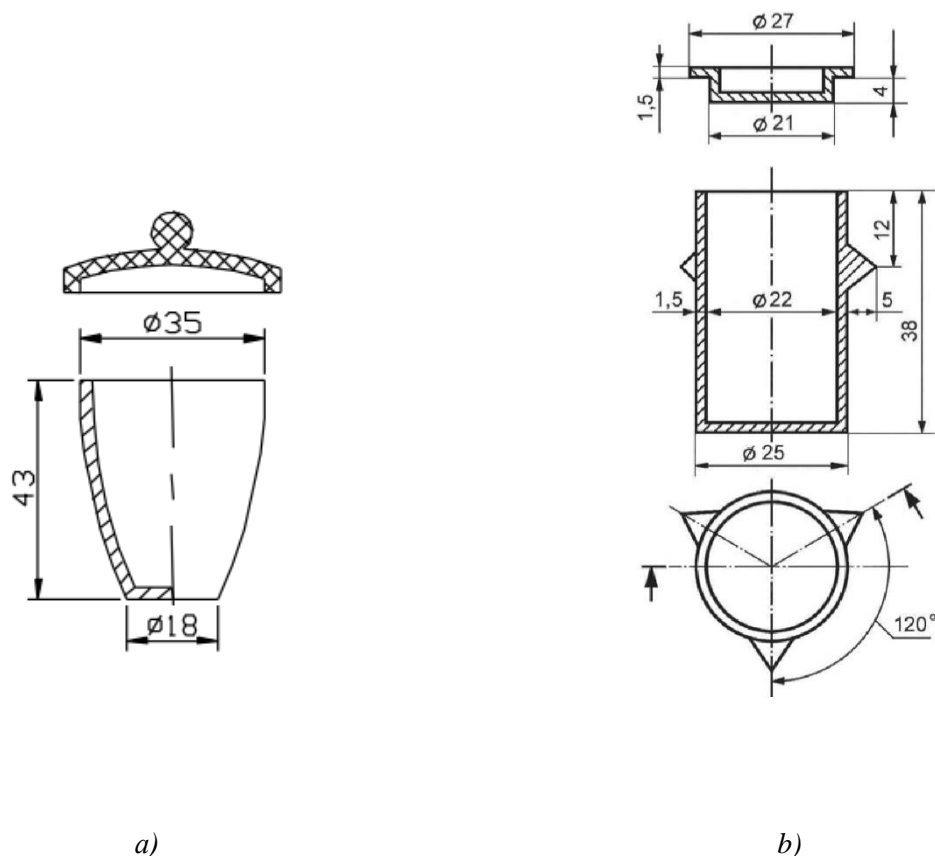


Fig. 31. Crucible with cover: a) porcelain; b) quartz

Crucibles with fitted and ground lids must be marked uniformly, fired at a temperature of $(900 \pm 5) ^\circ\text{C}$ to constant mass, and stored in a desiccator with a drying agent.

The support on which the crucibles are placed in the muffle furnace must ensure the prescribed heating rate. The following supports are allowed:

- For a single determination – a ring made of heat-resistant steel wire with a ceramic or asbestos disc 25 mm in diameter and 1.5–2 mm thick, placed on the internal projections of the support;
- For simultaneous determination of multiple samples (two, four, or six) – a frame made of heat-resistant steel wire with ceramic plates 2 mm thick for placing the crucibles, or a support made of heat-resistant sheet steel.

The cell dimensions in the supports must ensure that the distance between the crucible bottom and the furnace floor is approximately 20 mm.

Additionally, in laboratory conditions for testing, analytical balances with a weighing error of no more than 0.1 mg are used; balances with an error of up to 0.2 mg are permissible. A desiccator – a vessel maintaining a controlled air humidity (usually near zero), made of thick glass or plastic, where the tested substance is dried – is used. Crucible tongs 25–30 cm long, a special spoon or spatula for mixing samples and taking a sample portion are also employed.

Testing Procedure. The muffle furnace is heated to $(900 \pm 5)^{\circ}\text{C}$. The empty crucible with its lid is weighed. The analytical sample of fuel is mixed and a 1 ± 0.1 -gram sample is taken from two or three places at different depths. The crucible with the sample is covered with a lid and weighed. The crucibles are placed on the stand, and all free spaces on the stand are filled with empty crucibles with lids.

The stand with the crucibles is quickly placed in the muffle furnace and the furnace door is closed. The temperature in the furnace should return to $(900 \pm 5)^{\circ}\text{C}$ within no more than 4 minutes. Otherwise, the test is repeated. The stand with the crucibles is carefully removed from the furnace using tongs and cooled for 5 minutes on a metal or asbestos plate. Without removing the lids, the crucibles are transferred using tongs to the desiccator to cool to room temperature. After cooling, the crucibles are weighed to an accuracy of 0.1 mg. If black deposits appear on the outer surface of the crucible or its lid, the determination is repeated.

The non-volatile residue (coke) left in the crucible after volatile matter determination is characterized based on its appearance and strength: powdery; sticky (breaks into powder when lightly pressed with a finger); weakly sintered (breaks into separate pieces with light finger pressure); sintered, not fused (requires effort to break into separate pieces); fused, not swollen (flat disc with a silvery metallic surface); fused, swollen (swollen non-volatile residue with a silvery metallic surface, less than 15 mm high); fused, strongly swollen (swollen non-volatile residue with a silvery metallic surface, more than 15 mm high).

For coal with a volatile matter content greater than 20%, if the non-volatile residue is powdery or sticky, the test is repeated with briquetted samples, and the volatile matter yield is calculated based on the second test results.

In the case of testing coal with a volatile substance content of more than 20%, where the residue is powdery or sticky and non-volatile, the test is repeated with briquetted samples of this coal, and the volatile matter is calculated based on the results of the second test. The non-volatile residue in this case is characterized by the result of the non-briquetted sample.

When determining the volatile matter yield for brown coal samples, as well as for hard coal samples with volatile matter content greater than 20%, which produce a powdery or sticky non-volatile residue, the samples are pre-briquetted in a laboratory press.

In the processing of results, the average value of the volatile matter yield in the analytical sample is determined using the formula, %:

$$V_{av}^a = \frac{V_1^a + V_2^a}{2}, \quad (119)$$

The volatile matter yield, recalculated for the combustible mass in %, is calculated using the formula:

$$V^{daf} = V_{av}^a \frac{100}{100 - W^a - A^a}, \quad (120)$$

where W^a, A^a – the moisture and ash content of the analytical sample of the coal under study, %.

The volatile matter yield for the working mass of coal is calculated using the formula, %:

$$V^r = V_{av}^a \frac{100 - W^r}{100 - W^a}, \quad (121)$$

where W^r – the moisture content in the working mass of the coal, %.

The yield of the non-volatile residue (coke) from the analytical sample of coal, %:

$$(NV)^a = 100 - V^r - W^r, \quad (122)$$

Test results are calculated to two decimal places, and the final result is rounded to one decimal place. The volatile matter yield in each sample is determined in parallel for two portions. The final result is accepted as the arithmetic mean within the allowable discrepancies.

The allowable discrepancies between the results of two parallel volatile matter determinations for a single analytical sample should not exceed the values specified in Table 10.

Allowable errors in volatile matter determination

Table 10.

Volatile matter content, %	Allowable deviations of the measured results	
	in a single laboratory, %	in different laboratories, %
up to 10	0.3 abs.	0.3 abs.
more than 10	3.0 from the mean result	4.0 of the larger result

Otherwise, a third measurement is performed. The final result is taken as the arithmetic mean of the two closest values.

11.3. Determination of slaking norms and lower explosion limits of coal dust

Coal seams with a volatile substance content of 15% or more, as well as coal seams (excluding anthracites) with a lower volatile substance content, the explosiveness of whose dust has been established through laboratory testing, are considered hazardous with respect to dust explosions.

The lower explosion limits of dust and the slaking norms are determined in the laboratory: for coal from mining seams being developed, with a volatile substance content of less than 15% (excluding anthracites) – annually; for newly put into operation mining seams – before their commissioning; for coal from mining seams being exploited, with a volatile substance content of 15% or more – once every three years. Coal from all newly commissioned mining seams is also subject to testing.

The volatile matter yield (V^{daf}) of a mining seam is determined in the laboratory of the institute when the actual volatile matter yield (V^{daf}) data from the WTC changes by more than 10% for at least 2 months from the stable background values, but not less than once every 3 years. The lower explosion limits of dust and the slaking norms for coal seams with a volatile substance content of 15 to 30% are determined and adjusted according to the normative methodology [58], and for newly commissioned mining seams – based on laboratory test results. Repeated determination of the lower explosion limits of dust and adjustment of slaking norms is performed once a year.

In mines developing seams that are hazardous due to dust, measures must be implemented to combat coal dust explosions, based on the use of inert dust (shale dust), water (hydrodust explosion protection), or a combination of water and inert dust (combined dust protection).

To ensure reliable dust explosion protection in mines, the amount of coal dust deposited in mine workings should not exceed the lower limit of its explosiveness (the maximum permissible amount of coal dust in g/m³, which is not hazardous with respect to explosion). Additionally, when slaking is used, the ash content of the slaked dust must not be lower than the slaking norm established for that particular mining seam.

The control of dust explosion safety in mine workings is carried out by the DVGRS workers in the presence of a mine representative, visually at least once a quarter according to a plan developed together with the mine. If, as a result of a visual inspection, the working face is found to be explosion-hazardous, dust samples are taken for laboratory analysis.

In mine workings with hydrodust explosion protection, coal dust samples are taken for laboratory determination of moisture content, and in slaked workings – dust samples are taken to check for the presence of non-combustible substances. At operating coal enrichment plants, the dust regime is introduced by an order from the enterprise based on control tests of coal dust explosiveness conducted in the laboratory and the mine's data on gas emission from coal seams. The results of explosiveness tests for coal dust are sent to the enterprise within 30 days. Repeated tests are conducted once every 3 years, and in case of changes in the raw material base, unscheduled testing is carried out.

The lower explosion limits of dust δ_{sc} (g/m³) for coal seams with a volatile substance content (V^{daf}) from 15 to 30% are determined based on the volatile matter yield and the content of non-combustible substances (A_f) using a nomogram for determining the lower explosion limits of deposited coal dust, as shown in Figures 32 and 33.

$$\delta_{sc} = 262,5 \cdot \exp(-0,07 \cdot V^{daf}) + 3,3 \cdot \exp(-0,06 \cdot V^{daf}) \cdot A_f, \quad (123)$$

where V^{daf} – the volatile substance yield, %;

A_f – the content of non-combustible substances in the coal, %. These characteristics of the coal are determined based on laboratory research results.

If the content of non-combustible substances in the seam sample exceeds 30%, the value of the non-combustible substance content for determining dust explosiveness is assumed to be 30%.

At mines developing coal seams with a volatile substance content of 15% or more, if there is a change in the volatile substance yield (V^{daf}) or the content of non-combustible substances (A_f) by more than 1% according to the mine's data, the head of the Mine Safety Department must adjust the lower explosion limits of dust and the slaking norms. Slaking norms for seams with volatile substance contents from 15 to 30% are adjusted as follows. First, the addition of inert dust is adjusted using the formula:

$$D_c = D_k - a(V_k^g - V_f^g) + b(A_k - A_f), \quad (124)$$

where D_c – the corrected addition, %;

D_k, V_k^g – the addition of inert dust and volatile substance yield, as established by laboratory tests for this mining seam respectively, %;

A_k – the content of non-combustible substances in the coal for this mining seam, determined by laboratory tests;

V_f^g, A_f – respectively, the volatile substance yield and content of non-combustible substances in the most recent seam sample according to the mine's data, %;

a, b – coefficients that account for the impact of changes in volatile substance yield and non-combustible substance content on the addition size. The values of the coefficients a and b are given in Table 11.

Values of coefficients a and b depending on V_k^g

Table 11.

V_k^g	15	16	17	18	19	20	21	22	23	24	25	26	27	28	29	30
a	2,0	1,7	1,3	1,3	1,3	1,2	1,2	1,0	1,0	0,8	0,8	0,6	0,6	0,5	0,4	0,4
b	0,74	0,66	0,59	0,54	0,5	0,46	0,43	0,4	0,38	0,36	0,34	0,33	0,31	0,3	0,29	0,28

The corrected inert dust addition standard is calculated according to the formula:

$$N_c = \frac{A_f(100 - D_c)}{100} + D_c, \% \quad (125)$$

The inert dust addition is determined for coal with a volatile matter content of 15% or more using the nomogram for determining inert dust addition shown in Figures 32 and 33. The grounding standard for the main mine-wide roadways (common to all seams) is taken as the highest of the standards established for the seams mined by the given mine, while for group roadways it is taken as the highest within the group of seams being mined. The results of coal dust explosiveness tests conducted in the laboratory are documented in a report.

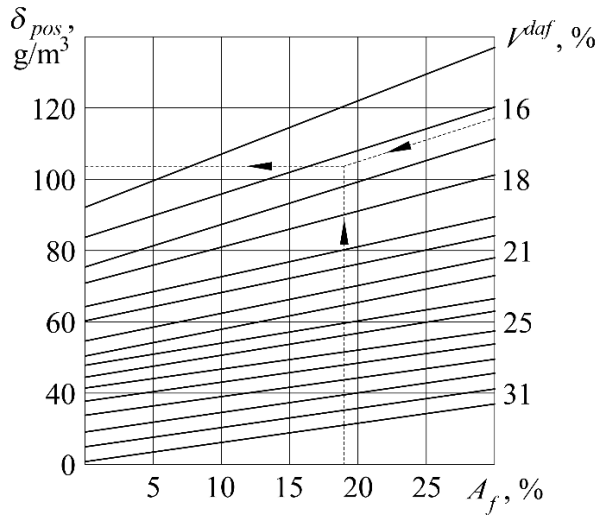


Fig. 32. Nomogram for assessing the lower explosive limits of deposited coal dust

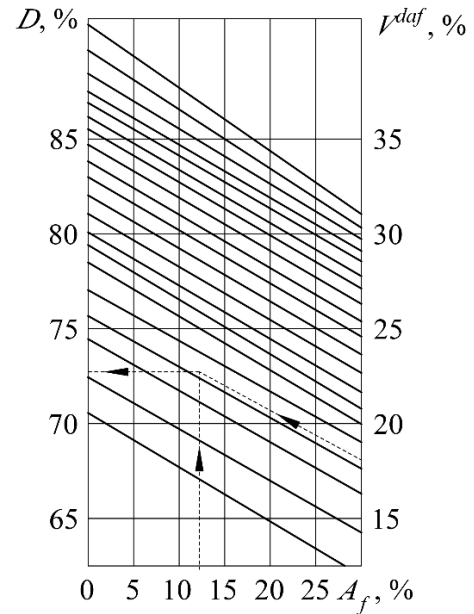


Fig. 33. Nomogram for assessing the required inert dust addition

The content of non-combustible matter in a seam sample of hard coal, when determining the lower explosive limit of deposited dust and adjusting the grounding standard, should not exceed the content of non-combustible matter in the marketable coal of the respective coal seam. If the content exceeds 30%, it is taken as 30%. For brown coal with a non-combustible matter content above 30%, the lower explosive limit of deposited dust is assumed to be 48 g/m³.

12. Selected results of the volatile matter content of the coal seam, coal dust lower explosive limits, and inert dust addition standards

The results of determining the characteristics of the seam, including the volatile matter yield of the coal seam, the lower explosive limits of coal dust, and the grounding standards, obtained according to the methodology described above for several coal mines in Ukraine, are presented below (see Table 12).

Results of coal dust explosiveness tests, volatile matter yield, and grounding standards conducted in the laboratory of the Department for Managing Dynamic Manifestations of Rock Pressure, IGTM NAS of Ukraine, Dnipro

Table 12

Sample No.	Mine management, Mine, Concentration plant, etc.	Name or geological symbol of the coal seam, date of measurements	Name and place of sampling	Content of non-flammable substances $Ac+(CO_2)_k$, %	Volatile substances output V^{def} , %	Lower explosion limit of deposited coal dust δ_{dep} , g/m ³	Addition of inert dust D, %	Norm of rock-dusting N, %
002	SE "Krasnolyanskaya Coal Company"	seam l_3	windway of the 1st northern longwall №1 seam l_3 picet 15+17,5, right side $\Delta J=2,41$ mg/g, left side $\Delta J=2,13$ mg/g	21,95	32,94	36,20	83,42	87,06
003			windway of the 1st northern longwall №1 seam l_3 picet 15+19,0, right side $\Delta J=1,72$ mg/g, left side $\Delta J=1,96$ mg/g	20,86	32,09	37,81	83,74	87,13
004			windway of the 1st northern longwall №1 seam l_3 picet 15+13,0, pama 385, right side $\Delta J=1,90$ mg/g, left side $\Delta J=2,22$ mg/g	19,25	29,84	43,11	84,23	87,26
005			windway of the 1st northern longwall №1 seam l_3 picet 16+0,5, right side $\Delta J=2,16$ mg/g, left side $\Delta J=1,96$ mg/g	20,51	31,86	38,23	83,85	87,16
006			windway of the 1st northern longwall №1 seam l_3 picet 16+1,5, right side $\Delta J=2,92$ mg/g, left side $\Delta J=2,41$ mg/g	19,18	28,78	46,27	84,25	87,27
007			windway of the 1st northern longwall №1 seam l_3 picet 16+31, right side $\Delta J=1.78$ mg/g, left side $\Delta J=2,03$ mg/g	20,74	31,88	38,29	83,78	87,14

Sample No.	Mine management, Mine, Concentration plant, etc.	Name or geological symbol of the coal seam, date of measurements	Name and place of sampling	Content of non-flammable substances $Ac+(CO_2)_k$, %	Volatile substances output V_{daf} , %	Lower explosion limit of deposited coal dust δ_{dep} , g/m ³	Addition of inert dust D, %	Norm of rock-dusting N, %
001	LLC "1-3 Novogrodovka"	Hard coal, grade G (G1) energy 15.02	The sample was selected and distributed according to the state standard 4096-2002, seam 1 ₁ , 18 southern longwall	10,1	39,7	32,2	86,7	88,3
729	LLC "Central Factory "Kurakhovska"	coal, grade G (G1) 0-100 mm 11.19	The sample was selected and distributed according to the state standard 4096-2002, loading conveyor	8,6	41,2	28,9	87,4	88,5
719	LLC "ZF Coal Energy Complex"	hard coal, grade DG (0-100) 07.19	The sample was selected and distributed according to the state standard 4096-2002	32,2	41,1	49,8	80,3	86,7
001	Mine named after Heroes of Space	Coal seam C ₁₁ 1130 belt entry	The sample was selected and distributed according to the state standard 4096-2002	36,2	38,03	30,53	79,14	86,69
002		501 windway		35,5	39,75	27,03	79,35	86,68
001	Heroes of space mining management	Coal seam C ₅ 501 windway, 06.15	The sample was selected and distributed according to the state standard 4096-2002	35,4	39,70	27,09	79,38	86,68
004	Belozersk Mine	seam m ₄ ⁰ 08.21	Well No1, 672,4 m	25,9	34,2	58,93	82,23	86,83
005			Well. No2, 675,9 – 677,3 m	27,8	34,6	60,23	81,66	86,76
008	PRIVATE LIMITED "MINING MANAGEMENT "POKROVSKE"	seam d ₄ 06.24	2 southern belt entry block №9 pic. 200+8,0	10,53	24,05	62,20	86,84	88,23
009			2 southern belt entry block №9 pic. 200+8,0	10,75	24,54	61,31	86,78	88,20
010			2 southern belt entry block №9 pic. 201+0,0	9,86	22,51	65,16	87,04	88,32
011			2 southern belt entry block №9 pic. 201+0,0	10,78	24,61	61,18	86,77	88,19

Sample No.	Mine management, Mine, Concentration plant, etc.	Name or geological symbol of the coal seam, date of measurements	Name and place of sampling	Content of non-flammable substances $Ac+(CO_2)_k$, %	Volatile substances output V_{daf} , %	Lower explosion limit of deposited coal dust δ_{dep} , g/m ³	Addition of inert dust D, %	Norm of rock-dusting N, %
012			2 southern belt entry block №9 pic. 201+1,0	10,44	23,84	62,60	86,87	88,24
013			2 southern belt entry block №9 pic. 201+1,0	10,50	23,98	62,34	86,85	88,23
014			2 southern belt entry block №9 pic. 201+3,0	10,36	23,66	62,94	86,89	88,26
015			2 southern belt entry block №9 pic. 201+3,0	10,57	24,12	62,09	86,83	88,22
016			2 southern belt entry block №9 pic. 201+5,0	9,74	22,24	65,69	87,08	88,34
017			2 southern belt entry block №9 pic. 201+5,0	10,46	23,88	62,53	86,86	88,24
018	PRIVATE LIMITED "MINING MANAGEMENT "POKROVSKE"	seam d ₄ 06.24	Setup room No 1 block No. 10 picet 24+2,5	11,59	26,45	57,91	86,52	88,09
019			Setup room No 1 block No. 10 picet 24+2,5	11,49	26,23	58,29	86,55	88,10
020			Setup room No 1 block No. 10 picet 24+4,5	11,53	26,32	58,13	86,54	88,09
021			Setup room No 1 block No. 10 picet 24+4,5	11,51	26,28	58,20	56,55	88,10
022			Setup room No 1 block No. 10 picet 24+5,5	11,65	26,59	57,67	86,51	88,08
023			Setup room No 1 block No. 10 picet 24+5,5	11,73	26,78	57,34	86,48	88,07
024			Setup room No 1 block No. 10 picet 24+7,5	10,51	24,00	62,30	86,85	88,23
025			Setup room No 1 block No. 10 picet 24+7,5	11,63	26,55	57,74	86,51	88,08
026			Setup room No 1 block No. 10 picet 24+9,5	10,43	23,82	62,64	86,87	88,24
027			Setup room No 1 block No. 10 picet 24+9,5	10,55	24,09	62,13	86,84	88,22

13. The Issue of Reclassifying a Fire as Extinguished and the Specifics of Conducting Work in This Area

It is important to note that, from the safety perspective of operations, the issue of reclassifying a fire as extinguished, further uncovering of isolation barriers, restoring ventilation of the emergency area, and the ventilation of the entire working horizon are of significant importance. Only after this, the questions regarding further work in the fire zone area are considered [6, 8, 23, 35]. Let us examine these issues further.

13.1. Reclassification of Fires as Extinguished and Opening of Sections with Extinguished Fires

It should be noted that fires occurring at mining enterprises must be recorded, regardless of their location, causes, or consequences. The accounting of fires and their consequences is maintained by business entities, regardless of ownership forms, and by the Ministry of Energy – for mining enterprise facilities that fall under its jurisdiction. The official document confirming the fact of a fire is a fire report (act), which is drawn up by a commission of the enterprise with the involvement of representatives from the fire accounting authority and the rescue service that participated in extinguishing the fire.

Each endogenous fire is assigned a number according to the order of its detection at a given mine. A fire that reoccurs retains its original number, adding the letter "R" and the date of its recurrence. The location, number, and date of occurrence of an endogenous fire must be marked on all mine layout plans. Fires that have not been extinguished by active methods must be isolated with stoppings made of non-combustible materials; for gassy mines, explosion-proof stoppings are used.

The restoration and resumption of operational activities in isolated fire zones is permitted only after the fire has been officially decommissioned by a commission formed by the employer, with the participation of representatives from the territorial bodies of the State Labor Service, the Institute of Geotechnical Mechanics of the National Academy of Sciences of Ukraine (IGTM NASU), Dnipro University of Technology and Rescue Mining Units (DVGRC).

Signs of extinguished fire:

- Hydrogen and carbon monoxide are absent in air samples taken from the fire area, or their concentrations do not exceed background levels;
- The coal temperature in the fire zone, determined by the ratio of unsaturated hydrocarbons, is below the critical threshold for the given seam;
- The temperature of air and water coming from the isolated area does not exceed the typical values for isolated workings on that horizon by more than 3–5 °C.

The description of a fire should consider the combination of all these signs and their dynamics. The main indicators of an extinguished fire are the levels of carbon monoxide and hydrogen in the mine air samples from the fire area, which do not exceed background values. The determination of background values of carbon monoxide and hydrogen, used for making decisions about declaring a fire extinguished, is carried out by the enterprise in accordance with approved methodology.

DVGRC personnel must collect air samples once a year from the outgoing ventilation streams of mining areas, dead-end workings, mine seams, wings, and pipelines to analyze the content of carbon monoxide and hydrogen, as well as other thermophysical parameters, in accordance with regulatory documents. If the average (background) concentrations of carbon monoxide and hydrogen in degassing pipelines change by 50% or more, the mining area is reclassified as highly hazardous, and additional measures must be taken to assess fire hazards. Background values must be determined for all mine seams, regardless of the spontaneous combustion tendency of the coal. The technical director of the enterprise defines the locations for determining the background values of CO and H₂, based on the need for sufficient data to support fire-extinguishing decisions anywhere in the mine.

For fire zones where coal extraction or other activities (equipment dismantling, removal of metal supports, etc.) or mining from underlying seams are planned, monitoring must continue for at least two months after CO

and H_2 content returns to background levels or disappears. For other zones, at least one month is required. Samples must be taken every 15 days. Once reliable results are obtained confirming the absence of fire, it may be decommissioned.

Before fire decommissioning, monitoring periods must be:

- At least two months for areas planned for reopening or mining from nearby seams;;
- At least one month for areas with no such plans.

Sample collection should occur at least once every 10 days. The monitoring period may be shortened only upon conclusion from IGTM NASU. After reliable results confirming the fire's absence are obtained, it can be officially written off.

Exploration and reopening of zones with extinguished and written-off fires must be carried out according to a plan and project developed by the chief engineer of the mine, together with the commander of DVGRC, and formalized as technical work execution. The project must include:

- Results of air composition testing and zone condition monitoring before reopening;
- Worker safety measures;
- The method for reopening;
- Ventilation mode for the area;
- Conditions under which the area is considered ventilated;
- Conditions requiring cessation of ventilation and resealing of stoppings;
- Locations for air quality checks and temperature control, including CO , methane, hydrogen, ethylene, and acetylene in the outgoing stream;
- Plan and route for DVGRC unit movement based on copies of the mine layout plan.

The plan must also define:

- The procedure for inspecting the zone before reopening;
- Safety measures for removing stoppings (washing coal dust, applying rock dust, installing water or rock-dust barriers, preparing materials/tools for resealing, adjusting air flow, power shutdown, having gas detectors and first aid kits);
- Ventilation fan mode (main ventilation fans);
- Locations of methane sensors;
- Routes of DVGRC units shown on the surveyed mine plan;
- Locations of air sampling and temperature measurements.

Only DVGRC workers are allowed to carry out reopening, exploration, and initial ventilation. Persons not involved must be evacuated from the affected wing or the entire mine. During initial ventilation, all workers must be removed from areas where outgoing air from the reopened zone passes; power must be cut off. The outgoing stream from a reopened zone with an extinguished fire may be directed into the general mine airflow.

If CO , hydrogen, ethylene, or acetylene levels in the outgoing stream exceed background values, ventilation must be stopped and the stoppings resealed.

During ventilation planning, the concentration of combustible gases in the stream from the zone must not exceed 1%, and 0.75% in the mine's outgoing stream. During initial ventilation, methane content in the outgoing stream must not exceed 1%.

13.2. Mining Operations in Areas Affected by Fire Hazards

Mining operations in zones with potential penetration of combustion products and other hazardous fire-related factors must be conducted while leaving protective coal pillars, in accordance with the extraction district plan. This plan must include a dedicated section outlining the procedures for operations near fire-affected areas and additional safety measures.

Operational work is strictly prohibited in fire-affected areas where an active fire source remains in the goaf (mined-out space).

It is forbidden to conduct mining operations on adjacent seams near sections with active fires located less than 15 meters away. Likewise, longwall mining on steep or steeply inclined seams is not allowed in the lower extraction panels adjacent to the fire boundaries.

Mining on adjacent seams close to active fires and longwall mining on steep or steeply inclined seams in the lower-lying and adjoining extraction panels near the fire zone are also not permitted. However, the excavation of main entries (main drifts) on the lower horizon beneath an active fire, or beneath adjacent seams with fire sources, is allowed.

Ventilation entries on the lower horizon beneath an active fire or in adjacent seams lying under fire-affected seams may be developed with the approval of the State Labor Service of Ukraine. Their construction must be based on an approved project plan.

Mining beneath workings affected by extinguished and written-off fires on the same seam or on lower adjacent seams must be conducted according to a project approved by the technical director of the production association. This project should include measures to prevent possible fire reoccurrence, such as additional isolation of former fire zones, enhanced monitoring for early signs of coal self-ignition, and timely localization of any newly detected fire outbreaks.

Longwall operations near fire-affected zones must maintain barrier coal pillars. The width of these pillars is determined by calculation but must not be less than 20 meters, according to a special project. The project should also include enhanced sealing of isolation stoppings, constant monitoring of the fire source, and reliable ventilation of the working face. In gassy mines, the stoppings must be explosion-resistant.

If necessary, mining on adjacent seams beneath areas with extinguished and written-off fires – where there is aerodynamic connectivity through deformed interseam rock – must be conducted with complete backfilling of the goaf.

13.3. Methodology for Reclassifying a Fire as Extinguished and Conducting Work in the Affected Area

The process of reclassifying an underground fire as extinguished requires a comprehensive and systematic assessment of the fire source, the surrounding geological and atmospheric conditions, and all relevant safety parameters. This assessment ensures that both residual heat and hazardous gas concentrations are monitored and stabilized before any decision is made regarding re-entry or resumption of work. The methodology typically includes a series of structured steps, encompassing preliminary inspections, continuous temperature and gas monitoring, controlled safety verification, and the establishment of safe operational protocols for subsequent activities in the affected area. The methodology typically includes the following steps:

Preliminary Assessment:

- Conduct an initial inspection of the fire-affected area using available monitoring data (temperature, gas composition, smoke presence);
- Verify that all active combustion zones have ceased flaming and that the heat release from smoldering materials has decreased to safe, stable levels;
- Confirm that ventilation and gas extraction systems maintain oxygen levels within safe limits, reducing the risk of re-ignition.

Temperature and Gas Monitoring:

- Perform continuous measurement of the rock and air temperature in the fire zone and surrounding workings to ensure they do not exceed critical thresholds;
- Analyze gas composition, focusing on concentrations of carbon monoxide, methane, and other combustible or toxic gases;
- Compare readings to established safety criteria for re-entry, ensuring that both temperature and gas levels remain stable over a defined period.

Safety Verification and Clearance:

- Conduct a controlled inspection of the fire area using protective equipment, sensors, or remotely operated tools where necessary;
- Identify potential hotspots or residual smoldering zones and implement additional cooling or inertization if needed;
- Only after verifying that the fire source is fully stabilized and that environmental conditions comply with safety standards should the fire be officially reclassified as extinguished.

Procedures for Conducting Work Post-Fire:

- Establish safe access routes and ensure continuous monitoring of temperature and gas conditions during work;
- Implement strict operational protocols, including limiting personnel exposure time and equipping teams with gas detection and respiratory protection devices;
- Continue periodic checks of the area after work completion to promptly detect any signs of re-ignition.

Documentation and Reporting:

- Record all monitoring data, inspection results, and mitigation measures taken;
- Update fire safety plans and provide detailed guidance for future emergency response and re-entry operations.

This methodology ensures that the fire area is reclassified in a scientifically justified and safe manner, minimizing risks to personnel and equipment while enabling the resumption of mining operations or other planned work.

The reclassification of an underground fire as extinguished and the subsequent resumption of work in affected areas require a systematic, multi-stage approach that integrates continuous monitoring, safety verification, and strict operational protocols. Key steps include preliminary assessment of the fire zone, comprehensive temperature and gas monitoring, controlled verification of environmental stability, and establishment of safe access routes for post-fire operations. The methodology emphasizes adherence to regulatory thresholds for combustible gases and temperatures, the maintenance of barrier coal pillars, and the implementation of protective measures for personnel. Documentation of monitoring data, inspection results, and mitigation measures is essential to ensure that re-entry and mining activities are conducted safely and in a scientifically justified manner. This approach minimizes the risk of fire reoccurrence while enabling the controlled restoration of mining operations in previously affected areas.

Conclusions

Based on the conducted research, the following conclusions were drawn:

1. The airflow distribution in workings and goaf zones of the isolated ventilation district (IVD) was analyzed. A ventilation scheme for isolated workings was developed, accounting for air recirculation, counterflows, and differences in heat exchange conditions across various areas.
2. An analytical expression for air density was obtained as a function of humidity, methane content, and temperature dynamics. Research showed that humidity reduces air density by 25%; full replacement of air with methane can halve the gas mass in the emergency workings; heating air to 1000 °C increases its volume nearly threefold.
3. The heat balance model for the fire source within the IVD was developed. It enables forecasting the average air temperature in the source and surrounding rock mass, considering the temperature-dependent air density over a long period (up to several months after fire ignition).
4. Analytical relationships were derived for air temperature in the fire source and adjacent zones as functions of IVD aerodynamic parameters. This allows modeling how ventilation regimes affect the thermal regime of the IVD.
5. It was established that the fire's impact on the ventilation regime of the IVD is governed by three factors: thermal resistance coefficient, local thermal depression, and global thermal depression.
6. The findings allow for reliable forecasting of the ventilation regime at various stages of accident mitigation. Mathematical modeling helps assess the feasibility and effectiveness of different ventilation and fire suppression methods.
7. The process of indicator gas release during combustion of destroyed coal mass was analyzed. It was shown that carbon monoxide (CO) is more stable at high temperatures, whereas carbon dioxide (CO₂) is more stable at lower temperatures.
8. Several methods for assessing coal self-ignition were reviewed, including pyrite-based, bacterial, phenol-based methods, and the "coal-oxygen" complex theory.
9. A methodology was presented for determining the incubation period of coal self-ignition under mine conditions.
10. A procedure was proposed for determining the yield of volatile substances from coal seams and the lower explosive limits of coal dust.
11. To assess the stage of coal self-heating during seam extraction in specific geological and mining conditions, a set of indicators was proposed, along with a passport for endogenous fire hazard of the seam.
12. For work safety, significant attention is given to reclassifying fires as extinguished, reopening isolation seals, restoring ventilation in the affected area, and reventilating the entire exhausted level. Corresponding recommendations were developed to guide these processes.

References

- [1] Ageev V. G. (2016).: Scientific foundations for creating methods and means of localization of shock waves during mine rescue operations for fire isolation in mines (Doctoral dissertation). State Research Institute of Mine Rescue, Fire Safety and Civil Protection “Respirator,” Donetsk.
- [2] Bulat A. F., Mineev S. P., Smolanov S. N., & Belikov I. B. (2021).: Fires in mine workings: Isolation of emergency areas. Kharkiv: V Deli.
- [3] Mineev S. P. (2016).: Prediction and methods of combating gas-dynamic phenomena in Ukrainian mines. Dnipropetrovsk: Eastern Publishing House.
- [4] Mei Y. (2023).: A rapid dual-drive technology for extinguishing large high-gas coal mine fires. *Frontiers in Earth Science*, 11. <https://doi.org/10.3389/feart.2023.1269092>
- [5] Smolanov S. N. (2018).: Development of scientific foundations for the elimination of complex underground fires in coal mines by ventilation impact methods (Doctoral dissertation abstract). M. S. Polyakov Institute of Geotechnical Mechanics, NAS of Ukraine, Dnipro.
- [6] Bulat A. F., Mineev S. P., Yanzhula O. S., Smolanov S. N., & Belikov I. B. (2024).: Fires in mine workings: Isolation of fires. Dnipro: Belaya.
- [7] Smolanov S. M., Holinko V. I., & Hryadushchyi B. A. (n.d.).: Fundamentals of mine rescue operations. Dnipropetrovsk: National Mining University.
- [8] Mineev S. P. (2017).: Enemy or friend – mine methane? People decide. *Occupational Safety, Supplement to Journal*, (12), 49–53.
- [9] Mineev S. P. (2018).: On the prevention of accidents related to methane explosions in coal mines. *Coal of Ukraine*, (1–2), 50–59. <http://ir.nmu.org.ua/handle/123456789/151975>
- [10] Smolanov S. N. (2002).: Elimination of complex underground emergencies by ventilation methods. Dnepropetrovsk: Nauka i Obrazovanie.
- [11] Pashkovsky P. S. (2013).: Endogenous fires in coal mines. Donetsk: Knowledge.
- [12] Topchienko B. I., & Zinchenko I. N. (1994).: Scheme of ventilation connections of an isolated section under fire gas recirculation. *Mine Rescue Work: Collection of Scientific Papers*, Research Institute of Mine Rescue, Donetsk, 61–63.
- [13] Xiaowei Z. (2019).: Colloid technology for preventing and extinguishing the spontaneous combustion of coal. In *Coal and Peat Fires: A Global Perspective* (pp. 217–241). <https://doi.org/10.1016/b978-0-12-849885-9.00012-3>
- [14] Dobriansky Yu. P. (1991).: Calculation of thermal and humidity regimes of underground structures using computers. Kyiv: Naukova Dumka.
- [15] Dehnert J., Stopp J., Windisch P., & Schönherrt, B. (2020).: Correction to: Quick-erect stopping system for radiation protection and mine rescue in small-scale mining. *Mining, Metallurgy & Exploration*, 37(6), 1819. <https://doi.org/10.1007/s42461-020-00353-z>
- [16] Baltaitis V. Ya., & Yarembash I. F. (1972).: The danger of convective-diffusive transfer of combustion products toward the ventilation flow. *Coal of Ukraine*, (12), 46–47.17.
- [17] Alekseenko S., Zavialov G., & Shaikhislamova I. (2016).: Energy indicators of the rescue units members. *Mining of Mineral Deposits*, 10(3), 90–96. <https://doi.org/10.15407/mining10.03.090>
- [18] Kim Y.-S., Kwon Y.-J., Kang H., & Kweon O.-S.: (2025). An Analysis of Ceiling Jet Velocity Characteristics in Horizontal Corridors during Fires. *Fire Science and Engineering*, 39(5), 1–12. <https://doi.org/10.7731/kifse.6a8b7f32>

- [19] Oka Y., & Oka H. (2020).: Temperature and velocity distributions of a ceiling-jet along a flat-ceilinged tunnel with natural ventilation. *Fire Safety Journal*, 112, 102969. <https://doi.org/10.1016/j.firesaf.2020.102969>
- [20] Leblond P. H. (1969).: Gas diffusion from ascending gas bubbles. *Journal of Fluid Mechanics*, 35(4), 711–719. <https://doi.org/10.1017/s002211206900139x>
- [21] Limantseva O. A. (2014).: Elucidation of the hierarchy of processes transforming the pore space of water-hosting rocks based on thermodynamic simulation results. *Geochemistry International*, 52(11), 979–991. <https://doi.org/10.1134/s0016702914090079>
- [22] Mineev S. P., Smolanov S. N., Belikov I. B., & Samopalenko P. I. (2018, September).: Methodology of temperature prediction in the field of fire. *Modern Scientific Researches*, (5, Part 1), 30–39. Minsk, Belarus.
- [23] Charter of the State Mine Rescue Service on the organization and conduct of mine rescue operations. (1993). Kyiv, Ukraine.
- [24] Mineev S. P., Rubinsky A. A., Vitushko O. V., & Radchenko A. E. (2010).: Mining operations in complex conditions on outburst-prone coal seams. Donetsk: Eastern Publishing House.
- [25] Mineev S. P., Prusova A. A., & Kornilov M. G. (2007).: Activation of methane desorption in coal seams. Dnipropetrovsk: Weber.
- [26] Mineev S. P. (2009).: Properties of gas-saturated coal. Dnipropetrovsk: National Mining University.
- [27] Mineev, S. P., Smolanov, S. N., Belikov, I. B., & Samopalenko, P. M. (2018, October). Justification of the choice of emergency ventilation modes during fire extinguishing. *Modern Scientific Researches*, (5, Part 2), 16–21. Karlsruhe, Germany.
- [28] Bulat A. F., Mineev S. P., Smolanov S. N., Belikov I. B., & Samopalenko P. M. (2018).: On the peculiarities of methane emission control during the elimination of the consequences of methane-air mixture explosions. *Coal of Ukraine*, (8), 29–34.
- [29] Mineev S. P., & Demchenko S. V. (2021).: Modeling of processes occurring during heating and ignition of coal particles in methane-air mixtures near the fire source. *Geotechnical Mechanics*, (156), 100–117. Dnipro.
- [30] Mineev S. P., Vostretsov N. A., Dubovik A. I., Losev V. I., et al. (2016).: Isolation of an air-supplying shaft during accident elimination. *Physico-Technical Problems of Mining Production: Collection of Scientific Papers*, (18), 153–162. Institute of Physics of Mining Processes, NAS of Ukraine, Donetsk.
- [31] Mineev S. P. (2018).: Methane explosion at the “Novodonetskaya” mine. *Geotechnical Mechanics*, (138), 137–149. Dnipro.
- [32] Bulat A. F., Mineev S. P., Smolanov S. N., Belikov I. B., & Samopalenko P. M. (2018).: On some peculiarities of methane emission control during the elimination of the consequences of methane-air mixture explosions in coal mines. In *Proceedings of the Forum of Miners 2018* (pp. 242–250). Dnipro: Serednyak T. K.
- [33] Liu Y., Shi Z., Jia Y., Chen Z., Yu B., Li K., Wang Z., Wang X., Chen Y., Fu P., & Zhou H. (2025).: Distinguishing the self-ignition and ignition temperatures of coal based on Semenov’s thermal explosion theory. *Fuel*, 384, 133982. <https://doi.org/10.1016/j.fuel.2024.133982>
- [34] Mineev S. P., Kocherga V. N., Dubovik A. I., Losev V. I., & Kishkan M. A. (2016).: Investigation of an accident with two explosions of a methane-air mixture. *Coal of Ukraine*, (9–10), 14–22.
- [35] NAPB B.01.009-2004. Fire safety regulations for coal industry enterprises of Ukraine, approved by

- the Ministry of Fuel and Energy of Ukraine Order No. 638, October 12, 2004. (2004). 161 p.
- [36] Koptikov V. P., Boki V. V., Mineev S. P., Yuzhanin I. A., & Nikiforov A. V. (2016).: Improvement of methods and means for safe mining of coal seams prone to gas-dynamic phenomena. Donetsk: Promin.
- [37] Safety rules in coal mines. (2015). Kharkiv: Fort.
- [38] Mineev S. P., Kocherga V. N., Yanzhula A. S., Samokhvalov D. Yu., et al. (2017).: Evaluation of indicator gas concentrations in the working faces of Pokrovske mine. Geotechnical Mechanics: Interdepartmental Collection of Scientific Papers, (133), 148–157. Dnipropetrovsk.
- [39] Kalinchak V. V., & Chernenko A. S. (2017).: Thermophysics of coal dust combustion. Odesa: I. I. Mechnikov Odesa National University.
- [40] Golovchenko A., Dychkovskiy R., Pazynich Y., Edgar C.C., Howaniec N., Jura B., & Smolinski A. (2020).: Some Aspects of the Control for the Radial Distribution of Burden Material and Gas Flow in the Blast Furnace. *Energies*, 13(4), 923. doi:10.3390/en1304092
- [41] Chernov O. I., Belaventsev L. P., Skritsky V. A., et al. (1982).: Influence of moisture on the development of coal self-ignition. *Industrial Labor Safety*, (5), 34–36.
- [42] Peng A., Zhou Y., Yang C., Chen G., & Wu H. (2025).: Ignition and Combustion of a Single Coal Particle under Pressurized Oxy-Coal Combustion Environments: A Modified Transient Coal Ignition Model. *Energy & Fuels*. <https://doi.org/10.1021/acs.energyfuels.5c02521>
- [43] Kernerman V. A., Mishenina K. A., & Slin'ko M. G. (2001).: Mathematical Modeling of Ignition and Extinction of Surface Exothermic Reactions. *Theoretical Foundations of Chemical Engineering*, 35(4), 389–396. <https://doi.org/10.1023/a:1010483321794>
- [44] Zborshchik M. P., & Osokin V. V. (1990).: Prevention of self-ignition of rocks. Kyiv: Tekhnika.
- [45] Zborshchik M. P., & Osokin V. V. (2012).: Pyrite-containing coals and rocks as sources of hazardous natural-technogenic phenomena. *Coal of Ukraine*, (11), 34–37.
- [46] Montgomery W. J. (1978).: Standard Laboratory Test Methods for Coal and Coke. *Analytical Methods for Coal and Coal Products*, 191–246. <https://doi.org/10.1016/b978-0-12-399901-6.50012-8>
- [47] Kobayakov A. I., & Kobayakov A. A. (2001).: Environmentally Safe Coal Processing. *Theoretical Foundations of Chemical Engineering*, 35(5), 498–502. <https://doi.org/10.1023/a:1012334305993>
- [48] Ceyhun İ. (2003).: Kinetic Studies on Karlova Coal. *Theoretical Foundations of Chemical Engineering*, 37(4), 416–420. <https://doi.org/10.1023/a:102504092283>
- [49] Akgun F., & Essenhigh R. H. (2001).: Self-ignition characteristics of coal stockpiles: theoretical prediction from a two-dimensional unsteady-state model. *Fuel*, 80(3), 409–415. [https://doi.org/10.1016/s0016-2361\(00\)00097-1](https://doi.org/10.1016/s0016-2361(00)00097-1)
- [50] Portola V. A., Labukin S. N., & Shelomentsev A. (1982).: Problems of detecting sources of coal self-ignition in mined-out areas. *Ecology and Occupational Safety*, 58–62.
- [51] Zborshchik M. P., Kostenko V. K., Pletnev V. A., & Suslov M. G. (2003).: Mechanism of formation of coal self-heating sources in zones of geological disturbances exposed by mine workings. *Miner's Week 2003, Seminar No. 4*, 1–4.
- [52] Kochetov S. I., & Voitenko Yu. I. (2017).: On the causes of coal self-ignition. *Mineral Resources of Ukraine*, (4), 11–14.
- [53] Holinko V. I., & Holinko O. V. (2021).: Algorithms and methods for performance improvement of automatic gas protection systems. *Scientific Works of Donetsk National Technical University, Series:*

- Problems of Modeling and Automation of Design, 1(17), 79–87.
- [54] Vovna O. V., Zori A. A., & Khlamov M. G. (2010).: Dynamic error compensation method for infrared methane concentration meter for coal mines. Bulletin of NTU “KPI”: Power Engineering and Conversion Technology, (12), 65–70. Kharkiv: NTU “KPI”.
 - [55] Institute of Geotechnical Mechanics, NAS of Ukraine. (2022). Research report: Development of recommendations for safe isolated methane removal in the presence of CO in degassing pipelines at Heroiv Kosmosu mine. Dnipro.
 - [56] Bulat A. F., Minieiev S. P., Kocherha V. M., et al. (2019).: Methodology for determining volatile matter yield of a coal seam and lower explosion limits of coal dust. Dnipro: Barvyks.
 - [57] Alekseev M. O., & Holinko O. V. (2018).: Automated diagnostics of stationary thermocatalytic gas analyzers. In Collection of Scientific Papers of NSU (Vol. 53, pp. 223–229). Dnipro: NGU.
 - [58] Bulat A. F., Minieiev S. P., Kocherha V. M., Krukovskiy O. P., et al. (2022).: Instruction for determining volatile matter yield of a coal seam and lower explosion limits of coal dust. Dnipro–Kyiv: Barvyks.
 - [59] Mineev S. P., Dyakun I. L., & Yashchenko I. A. (2018).: Influence of volatile matter yield on determining the explosibility of coal dust. Geotechnical Mechanics, (142), 45–52. <http://dspace.nbu.gov.ua/handle/123456789/158714>
 - [60] Holinko V. I., & Kotlyarov A. K. (2010).: Control of explosion-hazardous environments in mine workings and equipment of coal mines (Monograph). Dnipropetrovsk: Lira.
 - [61] Holinko V. I., & Kotlyarov A. K. (2004).: Developing a method to control the sensitivity of thermocatalytic methane sensors. Mining Electromechanics and Automation, (73), 54–60.
 - [62] Korenev A. P. (2012).: State and prospects of dust suppression and dust protection in coal mines. Coal of Ukraine, (9), 34–37.
 - [63] Bulat A. F., Yashchenko I. O., Minieiev S. P., Seleznev A. M., & Drozd S. V. (2018).: Method for determining the lower explosion limit of coal dust (Patent No. 124544, Ukraine). Ukrainian Institute of Geotechnical Mechanics, NAS of Ukraine.
 - [64] Pivnyak G., Falshtynskiy V., Dychkovskiy R., Saik P., Lozynskiy V., Cabana E., & Koshka O. (2020).: Conditions of suitability of coal seams for underground coal gasification. Key Engineering Materials, 844, 38–48. <https://doi.org/10.4028/www.scientific.net/kem.844.38>
 - [65] Minieiev S. P., Seleznev A. M., Yashchenko I. O., & Samokhvalov D. Yu. (2017).: Method for assessing the explosibility of coal dust near drivage workings (Patent No. 122296, Ukraine). Institute of Geotechnical Mechanics, NAS of Ukraine.
 - [66] Manka D. P. (1979).: Coke Oven Gas Analysis. Analytical Methods for Coal and Coal Products, 3–27. <https://doi.org/10.1016/b978-0-12-399903-0.50007-6>
 - [67] Hershkovitz F. (1985).: Mass Transfer Effects in Coal Conversion Chemistry. Chemistry of Coal Conversion, 45–65. https://doi.org/10.1007/978-1-4899-3632-5_3
 - [68] Heredy L. A. (1981).: The Chemistry of Acid-Catalyzed Coal Depolymerization. Coal Structure, 179–190. <https://doi.org/10.1021/ba-1981-0192.ch012>



Serhii Minieiev
– Doctor of Technical Sciences, Professor

Areas of scientific research:

- Problems of mine ventilation and labor protection;
- Mine atmosphere control,
- Industrial sanitation and civil safety;
- Forecasting and prevention of explosions, fires, and gas-dynamic phenomena in mines;
- Methane degasification and dust control.

Since 2014, he has served as the principal head of expert commissions investigating accidents (methane explosions, fires, gas-dynamic phenomena, etc.) at coal mines in Ukraine.

He is the author and co-author of about 700 published works, including 16 monographs, 13 manuals and regulatory documents, as well as more than 200 patents for intellectual property objects.



Roman Dychkovskiy
– Doctor of Technical Sciences, Professor

Areas of scientific research:

- Extracting the thin and very thin coal seams, including reserves with different structural changes;
- Substantiation of the mining technologies in zones of geologic infringements and stress borders;
- Underground coal gasification;
- Management of mining pressure;
- Simulation the mining processes and other problems related to mining activity.

Author and co-author of more than 260 publications (including 21: monographs, reference books and textbooks, 73 scientific articles in scientometric databases Scopus and WoS, and 28 patents for intellectual property rights). Dychkovskiy Roman is an honored worker of education of Ukraine.



Dariusz Prostański
– Doctor of Technical Sciences, Professor

Areas of scientific research:

- mining hazards — in particular: dust, coal dust, explosion hazards, dust deposition in excavations and methods of controlling it.
- mechanisation and mining technologies: mining machinery and equipment, their design, power supply, automation and safety.
- transformation of post-mining areas and power engineering — including concepts for the use of post-mining areas and energy storage.

He combines the analysis of mining hazards (dust, occupational safety) with work on the mechanisation and modernisation of mining. He is the Chairman of the Energy Machinery Hazards Section within the Commission for Hazards in Mining Plants, operating at the State Mining Authority.

Author and co-author of over 100 publications in technical journals and monographs, as well as over 100 patents and utility models, most of which have been implemented in industry.



Vladyslav Ryskykh
– Doctor of Philosophy in Technical Sciences

Areas of scientific research:

- underground mining of mineral deposits;
- 3d modeling and planning of mining production;
- geomechanics and management of mining pressure;
- simulation of the mining processes;
- AI in mining;
- neural networks in data processing and other problems related to mining activity.

Author and co-author of about 80 publications, including 3 monographs, 6 patents, reference books and textbooks and 13 scientific articles in scientometric databases Scopus and WoS.

